DG allocation and network reconfiguration for Energy Efficiency Performance of distribution system using Harmony Search Algorithm

A Dissertation submitted in fulfillment of the requirements for the Degree of

MASTER OF ENGINEERING

in

Power Systems

Submitted by

Pratima Pal
(Reg. No. 801742028)

Under the Guidance of
Dr. Pawan Kumar
Assistant Professor, EIED

THAPAR INSTITUTE
OF ENGINEERING & TECHNOLOGY
(Deemed to be University)

2019

Electrical and Instrumentation Engineering Department
Thapar Institute of Engineering & Technology, Patiala
(Declared as Deemed-to-be-University u/s 3 of the UGC Act., 1956)
Post Bag No. 32, Patiala – 147004
Punjab (India)

DECLARATION

I hereby certify that the work which is presented in dissertation entitled, "**DG allocation and network reconfiguration for energy efficiency performance of distribution system using harmony search algorithm**", in partial fulfilment of the requirements for the award of the degree of **Master of Engineering** in **Power Systems**, submitted to Electrical & Instrumentation Engineering Department of Thapar Institute of Engineering & Technology (Deemed to be University) is as authentic record of my own work carried under the supervision of **Dr. Pawan Kumar.** It refers others researcher's work which are duly listed in the reference section. The matter contained in this dissertation has not been submitted, neither in part nor in full to any other degree to any other university or institute except as reported in text and references.

Pratima

Place: TIET,

Date: 14/08/19

(Pratima Pal)

Roll No.: 801742028

It is certified that the above statement made by the student is correct to the best of my knowledge and belief.

Date: 14/08/19

(Dr. Pawan Kumar)

Assistant Professor

Electrical & Instrumentation Engineering Department

Thapar Institute of Engineering & Technology, Patiala

ACKNOWLEDGEMENT

I express my deep sense of gratitude and indebtedness to my supervisor Dr. Pawan Kumar (Assistant professor), Thapar Institute of Engineering & Technology, Patiala, Punjab for his guidance, support and encouragement in steering this thesis work. I feel privileged to have been associated with him as my project supervisor.

I wish to thank Prof. R. S. Kaler, Head, Electrical and Instrumentation Engineering, Thapar Institute of Engineering & Technology, Patiala, Punjab for permitting to pursue this work.

Also, I would like to thank all the faculty members of Electrical & Instrumentation engineering department, Patiala and my colleagues for their unconditional support for the completion of this thesis work.

TABLE OF CONTENTS

LIST OF FIGURES

LIST OF TABLES

NOMENCLATURE

V	Voltage
I	Current
R	Resistant
X	Reactance
P	Real power
Q	Reactive power
S	Apparent power
TP_L	Total power-loss
PL_O	Initial power-loss
QL_0	Initial power-loss
n_p	Real power voltage exponents
n_q	Reactive power voltage exponents
F_{si}	Loadability factor at node ‘i’
P_{FD}, Q_{FD}	Nominal active and reactive load demands
S_{FC}	Feeder KVA loading at substation
$V_{i, min}$	Minimum voltage
$V_{i\ max}$	Maximum voltage

LIST OF ABBREVIATIONS

DG	Distributed Generation
HSA	Harmony Search Algorithm
EEP	Energy Efficiency Performance
ZIP	Constant Impedance, Current, and Power
HMCR	Harmony Search Considering Rate
PAR	Pitch Adjusting Rate
LM	Load Model
BW	Bandwidth
HM	Harmony Memory
HMS	Harmony memory search
SLD	Single Line Diagram
TSA	Tabu Search Algorithm
ACSA	Ant Colony Search Algorithm
RLF	Radial Load Flow
DNRC	Distribution Network Reconfiguration
DFR	Distribution Feeder Reconfiguration
GA	Genetic Algorithm
MISCOCP	Mixed Integer Second Order Conic Programming
DNO	Distribution Network Operation
DGO	Distributed Generated Owners
OPF	Optimal Power Flow

ICA	Imperialistic Competition Algorithm
PEM	Point Estimate Method
ODGP	Optimal Distributed Generation Placement
PPF	Probabilistic Power Flow
EEDP	Energy Efficiency Defining Parameters
EEPI	Energy Efficiency Performance Index
VS	Voltage Security
NVSI	Node Voltage Security Index
NVQI	Node Voltage Quality Index

ABSTRACT

In the ever-growing load demand scenario, the representation of loads and the integration of DG in coordination with network reconfiguration plays an important role in the distribution system operation. Though, distribution system usually required to change the network topology due to frequent change in loading pattern and to operate the system in energy efficient manners. The frequent change in network topology further required to alter the DG size as per the demand and the operating constraints. In the past, several researches have presented the reconfiguration and DG allocation exclusively under fixed loading conditions.

This work considered several practical combinations of loading pattern for the representation of loads in load flow studies. For optimal load flow there exists several natures inspired optimization techniques. In this work, optimization is performed using harmony search algorithm. The results are demonstrated on a 33-node radial system under five different loading patterns for single and multi DG allocation. From the results, it can be observed that in the proposed approach the optimal configuration and DG size found to be significantly different as compared to the results obtained for constant power loading in the literature. Moreover, the proposed approach explores the most efficient operation under large change in loading in order to find the energy efficient operation of distribution system.

Chapter 1

Introduction

1.1 Overview

The distribution system is defined as the constant or consecutive discharge of motions, strategy, system composition and related to facilitating the monitoring of service evolution from the substations to consumers. Distribution system is all about to provide the voltage to end of consumer without interruption as much as they required to run the appliances. The main aim of this system is providing the energy to the consumers with individuals zone. The distribution of the electrical energy is done with low amount of voltage level.

Distribution system is basically final operation of the electrical energy system to provide energy to consumer side. It carries energy to the distinct zones of consumers side from the transmission system. With the help of transformer between the transmission to distribution system, voltage up to medium range 2kV-35kV. Medium range of voltage carries by distribution lines to the transformer of distribution system which is located nearest to consumers zone.

Distribution transformer further diminished the value of the voltage according to the consumers requirement (to feed household appliances) through the secondary distribution lines. It has consisted following major parts:

- Sub-systems of distribution
- Primary distribution System
- Transformers of distribution
- Mains service distributors

1.2. Classifications of distribution system

The distribution system or scheme can be classified in different manners based on the load supplied, network structure and connection schemes. In power system power supply from the substation to consumer side with two different structure. The overhead system is usually used due to low cost. Underground system is used for impracticality. First one is overhead distribution and second is underground distribution supply system, which are defined below:

1.2.1 Overhead distribution system

An overhead power line is a construction, used to transmit the electrical energy to the load side. It consists one or more conductors in it which are suspending over the towers. They are cost effective rather than the underground.

1.2.2 Underground distribution system

Undergrounding is the alternative of overhead cables transmit electrical electricity or telecommunications, with underground cables. It demonstrates the better technology in evolved nations for fireplace prevention and to make the energy lines less dispose to outages or discontinuity all through heavy snow or ice storms. Underground may be expensive in the beginning but after implanting operational cost may decrease with respect to the lifetime of the cable.

1.3 Scheme of connections

In distribution system, basically scheme of connections are:

- Radial distribution system
- Ring main distribution system

1.3.1 Radial distribution System

In last few years, distribution system evolved in different manner such as, distinct feeders radially came from the sub-station end and feeders are straight attach to the primary end of the transformer in distribution system.

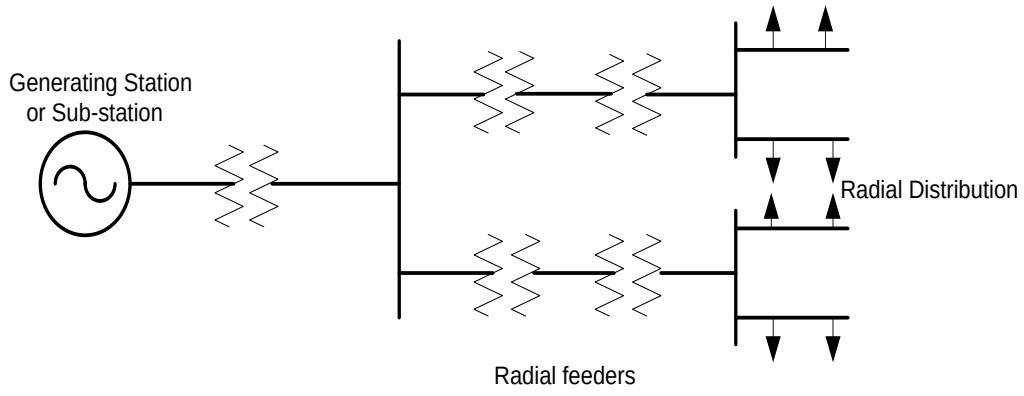

Fig 1.1 Radial feeder of distribution system

But there is a major issue with the radial pattern of distribution system which is, whenever any of the feeders' damage due to the faults then total power supply interrupt to the consumer side

because there is not second option feed the transformer. Hence if the any of reason transformer failure also occurs in radial pattern then complete supply blocked to the consumer side, so that with this reason radial pattern of distribution system is not feasible as compare to ring distribution system.

1.3.2 Ring main distribution system

Ring main distribution system came after the radial main, hence the time radial main fail to solve the problem of system then ring main operate or come to prevent the power interruption issue from the system which makes the system more reliable as compare to radial to consumer point of views as well. It designed as, a single ring network or system fed through single or multiple number of feeders.

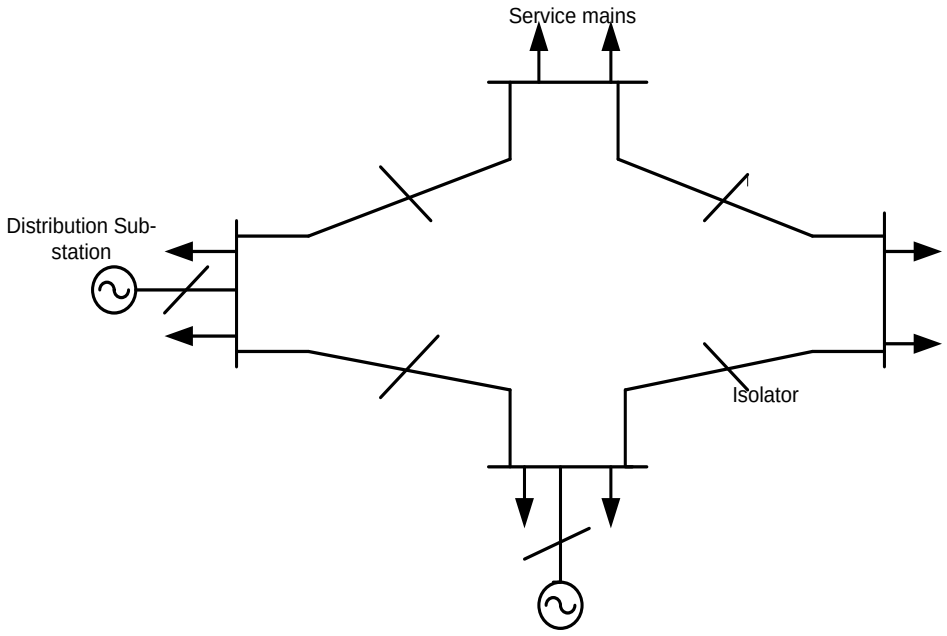

Fig 1.2 Ring main feeder of distribution system

If fault occurs in system and it damage any feeder, but it will not make difference into the system power supply to the consumer side which proves itself, the advantage of ring main over the radial main. Hence due to the ring main, consumer gets eternal power supply which is much an augurate manner. And there is some of the advantage in it, in ring main different ring sections are open to each other hence whenever any fault occurs in the any single of ring section, affected section can easily isolate. with help of associate section, the power supply will continue to consumer side.

1.4 Load class

In power system, load class is mainly classified into three different load class, namely: residential load, commercial load and industrial loads. These three loads are used as the requirement of the consumer demands. They are defined below:

1.4.1 Residential load

Residential or Domestic load consists of home electric appliances such as light, fan, small motors etc. And maximum appliances are operating in daytime for few hours.

1.4.2 Commercial load

Commercial load consists of electric load which purpose to be used commercially as: Restaurant, Shop, and Mall etc. This type of load operated more than the residential operating hours.

1.4.3 Industrial load

Industrial load consists load demand by individual industries and it includes all electrical loads in industry even employed machinery. Industrial load can operate a whole day which means, operating time of the industrial load is more than the residential and commercial load**.**

1.5 Load model

Mostly, power supply consumption totally depends on the morning to night hours, which means It varies with daytime, node voltage and frequency. But if it comes to the frequency, variations in the frequency does not make more difference in the system so that it can be negligible. Generally, in load flow studies, usually loads are considered as static model.

$$PL = PL_0(V|V_0)^{np} \quad (1)$$

$$QL = QL_0(V|V_0)^{nq} \quad (2)$$

where np & nq are voltage components which clarified Dependent voltage properties of active and reactive load elements. These are the different load models which all are considered as static loads it is also referred as constant power, current and impedance. Z is steady loads of impedance with $n_p=n_q=2$, represent constant current loads with $n_p=n_q=1$ and 'P' referents constant power loads with $n_p=n_q=0$. Generally, these three loads are disturbing the EEP of distribution system with the variations of voltage exponent values.

1.6 Types of load

There are different kind of loads are present in electrical power system which are given below in tabular form with their suitable example, they are such as: constant power, impedance and currents loads.

Table 1.1 Types of load

S. No.	Types of Load	Voltage exponents		Example
		α	β	
1	**Constant Power (P)**	0.0	0.0	Induction motor running at steady slip, maintaining power consumption as steady even at low voltage by drawing greater energy.
2	**Constant Impedance (Z)**	2.0	2.0	Room heater, the efficient impedance of the circuit stays continuous, while the energy differs as the voltage square.
3	**Constant Current loads (I)**	1.0	1.0	The method of welding the transformer and electroplating remains continuous.
4	**Exponential loads**	1.38	3.22	This is the combination of several P, I, Z loads

1.7 Load combinations

The different load combinations formulated in this work are discussed as follows

A. **Load combination 1:** This considers all load kinds (i.e. continuous ZIP) and therefore this model is a complicated load at a separate distribution scheme node.

B. **Load combination 2:** This considers all loading classes and therefore this model is the complicated load at a separate distribution scheme node.

C. **Load combination 3:** All load kinds (i.e. ZIP including exponential) are therefore regarded in this model the complicated load at the distribution system's node.

D. **Load combination 4:** Complex load on the distribution scheme where distinct nodes are grouped with comparable load kinds.

E. **Load combination 5:** Composite allocation system load where distinct nodes are grouped with comparable load classes.

1.8 Conclusion

In this chapter, distribution system discussed in terms of definition, classification, load classes in different types like, residential, commercial and industrial, types of construction ring and radial form, load type like constant voltage, constant current and constant impedance load, load model and load combinations as well. Hence in this chapter a brief information delivered.

Chapter 2

Literature Review

2.1 Overview

Mostly, energy management is now a serious problem in the distribution system, we can maintain the voltage profile on load side with the help of reconfiguration, which has an authority to balance the voltage profile toward the linear/ non-linear loads at different feeders.

2.2. Literature survey

Ali et al. [1] discussed a method with respect to the practical loads, reconfiguration of energy efficiency by developing a cumulative index of improved system performance. All EEDPs are accountable for finding a truly energy-efficient configuration. There are three distinct instances of changes in working circumstances and specifications, and the findings show that various EEDPs play a crucial role in setting the network reconfiguration criterion for distinct load models.

Kumar et al. [2] This article provided the distribution system's energy efficiency assessment in various configurations for practical loads. Due to the experimental results, power demand along with the capacity of the feeder is also vary in distinct configuration in case of voltage dependent loads. and with the improvement in node voltages, load profile will be improved, hence energy efficiency will be improved as well.

Kumar et al. [3] introducing effective heuristic and meta-heuristic solutions to the reconfiguration of the distribution scheme through the imposition of VS and network radiation. Improvement of the: loadability limit, load profile, operating efficiency and reduction in power as well dur to the VS. Inflicting of VS, to meet the objectives of NVSI and NVQI heuristic approach implementation will consider and for the loss reduction meta-heuristic approach will be consider.

Venkatesh et al. [4] introduced a scheme, which is based on the derived maximum loadability index. It is also using fuzzy modelling technique to obtain reliable voltage profile and model bi objectives of loadability at maximum margin. Sivanagaraju et al. [5] with the improvement of loadability margin at a node, the voltage stability reform can be achieved with the voltage stability index.

Saffar et al. [6] optimum reconfiguration to achieve better voltage regulation in terms of equal load balancing of feeders and energy loss. in this a technique used which has two distinct methods involved itself, first one is multi-objective function, and another is based on fuzzy variables. And this technique aims at balancing loads and reconfiguring power losses in feeders for system. Both load balance and feeder loss reduction goals were considered in this method.

Baran et al. [7] proposed general formulation and methodology to lowering, loss in power and balance of load as well. In terms of load balance, a load balance is defined. For both balanced and unbalanced radial distribution system, a very simple reconfiguration algorithm is used. There is less mathematical formulation in this algorithm, and it is and effective way to reduce energy loss.

Subrahmanyam et al. [8] presented, algorithm of reconfiguration used for both balanced and unbalanced radial distribution schemes had been implemented. This suggested algorithm includes less complicated mathematical expressions and with decreased power losses, a more effective network set up can be achieved.

Rao et al. [9] In this context, harmony search algorithms are used to resolve the system reconfiguration problem in order to obtain optimal switching in the distribution system to reduce losses. Ababei et al. [10] introduced an efficient heuristic algorithm to fix network loss decrease. The primary strategy of concurrent branch exchanges results in a greater decrease of losses within tiny iterations.

Nara et al. [11] Introduction of genetic algorithms in the distribution system to reduce loss. Also known as the optimization algorithms is GA based on mechanics of natural selection and natural genetics.

Zhang et al. [12] Presents an enhanced loss minimization reconfiguration tabu search algorithm in a large-scale distribution scheme. TSA is an effective algorithm method. Raju et al. [13] It utilizes present data from a power flow instead of an ideal stream pattern used in other methods to decide which switch to open, in a sequential manner. During the second stage, the operation of the branch exchange is studied to further reduce losses.

Tzong et al. [14] Presents an ant colony search algorithms (ACSA) to decrease losses in the distribution scheme as well as a new optimization method. With the help of ACSA, the optimum solution to the network reconfiguration problem can be adequately achieved.

Hooshmand et al. [15] Introducing a new method employing heuristic rules is presented for optimal reconfiguration of distribution networks with the aim of loss reduction and load balancing. We use two separately algorithms for each objective. Moving from the original setup to the final setup, for the two above algorithms, network parameters (contain loss and load balancing index) are calculated for each configuration and all intermediate configurations are stored.

Farahani et al. [16] Loops selection sequence impacts ideal setup and network loss in this easy technique of branch return. This technique has therefore been enhanced by optimizing the sequence of selected loops to minimize energy losses.

Jabr et al. [17] Introduction of a conical mixed-integer programming formula for network reconfiguration with minimal loss. This formulation has two characteristics: first, it uses a convex representation of the network model based on the conical quadratic format of the energy flow equations and, second, it optimizes the accurate value of network losses.

Oliveira et al. [18] Presents a heuristic algorithm step by step to reconfigure radial distribution devices in order to minimize power losses. The methodology suggested is Based on the Strategy for Dynamic Switches, updated to avoid premature algorithm convergence into sub-optimal solutions due to topological changes in the electrical network. This technique includes only evaluating a straightforward algebraic voltage magnitude expression and no trigonometric function unlike the conventional load flow situation.

Aman et al. [19] Introduced RLF analysis based on smart graph theory to fix "dynamic" issues. The suggested algorithm will assist to arrange line information for Any combination of position of tie switches, verify the system's radiality and guarantee That all nodes are linked to the source node. Andervazh et al. [20] Proposes a multi-objective network reconfiguration (DNRC) technique based on Pareto using a discrete particle swarm optimization algorithm. The methods are minimizing energy loss, the number of switching activities, and the amount of bus voltage deviations from their rated values subject to system limitations.

Menzoda et al. [21] Proposes and applies a multi-objective reconfiguration approach based on evolution in electrical power medium voltage distribution system. This method is approaches for two main motives, Reduction of power loss and indices of reliability. Naramani et al. [22] Implemented an effective technique for Multi-objective reconfiguration with regard to distributed generators of radial distribution systems. The problem of conventional feeder

reconfiguration (DFR) cannot meet the reliability requirements, while the primary strategy is to reduce energy loss and voltage deviation.

Gupta et al. [23] Introducing genetic algorithms (GAs) to resolve the two problem in distribution network as improvement of the reliability and power quality. This is very important method because it is stands for solve two different problem in network. Lopez et al. [24] Proposes a method Multi-objective reconfiguration of distribution systems for distributed generators. The problem of conventional feeder reconfiguration (DFR) cannot meet reliability requirements, Consideration of minimizing the loss of active power and limiting reliability. A MISOCP model's primary strategy ensures convergence to optimality with the assistance of current convex optimization solvers.

Ghazani et el. [25] using genetic algorithms tools to protect the distribution network and there is penalty function is also used for mathematical constraints to reach the satisfied result with respect to the minimum power loss and voltage deviation.

Ali et al. [26] In order to evaluate the efficiency of the distribution scheme, distinct configurations were suggested using distinct soft computing techniques. The outcomes are regarded after enhanced energy loss in the distribution network, such as Profiles of voltage, limit of loadability, and release of energy demand and feed capacity.

Kumar et al. [27] Use harmony search algorithms (HSA) to find the optimum solution for distinct static loads. There are two primary approaches in the distribution network, such as loss decrease and tension profile maintenance. Deregulation in power is a very prevalent problem in the electricity industry, because of this problem there are so many possibilities to explore some fresh technology. One of those technologies used to satisfy the ever-increasing demand for electricity is distributed generation or disperse generation. The word dg generates electricity on a small scale close to the point of consumption. By using dg allocation, we are able to take maximum advantage of the appropriate positioning of dg units at the appropriate location with ideal capacity and the appropriate DG unit type.

Celli et al. [28] It has been defined that many Objective Functions can be adopted in order to drive research into the optimal allocation of dg’s towards a solution that is not only economically and technically convenient but also robust in terms of the objectives selected. Chiradeja et al. [29] DG in a distribution scheme provides several benefits for utilities, customers and society, such as reduced line losses and transformer losses, reduced reserve

requirements for main generating stations, Improved system voltage profile, increased system reliability and improved power quality, peak shaving, reduced impact on the environment and reduced transmission and distribution congestion.

Hung et al. [30] Proposed analytical terms for Optimizing the size and power factor of separate generators to minimize losses in major distribution systems. The validity of the suggested analytical expressions for ideal size is evaluated and verified using exhaustive load flow alternatives on three different size and complexity test distribution devices.

Khaleshi et al. [31] Introducing dynamic programming as an instrument for optimization, a novel way of finding the best place for distributed generation assembly in a variable load model network has been provided. Network load was modelled at distinct levels and the issue was optimized in view of the constraints on the continuous operation of the distribution scheme.

Ganguly et al. [32] DG integration is only beneficial for certain specific nodes in a network to significantly improve energy loss and node voltage. Soroudi et al. [33] Introduces a dynamic, multi-objective formulation of the DG -planning problem and an immune-GA-based approach to the problem formulated. The proposed two-step algorithm defines non-dominated options in the first stage by maximizing the advantages of DNO and DGO concurrently and employs a blurred adequate method to select the candidate's best alternative in the second stage.

Dent et al. [34] Changing the voltage step when a distributed generator is suddenly disconnected is one of the areas of interest for distribution network operators to determine whether DG can be linked, although there are differences in the use of utility boundaries. To study how constraints on the voltage phase affect the quantity of DG that can be attached to a distribution network, constraints of the voltage step were incorporated into the defined optimum energy flow (OPF) method to determine the ability of the DG network.

Mahari et al. [35] Suggested technique to solve the issue of nonlinear mixed-integer DG allocation and size optimization using ICA. The objective was to minimize the active power losses of the whole scheme by meeting different system limitations. The algorithm is tested with distinct load situations on the two radial distribution feeder systems 69-bus and 33-bus. The ICA-based method suggested has some important benefits over other methods.

Evangelopouse et al. [36] As a stochastic programming model, restricted programming was introduced and in view of the uncertainties of load growth, as a new methodology for solving

the ODGP problem, a PEM-based GA-based approach has been proposed. Wind, photovoltaics manufacturing and future volatile fuel and electricity prices.

Keane et al. [37] The IC of the primary work points was calculated to assist in the planning of non-firm generation projects with the feasibility of infringements of the voltage constraint. In addition, DG voltage management is suggested with a minimal cost reduction method, which encourages the operation of non-firm DG by stopping energy leakage through non-dispatchable generation.

Haghifam et al. [38] This paper presents a new strategy for DG placement, taking into account a fuzzy explicit representation of the uncertainties associated with the future load, as well as a fuzzy illustration of power flow uncertainties in feeders and substations, network node voltage and electricity market price. This model reduces financial and technical and economic risks at the same time.

Kaen et al. [39] DG's rapid development in its various forms and scales transforms traditional distribution network planning and operation. The power resources range is consistent with the computational techniques and approaches used to integrate them. As described in this article, each one has its benefits and disadvantages and depends on the situation.

Kamel et al. [40] introducing hybrid which is based on gray wolf optimizer algorithm. Due to this technique, optimal DG size and locations are deciding. It will also improve the voltage stability, loadability and reduced the active power losses.

Rawat et al. [41] this is based on heuristic optimization technique, which is helpful in improvement of the entire performance of the system like boosting the voltage stability and reducing power loss. In this paper, both operations are involved: reconfiguration and DG allocation radial in distribution system.

Rao et al. [42] introducing meta-heuristic HSA technique, this technique is applicable in radial distribution system with success. Aim of the technique to boost up voltage profile and reduction in power loss. the result of HSA is better than the others technique like GA, RGA and ITS. There is result comparisons for 33-node radial system, HSA over the others like: 24.85% loss minimization reach by HSA over the 18.01% in GA, 18.65% in RGA and 19.34% in ITS. Hence this technique is better with others.

Rao et al. [43] presenting HSA technique to reduce the power losses in distinct approach DG allocation, DG allocation after reconfiguration of networks. Improvement of power loss reduction is beneficial as number of DG are install in system from one to four but on there hand if locations are increased from one to four on every load then improvement rate will decrease.

Esmaeilian et al. [44] introducing a novel method, GA as metaheuristic and heuristic algorithm. This is helpful in the, maximization in robustness of system and less time computational time to achieve min loss configuration with the instalment of DG in the system.

2.3 Conclusion

In this chapter, literature review has been discussed. From the literature review it has been observed that the single problem can be solved in different way based upon the operating constraints and the methodologies. The objective of reconfiguration and DG placement have been solved by the researcher using several heuristic and meta-heuristic approaches. In the literature, the loading is considered constant power type whereas in practical system the loads vary with time and state of the economy. Therefore, it is a big challenge to solve the objective of reconfiguration and DG allocation in coordination under different loading pattern. In this work, this objective is thoroughly studied.

Chapter 3

Mathematical Formulation and Harmony Search Algorithm

3.1. Introduction

From the literature survey presented in Chapter 2 the system performance may be observed depends upon the several parameters. The various parameters are as under,

1. Active load demand
2. Reactive load demand
3. kVA capacity of transformer
4. System voltage profile
5. Active power loss
6. Reactive power loss
7. Loadability margin
8. Reliability of supplying power

Therefore, the energy performance of distribution system cannot be evaluated mere based upon the single parameter. This is due to the fact that the system voltage profile depends upon the load demand whereas the load profile is voltage dependent.

3.2. Calculation of node voltage and loadability index

For the calculation of different EEDPs an equivalent radial distribution system is considered, and it is represented in Fig.1. Here V_{i-1} and V_i are voltages of sending side and receiving side. If we assume α is Angle of the load factor and β is sending voltage angle, then we can derive voltage profile and power loss by using following equations.

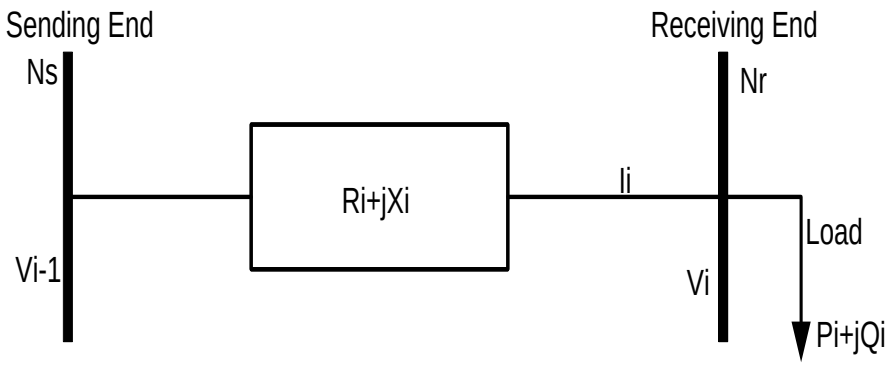

Fig 3.1 an equivalent scheme of radial distribution between two nodes

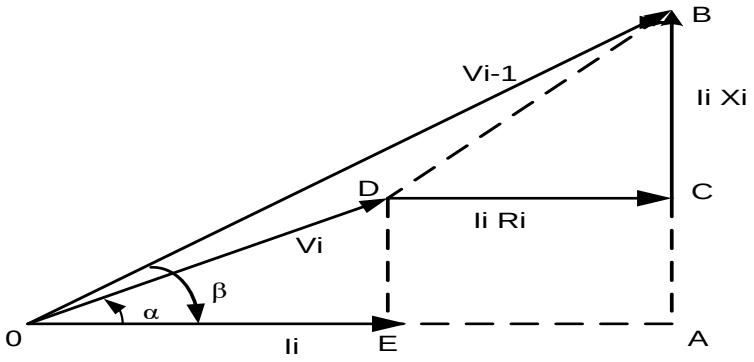

Fig 3.2 Phasor Diagram of equivalent distribution system

$$OA = V_{i-1}cos\beta = V_i cos\alpha + I_i\, R_i \tag{3}$$

$$AB = V_{i-1}sin\beta = V_i\, sin\alpha + \ I_i\ X_i \tag{4}$$

$$V_{i-1}^2 = OA^2 + AB^2 = OB^2$$

$$= (V_i\, cos\alpha + I_i\, R_i)^2 \ + \ (V_i\, sin\alpha + I_i\, X_i)^2 \tag{5}$$

After Solving the above equation, we get:

$$V_{i-1}^2 = \ V_i^2 + 2R_i\ P_i + 2X_i\, Q_i + (R_i^2 + X_i^2)[(\text{P\_i\^{}(2)+Q\_i\^{}2})/V_i^2] \tag{6}$$

$$where\ P_i = \ V_i I_i \cos\alpha$$

$$Q_i = \ V_i I_i \sin\alpha$$

$$I_i = \frac{(\ P_i^2 + Q_i^2)^{.5}}{V_i}$$

Due to re-arranging of the above equations

$$V_{i-1}^2 = V_i^2 + 2R_iP_i + 2X_iQ_i + R_i^2\, cos^2 \propto I_i^2(1 + tan^2 \propto) + x_i^2\, cos^2 \propto \tag{7}$$

To make rearrangement in (10) with respect to line parameters and generalized representation the receiving end voltage equation is obtained in the form for the ith node:

$$V_i^2 = \frac{V_{i-1}^2}{2} - (R_iP_i + X_iQ_i) \pm \left[\left\{\frac{V_{i-1}^2}{2} - (R_iP_i + X_iQ_i)\right\}^2 - (R_i^2 + X_i^2)(P_i^2 + Q_i^2)\right]^{\frac{1}{2}}$$

$$= X \pm Y \tag{8}$$

Where

$$X = \frac{V_{i-1}^2}{2} - (R_iP_i + X_iQ_i)$$

$$Y = \left[\left\{\frac{V_{i-1}^2}{2} - (R_i P_i + X_i Q_i)\right\}^2 - (R_i^2 + X_i^2)(P_i^2 + Q_i^2)\right]^{1/2}$$

As in equation (8) The voltage solution does not exist mathematically if Y2 becomes negative. That is, there will be a solution, when

$$\left\{\frac{V_{i-1}^2}{2} - (r_i P_i + x_i Q_i)\right\}^2 - (r_i^2 + x_i^2)(P_i^2 + Q_i^2) \geq 0 \quad (9)$$

The load capacity limit at that node is defined in equation (12) for the particular load. For the maximum load ability, the existing load is replaced by in other terms. The power factor is considered as constant. After modifying further equation (7), As a quadratic equation, it is equated to zero

$$MLI_i = \frac{V_{i-1}^2\left[-(R_i P_i + X_i Q_i) + \sqrt{(R_i^2 + X_i^2)(P_i^2 + Q_i^2)}\right]}{2(X_i P_i + R_i Q_i)^2} \quad (10)$$

3.3 Mathematical formulation (in terms of DG placement)

To place the distributed generation in distribution network, there are some problem induced due to various reasons number of DG, size of DG and place of installation. Usually capacitor is used for achieving maximum benefits. Maximum loadability with the help of minimum of MLI (minimum loadability index) and reduction of maximum loss by using DG placement in distribution network.

Subject to:

(1) $V_i \min < V_i < V_i \max$

(2) $I_i < I_{i\max}$

3.3.1. DG size calculation

Total active loss of power for the distribution system

$$TP_L = \sum_{i=1}^{n} I_i^2 R_i \quad (11)$$

The energy loss can be demonstrated by dividing the actual and reactive power parts of the present

$$TP_L = \sum_{i=1}^{n} I_{ai}^2 R_i + \sum_{i=1}^{n} I_{Ri}^2 R_i \quad (12)$$

Therefore

$$TP_L = TP_{La} + TP_{LR}$$

Where, TP_{LA}= Loss of power due to the active current component.

TP_{LR}= Loss of power due to the reactive current component.

Total energy loss in the DG scheme is I_{dgk} placed at a node

$$TP_L = \sum_{i=b(j)}^{k} (I_{Ri} + I_{DGk})^2 R_i \sum_{i \neq b(j)}^{n} I_{ri}^2 R_i + \sum_{i=1}^{n} I_{ai}^2 R_i \quad (13)$$

Subtracting equ15 from equ16 reduction in losses may be reduced as

$$\Delta TP_L = -2 I_{DGk} \sum_{i=b(j)}^{k} I_{Ri} R_i - I_{DGk}^2 \sum_{i=b(j)}^{k} R_i \quad (14)$$

Dg current provide maximum loss savings. It can be expressed as

$$\frac{\delta(\Delta TP_{Lk})}{\delta I_{DGk}} = -2\left(\sum_{i=b(j)}^{k} I_{Ri} R_i + I_{DGk} \sum_{i=b(j)}^{k} R_i\right) = 0 \quad (15)$$

The maximum loss saving DG current is

$$I_{DGk} = -\left(\frac{\sum_{i=b(j)}^{k} I_{Ri} R_i}{\sum_{i=b(j)}^{k} R_i}\right) \quad (16)$$

And the size of DG at the candidate node can be calculated as

$$P_{DGk} = I_{DGk} V_k \quad (17)$$

3.4 Load Flow Method

Both voltage-independent loads and voltage-dependent loads have implemented the method. 33 Bus radial distribution systems have been applied to this algorithm. With different types of static load, the power flow problem has been successfully solved.

3.4.1Algorithm to distinguish the nodes and branches above a specific branch

The algorithm representing a terminology to distinguish the nodes, above all branches and it will be very helpful to obtaining injected power of individual branch of the network. There are Step by step algorithm description shown in below:

Step 1: Enter data on the line of radial distribution system.

Step 2: Input k isolated.

Step 3: Count input as isolated and select re(k) to IE (k, count)**.**

Step 4: Input **i** as isolated.

Step 5: whenever **i** is less than or equal to count go to step 6 else go to step 12.

Step 6: Number equal to IE (K, i).

Step 7: Input **j** as isolated.

Step 8: If number equal to se(j) goes to step 9, go to step 10.

Step 9: Access the count and allow IE(K, count) with re(j)**.**

Step 10: Accession j and assume that j is less than or equal to the number of branches and then go to step 8.

Step 11: Accession **i** and go to step 5.

Step 12: Choose count to N(K)**.**

Step 13: Accession K & assume that K is less than or equal to the number of branches and then go to step 2.

Step 14: End.

3.4.2 Assumption

Considering a single line diagram of radial distribution system. It has contained 12 nodes in it. With the help of this single line diagram we can find out voltages and currents values in each node.

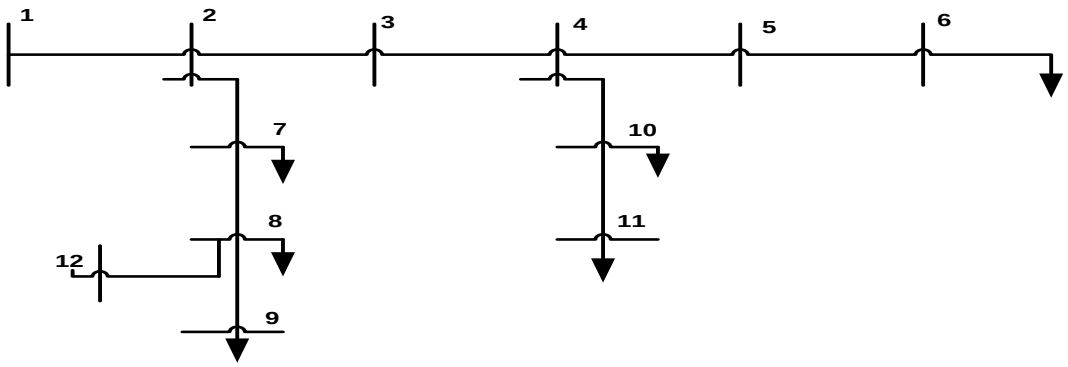

Fig 3.3 Single-line radial distribution system diagram

3.4.3 Solution Methodology

Fig 3.3 Radial distribution system or feeder single line diagram. Below are the branch number that sends the node and receives the given node from this feeder. If consider branch 1 then can write as the receiving end node voltage

$$V(2) = V(1) - I(1)Z(1) \tag{18}$$

Likewise, for the other branches,

$$V(3) = V(2) - I(2)Z(2) \tag{19}$$

And here V(1) is substation voltage which is known, and I(1) is known as well, with the help of these two values can calculate V(2) from equation 21.

If V(2) is known then can calculate V(3) in same manner with help to equation no. (22) and similarly we can calculate the voltages of node 4, 5 ,…….NB.

Hence the The generalized receiving and sending voltage equation, branch current and impedance

$$V(m_2) = V(m_1) - I(jj)Z(jj) \tag{20}$$

Where jj is the branch number.

$$m_2 = \text{IR(jj)} \tag{21}$$

$$m_1 = IS(jj) \tag{22}$$

Eq. (23) can be calculated for jj= 1, 2, ……..LN1(LN1=NB-1=no. of branches). Current over branch 1 is the sum of the load flows of all nodes except branch 1 plus the sum of the load currents of all nodes except branch 1, i.e

$$I(1) = \sum_{i=2}^{LN1} IL(i) + \sum_{i=2}^{LN1} IC(i) \tag{23}$$

The current over branch 2 is the sum of the load currents of all nodes except branch 2 plus the sum of the loading current of all nodes over branch 2, i.e

$$I(2) = IL(3) + IL(4) + IL(5) + IL(6) + IL(10) + IL(11) + IC(3) + IC(40 + IC(5) + IC(6) + IC(10) + IC(11) \tag{24}$$

Hence If nodes can be identified beyond all branches, all branch currents can be calculated. An algorithm is used to determine the nodes apart from all the branches.

The node's load current is,

$$IL(i) = \frac{PL(i) - jQL(i)}{V^*(i)} \quad i = 2,3 \ldots\ldots, NB \tag{25}$$

The charging current at node i is

$$IC(i) = y_0(i)V(i) \quad i = 2,3, \ldots\ldots NB \tag{26}$$

Iteratively calculated the load currents and charging currents. A flat voltage profile is assumed at the beginning and load current and load currents of all loads are calculated using equation 28 & 29. A detailed calculation of load flow is described earlier. The branch jj's real and reactive power loss is given by,

$$LP(jj) = |I(jj)^2|R(jj) \tag{27}$$

$$LQ(jj) = |I(jj)^2|R(jj) \tag{28}$$

3.5 Harmony search algorithm

The music act of spontaneity is a process of seeking a better agreement by trying different pitch mixes that should follow any of the three accompanying standards.

1. Play any pitch in the memory.

2. Playing the adjacent pitch from the memory.

3. Playing an uneven pitch within the imaginable spectrum or range.

In every factor determination of the HS calculation, this method is imitated. So, one of the three principles below should also be pursued:

- picking any an incentive from the HS memory;
- picking an adjoining an incentive from the HS memory;
- picking an irregular incentive from the conceivable esteem go.

The three principles in the HS calculation are adequately coordinated utilizing two fundamental parameters: concordance memory thinking about rate (HMCR) and pitch changing rate (PAR). Figure demonstrates the flowchart of the essential HS strategy, in which there are four main advances included.

Stage 1. Initiate the harmony memory. The underlying harmony memory comprises of a given number of haphazardly produced answers for the advancement issues under thought. A HM with the extent of HMS can be spoken to as pursues for a n-measurement issue:

$$\text{HM}=\begin{bmatrix} x_1^1 & \cdots & x_n^1 \\ \vdots & \ddots & \vdots \\ x_1^{hms} & \cdots & x_n^{hms} \end{bmatrix} \tag{29}$$

Where

$[x_1^i \quad x_2^i \ldots\ldots \quad x_n^i]$ (i= 1, 2, ... HMS) It's the candidate solution.

Harmony memory is usually set between 10 to 100 and even it depends on the size of given problem. To full utilization of the harmony memory members, a new solution method can used, named as S generation in HS method.

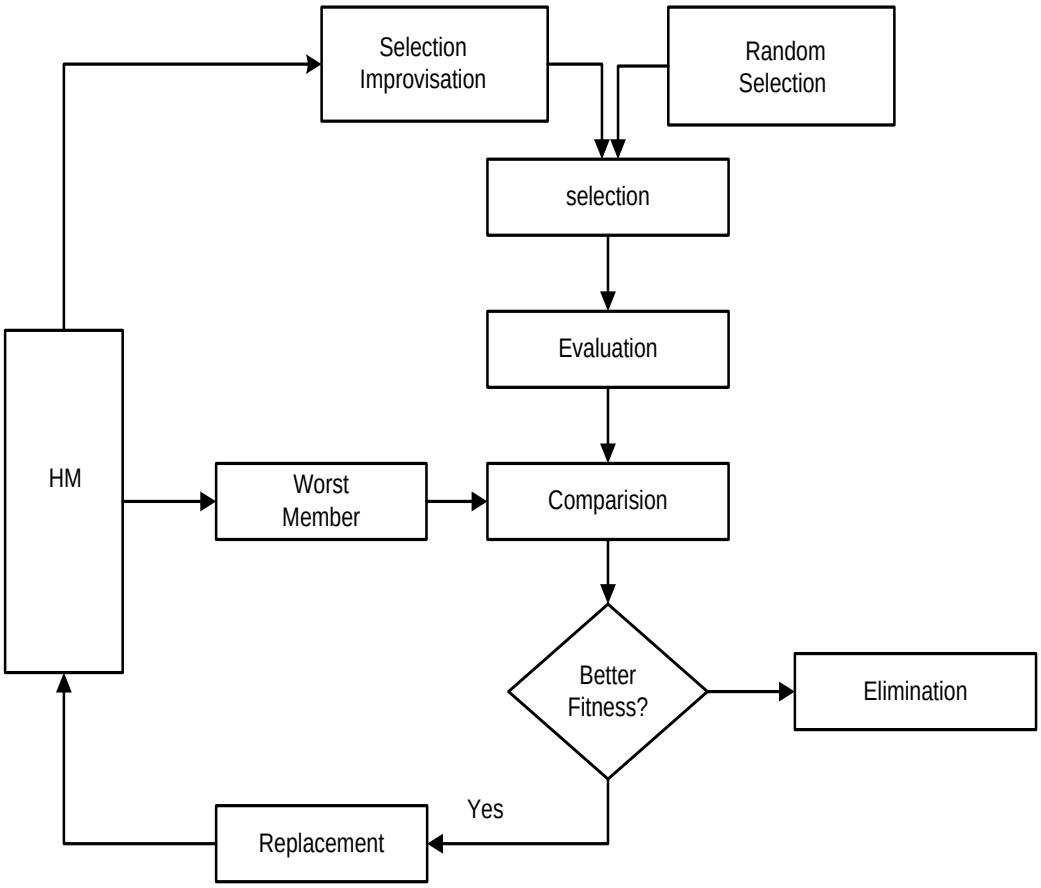

Fig 3.4 Flow chart of HSA

Stage 2. Improvising a new solution $(x_1' \quad x_2' \ldots . x_n')$ out of harmony memory. All components of this solution $x_j{}'$ is calculated based on HMCR. It is characterized as the possibility of choosing apart from the present HM individual and 1-HMCR is in this way possibility of producing it haphazardly. If originates from the HM, it is looked over the j^{th} measurement of an irregular HM part, and it very well may be additionally changed by the patch adjusting rate. It decides the possibililty of a hopeful from the HM to be changed. The GA makes crisp chromosomes utilizing just one (change) or two (basic hybrid) existing ones, while the age of new arrangements in the HS strategy utilizes all the HM individuals.

Stage 3. Revise or update the memory and updated arrangement from Step 2 is assessed. Off chance that it will yield a superior wellness than that of the most terrible part in the HM, it will supplant that one. Otherwise, it will be wiped out.

Stage 4. Repeat step 2 to step 3 until a current end model, e.g. the maximum number of emphases, is met. Obviously, the HMCR and PAR are two essential parameters in the HS

calculation, which control the part of the arrangements and even affect assembly speed. The previous is utilized to set the likelihood of using the notable data put away in the HM.

3.5.1 Harmony search algorithm parameter

An objective research is conducted to determine the impacts of distinct parameters of the HS algorithm on the quality of the solution and the convergence behaviour. 12 distinct cases are screened as Table 3.1 to demonstrate the effects of single parameter modifications. Each case is tested in three situations over 200 runs, and for all runs the highest amount of iterations is set at 250. In case 1, 2, and 3, respectively, HMCR, PAR, and HMS are diverse and two other parameters are constantly maintained.

Table 3.1 Results based on various HSA parameters for 33-bus system [42]

Scenario	**Parameters setting**			**Power loss(kW)**
	HMCR	PAR	HMS	
1	0.95	0.3	10	146.73
	0.73	0.3	10	142.11
	0.60	0.3	10	143.28
	0.30	0.3	10	153.60
2	0.85	0.3	10	139.55
	0.85	0.4	10	139.97
	0.85	0.5	10	140.40
	0.85	0.6	10	140.45
3	0.85	0.3	2	158.38
	0.85	0.3	15	147.96
	0.85	0.3	20	160.87
	0.85	0.3	30	162.67

Table 3.1 summarizes the complete energy loss for 33-bus allocation by varying the parameters. The HMCR determines the frequency of selecting one of the historical values stored in the HM. The bigger the HMCR, the less exploration is accomplished: the algorithm depends further on stored values in HM, which could lead to the algorithm being stuck in a local optimum. On the other hand, choosing the HMCR too tiny reduces the efficiency of the algorithm and the HS algorithm acts as a pure random search with less historical memory help. As shown in Table 3.1, big and low HMCR values lead to a reduction in the quality of the solution. Large and tiny HMS values reduce harmony memory efficiency as seen in Table IV. An HMS between N and 2N is appropriate for most issues. The algorithm is noted to have a low sensitivity to PAR values.

Harmony search has considered parameters which are:

- Harmony memory considering rate
- Pitch adjusting rate
- Band width

3.5.1.1 Harmony memory considering rate

It is known as the harmony memory consider rate and it is between 0 and 1 value. The decision variable value must be selected from the harmony memory. In this decision variable pays more attention to the algorithm to ensure that in less computational time, the find optima value is as much as it is. And the solutions later obtained are varied.

$$HMCR(t)= HMCR_{max} – ((HMCR_{max} – HMCR_{min}) *t)/ T_{max} \quad (30)$$

Where, t = Number of iterations specified

T_{max} = The number of iterations is maximum

$HMCR_{max}$ and $HMCR_{min}$ = Both are HMCR maximum and minimum.

3.5.1.2 Pitch adjusting rate

In HSA, the pitch adjustment rate controls local search as it claims that PAR can effectively prevent the search from being trapped in the best possible location. In general, in the initial search step, smaller PAR is beneficial in approaching the local optimal solution. If the greater value of PAR is compatible in the later steps to spring the optimal local out.

$$PAR(t) = ((PAR_{max} – PAR_{min}) / (\pi/2))* \arctan t + PAR_{min} \quad (31)$$

Where, PAR(t)= Specifies the rate of adjustment for the t^{th} generation

PAR_{max} and PAR_{min} = Maximum and minimum pitch adjustment rates.

3.5.1.6 Band width

The suitable BW may be helpful for adjusting the algorithm convergence rate to the optimal solution. Bandwidth changes in dynamical form with the following generation number as expressed:

$$BW(t)= BW_{max} – ((BW_{max} - BW_{min})/ T_{max})*I \quad (32)$$

Where, BW(t)= BW rate for t^{th} generation and BW_{max}, BW_{min} are the maximum and minimum bandwidth under consideration.

3.6 Conclusion

In this chapter, the mathematical formulation of various energy efficiency different parameters like node voltages, loadability index is presented for radial network/system nodes beyond particular node have been identified. An efficient load flow method, based on backward/forward sweep, is presented and fundamental of HSA are discuss for form.

Chapter 4

Reconfiguration

4.1 Introduction

Energy circulation is conveying through the distribution system to consumer. In general, distribution feeders are in radial network which helps to reduce over current protection, although transmission lines are framing with the meshed network. When fault occurs in the line due to any reasons, it makes interruption to consumer, to bring back power immediately to load side, Maximum feeders are connected to adjacent feeders. The distribution scheme should be economical with regard to the different limitations.

- Configuration in radial pattern
- Supply in entire load
- Coordinated over existing protective equipment
- Cables, transformers and other devices are within their current capacity's limits
- Magnitude of the voltage should be limited

Loads are varying with daytime, weekday, and year period. Each load type has an alternating time profile and each feeder provides a unique load mixture. The load layout of each feeder is therefore constantly fluctuating, as if each feeder had a unique load variety. This creates a convenience to keep losses to a minimum during the day to reconfigure the feeders. In order to accomplish this distribution automation, switches and control systems could be implemented at a price that must be adapted against loss compensation. Since there would be 10 decades of switches in the distribution scheme, the inquiry of the switches could certainly take too long. Similarly, it takes more computing time to test and apply the limitations and impeded the use of traditional optimization techniques. Anyhow, system economy boosts productively as the number of switches also boosts, so investigating big systems is important.

Reconfiguration of the RDS automation allowance and such an agreement could be beneficially used to improve execution. One of the main execution estimates that could be enhanced among some others is the MVA edge or margin to the point of ultimate loadability. To achieve this goal, two issues need to be addressed, namely the estimation of accurate proximity to the highest loadability. Loadability point and an optimal reconfiguration scheme to reconfigure the network to maximize loadability.

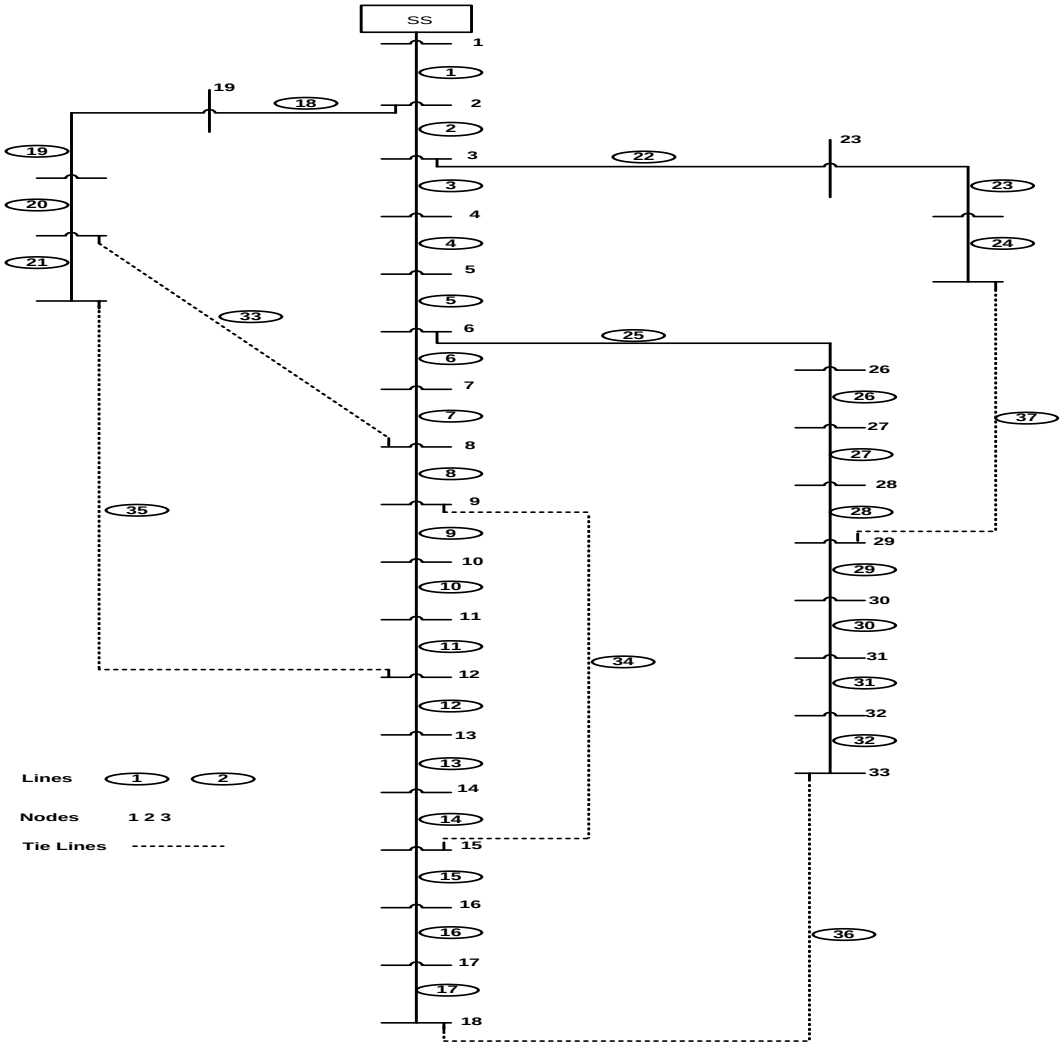

Fig 4.1 IEEE 33-node radial distribution system with reconfiguration

4.2 Algorithm

The following algorithm for the proposed network reconfiguration is given below to maximize MVA load at the minimum MLI node.

Step1: Read the line and load data.

Step2: Set the HSA parameter.

Step3: Initialize the HM.

Step4: Generate solution vector for HM.

Step5: Improvise the HM using

i. Random search
ii. Harmony memory consideration rate

iii. Pitch rate adjustment

Step6: Compare the new harmony with existing harmony.

Step7: If new harmony is better than old harmony, update the solution vector, else discard.

Step8: Repeat the step 5-7 till maximum improvisation.

Step9: Print the best harmony and load flow result.

Step10: Stop

4.3 Flowchart

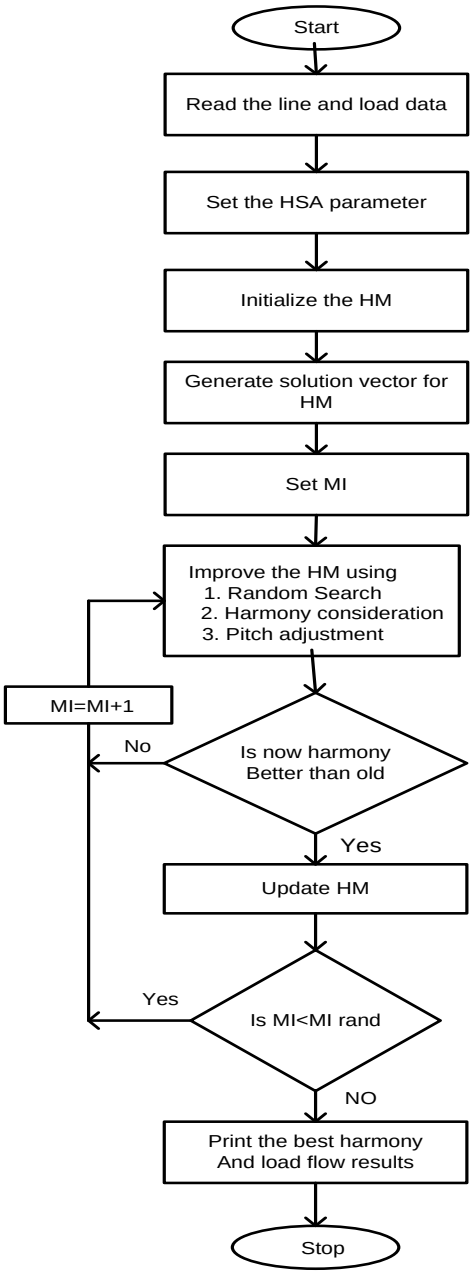

Fig 4.2 Flow chart for reconfiguration using HSA

4.4 Result and discussion

The base configuration of 33-node radial network is represented with tie-lines as 33, 34, 35, 36 and 37. The performance of the system under consideration is evaluated under three different load models. From the results it can be observed that the active and reactive power demand is different in different configuration under different load models. In the base configuration the active power demand is 3917kW whereas in optimal configuration it is found to be 3854.9kW for the same loading pattern. Similarly, in other case of other load models the difference in active, reactive and apparent power demand can be observed. In consequence of this, the voltage profile, loadability margin and the power loss in the same network configuration varies differently. Table 4.1 shows the test results for reconfiguration in base configuration under load model 1, 2 and 3. From the results it can be observed that the variation in different EEPD's in different. The power loss reduced from load model one to load model three is not uniform. Power loss reduction in LM-1,2, & 3 are 202.6647, 179.4494 and 161.0354kW respectively.

Table 4.1 EEP under different load models in base configuration

Parameters	**System performance under different load models**		
Load Model	**LM=1**	**LM=2**	**LM=3**
Configuration	33, 34, 35, 36, 37	33, 34, 35, 36, 37	33, 34, 35, 36, 37
$P_{FD,}$ (kW)	3917.1	3742.0	3740.0
$Q_{FD,}$ (kVAr)	2434.9	2314.0	1997.6
$S_{FC,}$ (kVA)	4612.2	4399.7	4240.0
Vi, (min)	0.9131	0.9187	0.9229
F_{si}	84.06	88.11	91.29
$P_{L,}$ (kW)	202.66	179.44	161.03
CT (sec)	0.1788	0.0375	0.0449

Table 4.2 shows the test results for reconfiguration in optimal configuration under load model 1, 2 and 3. From the results it can be observed that the variation in different EEPD's in different. The power loss reduced as significantly whereas the reduction loss from load model one to load model three is not uniform. Power loss reduction in LM-1,2, & 3 are 62.6851, 50.6816 and 42.0914 respectively.

Table 4.2 EEP under different load models in optimal configuration

Parameters	**System performance under different load models**		
Load models	**LM=1**	**LM=2**	**LM=3**
Configurations	7,14,9,32,28	7,14,9,32,37	7,14,9,32,37
P_{FD}, (kW)	3854.9	3732.0	3733.0
Q_{FD}, (kVAr)	2404.9	2316.4	2073.6
S_{FC}, (kVA)	4543.5	4392.5	4270.3
Vi, (min)	0.9413	0.9407	0.9440
F_{si}	85.34	88.26	90.66
P_L, (kW)	139.97	128.76	118.94
CT, (sec)	0.8023	0.5070	0.5853

Fig 4.3 to 4.5 show the convergence characteristics of the 33-node system under different load models while reconfiguration of network topology. Here, it can be noticed that the convergence has occurred in different number of iterations. The program is run for 250 iterations and the 5 runs. The computational time is evaluated from the average of the time taken to converge in each run. From Fig 4.3 it can be noticed that the convergence rate is slow as compared to the convergence rate in Fig 4.5.

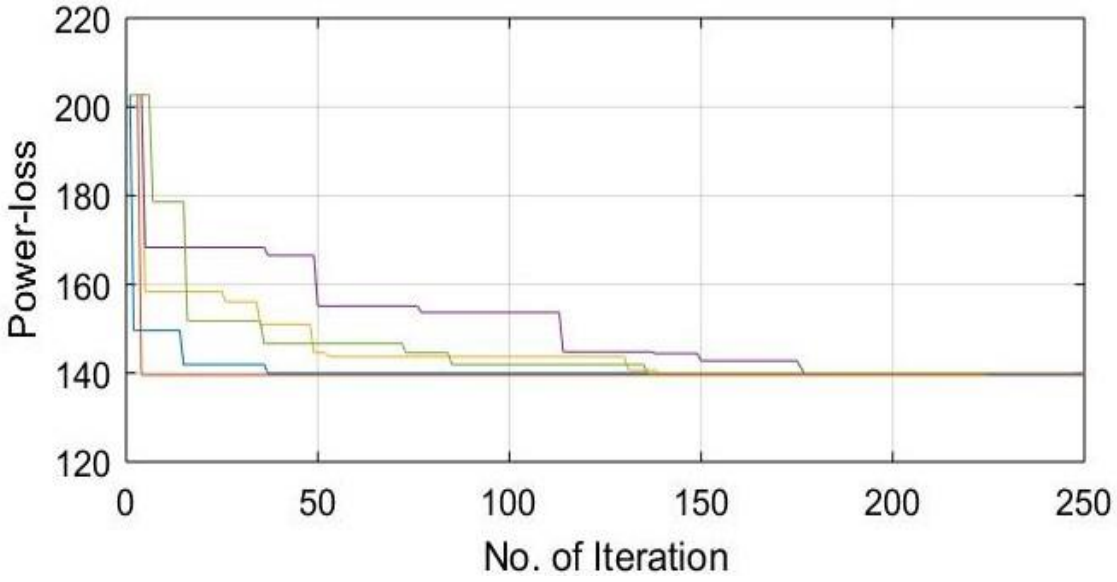

Fig 4.3 Convergence characteristic of optimal configuration under LM-1

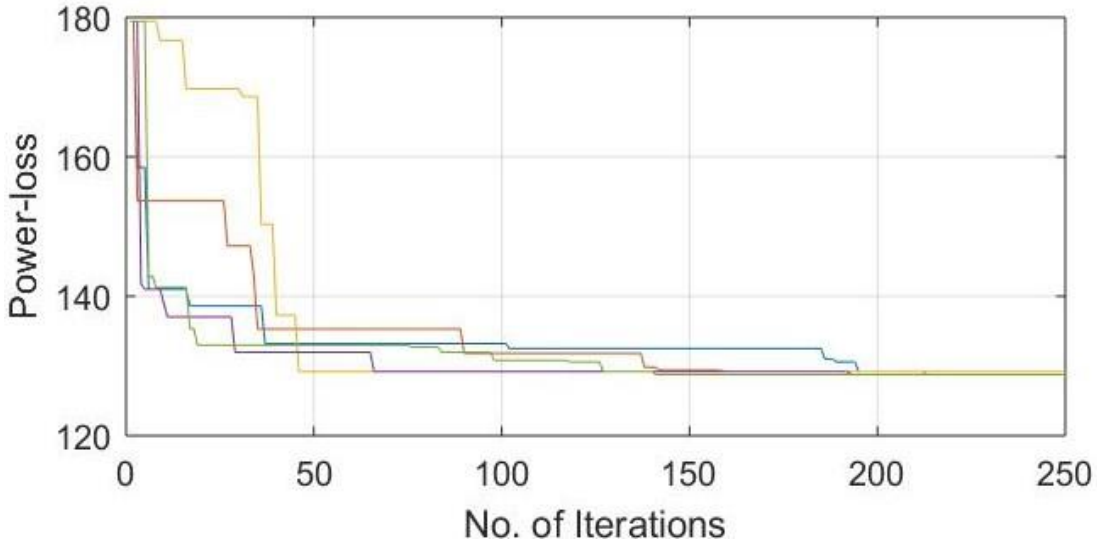

Fig 4.4 Convergence characteristic of optimal configuration under LM-2

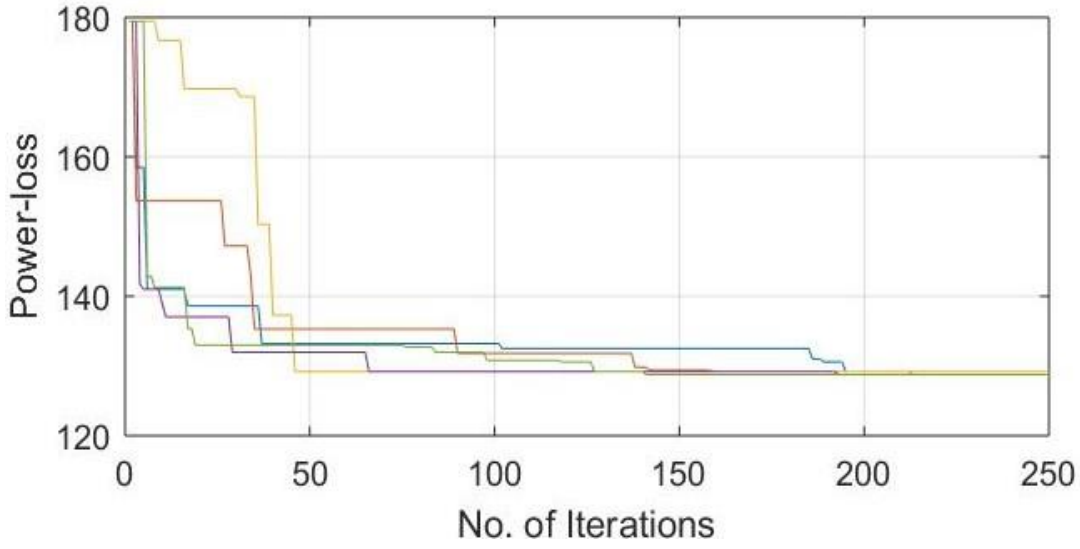

Fig 4.5 Convergence characteristic of optimal configuration under LM-3

4.5 Conclusion

This chapter presented the network reconfiguration of distribution system. Due to reconfiguration of network, power losses of distribution system can be minimized and with the minimization of power loss, voltage profile has improved. The proposed approach is also examined for distinct load models and the variation in different parameters have been observed. This variation is highly dependent on the level of voltage and proximity to the source node. Further, the convergence of algorithm found different under load model.

Chapter 5

Distributed Generation Allocation

5.1 Introduction

The design of the electrical device within the presence of distribution generation (DG) requires the definition of several factors, such as: the satisfactory technology to be used, the wide range and potential of the gadgets, the notable area, the type of network connection and many others. DG placement in the distribution system, leave the huge change in operating characteristics to makes the system more effective and efficient compared to the previous or without DG with respect to the voltage losses, voltage profile, stability, and reliability as well. There is some major issue with DG placement with respect to the size and location.it must be in appropriate manner otherwise placement of DG at non-optimal site increases the losses and that is why cost will also increase, therefore awareness of the site and size of DG is important.

5.2. Advantages of DG placement

There are several advantages of the DG placement in the distribution system.

- Load-centres being far-off to the substations, energy dissipation induced in the system. With the placement of the DG's in the system, this problem can reduce but the DG's must be near to the end-consumer or energy utility side which makes huge difference to the system stability.
- Placement of the DG in the system, helps the consumer to the dependency of the grid, so that system become more reliable.
- As DG's are placing at the appropriate site of the system, it reduces the losses and improving the voltage profile of the system as well. Hence the losses are reducing, and system becomes more efficient.
- With the increasing efficiency of the system, system become some economical to the end-consumer. Therefore, entire cost decreases and system become more reliable.

This thesis provides a DG positioning approach for improving the radial distribution system's node voltage profile and power losses using HSA. The elements to minimize the loss of active power within the voltage profile limit.

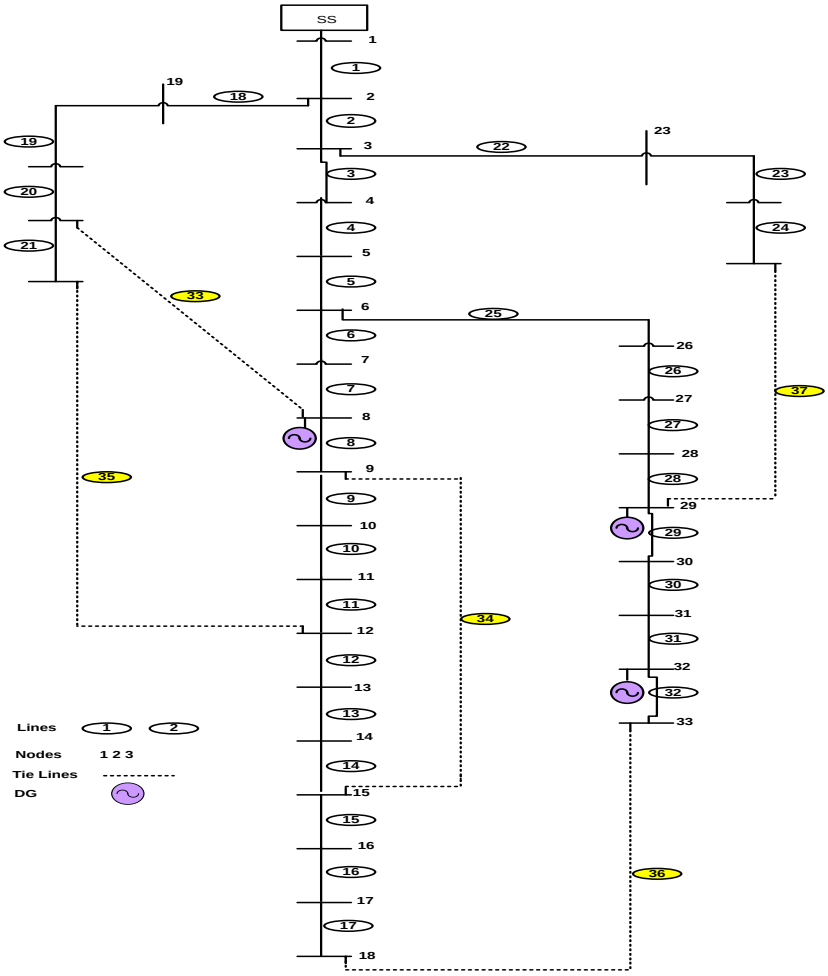

Fig 5.1 IEEE 33-node radial distribution system with DG placement

5.3. Algorithm

Step1: Read the line and load data.

Step2: Set the HSA parameters.

Step3: Generate solution vectors for

i. DG location

ii. DG size

Step4: Initialize the HM with discrete and continuous solution vector

i. Discrete vector: DG location

ii. Continuous vector: DG size

Step5: Improvise the HM based on HSA rules.

Step6: Compare the new harmony with existing harmony.

Step7: If new harmony is better than old harmony, update the solution vector, else discard.

Step8: Repeat the step 5-7 till maximum improvisation.

Step9: Print the best harmony and load flow result.

Step10: Stop.

5.4. Flowchart

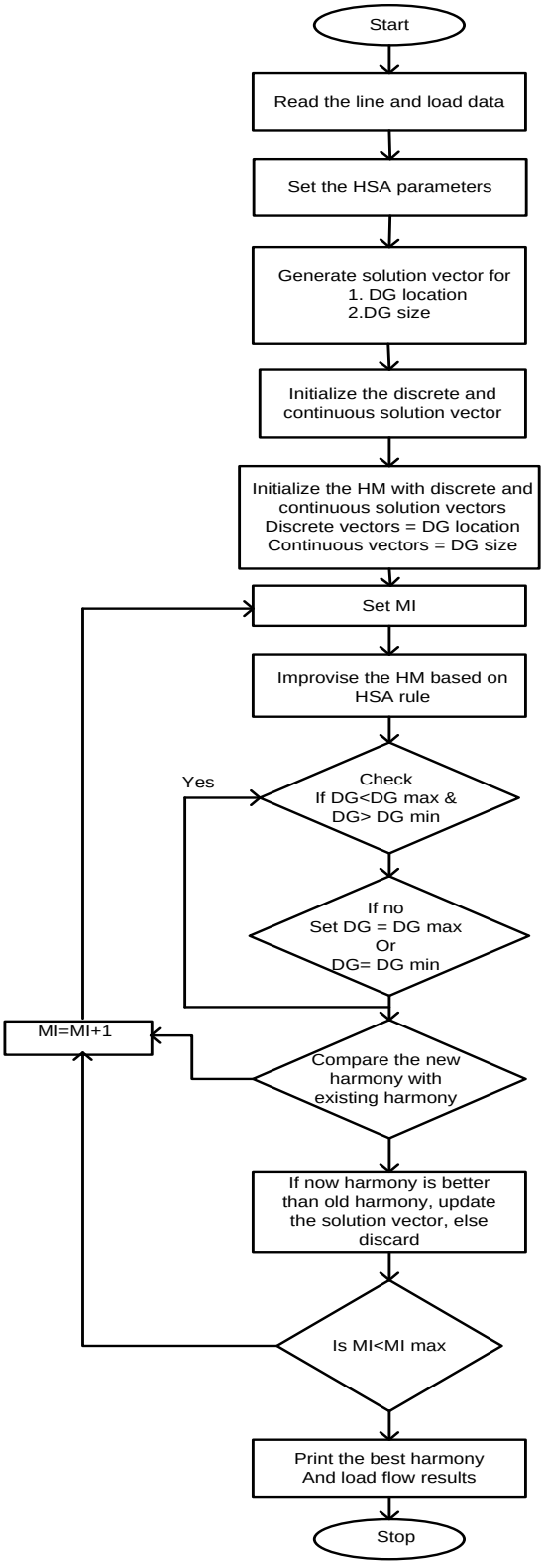

Fig 5.2 Flow chart for DG allocation using HAS

5.5. Results and discussions

In the DG allocation result and discussion, different load models along with variation of DG's and fixed size, location are discussed below:

5.5.1 Result and discussion for DG allocation in base configuration under LM-1

Table 5.1 shows the test result for DG allocation in the base configuration under load model 1. The DG allocation is performed for single and multi-placement. From the result it can be observed that the variation in various EEDPs is different and optimal DG allocation found to be at different nodes. This is due to the fact that the optimal DG size and location is highly dependent on the system loading pattern and the node voltage profile.

Table 5.1 EEP after DG allocation in base configuration under LM-1

Parameters	**System performance under LM-1**		
No. of DG	**DG=1**	**DG=2**	**DG=3**
Configuration	33, 34, 35, 36, 37	33, 34, 35, 36, 37	33, 34, 35, 36, 37
P_{FD} (kW)	3296.2	2015.1	1443.1
Q_{FD} (kVAr)	2382.3	2359.8	2350.5
S_{FC} (kVA)	4067	3103.1	2758.2
Vi, min	0.9475	0.9590	0.9730
f_{si}	95.68	116.28	149.2277
P_L (kW)	108.74	86.6	68.185
CT (sec)	0.1103	0.0776	0.2984
DG Locations (Node)	30	21, 28	9, 26, 30
DG sizes (kW)	527.5	950, 831	860, 822.1, 657.9

The power loss has reduced significantly whereas, the reduction in loss from single DG allocation to the multi DG allocation is not uniform rather with the increment in DG size the overall reduction in loss is 31.23kW, 53.37kW and 71.18kW when DG size is 527.5kW, 1781kW and 2340kW respectively.

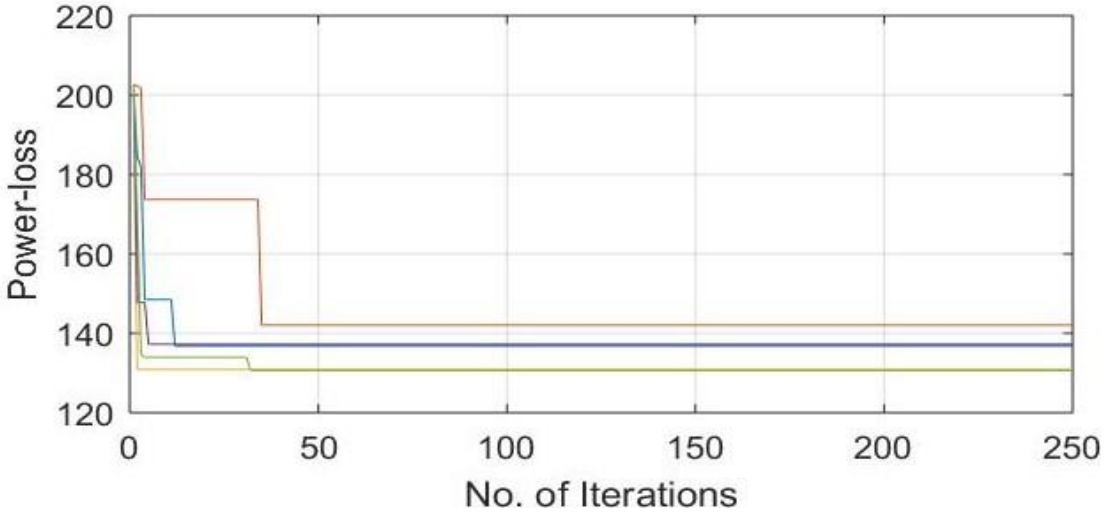

Fig 5.3 Convergence characteristic of base configuration under LM-1 with 1-DG

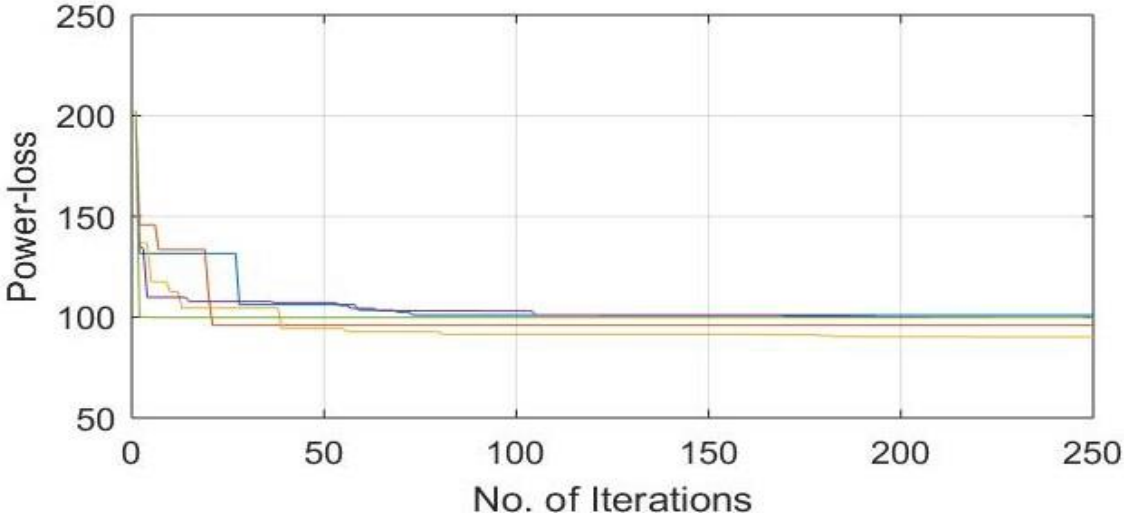

Fig 5.4 Convergence characteristic of base configuration under LM-1 with 2-DG

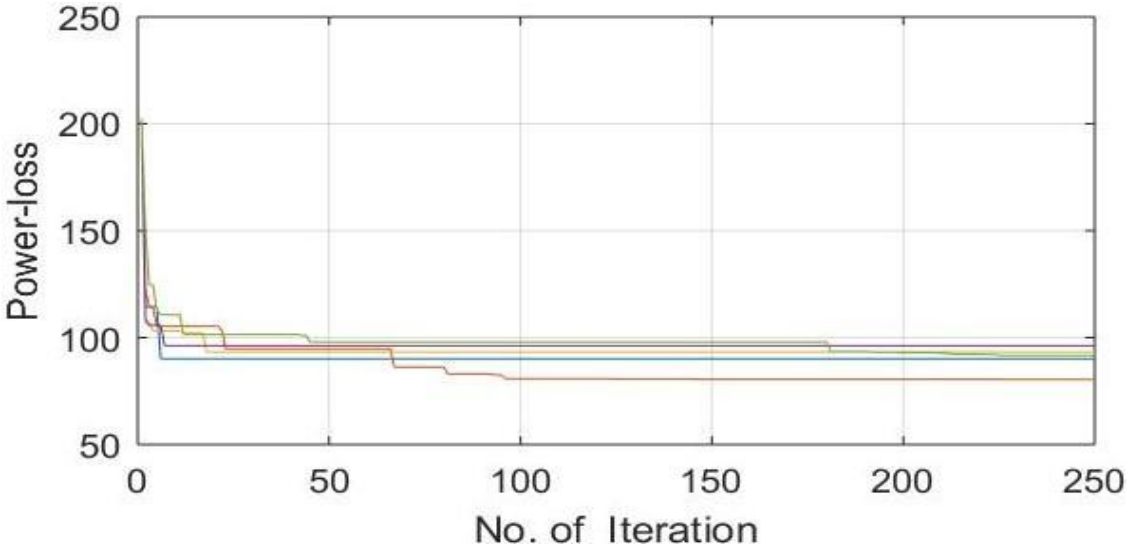

Fig 5.5 Convergence characteristic of base configuration under LM-1 with 3-DG

Fig 5.3 to 5.5 show the convergence characteristics of the 33-node system under different load models with single and multiple DG allocation while reconfiguration of network topology. Here, it can be noticed that the convergence has occurred in different number of iterations. The program is run for 250 iterations and the 5 runs. The computational time is evaluated from the average of the time taken to converge in each run. From Fig 5.3-5.5 it can be observed that the convergence rate is slow in Fig 5.3 as compared to the convergence rate in Fig 5.4 and 5.5.

5.5.2 Result and discussion for DG allocation in optimal configuration under LM-1

Table 5.2 shows the test result for DG allocation in the base configuration under load model 1. The DG allocation is performed for single and multi-placement. From the result it can be observed that the variation in various EEDPs is different and optimal DG allocation found to be at different nodes. This is due to the fact that the optimal DG size and location is highly dependent on the system loading pattern and the node voltage profile.

The power loss has reduced significantly whereas, the reduction in loss from single DG allocation to the multi DG allocation is not uniform rather with the increment in DG size the overall reduction in loss is 39.76kW, 81.31kW and 67.79kW when DG size is 885.9kW, 1700.2kW and 1481.5kW respectively.

Table 5.2 EEP after DG allocation in optimal configuration under LM-1

Parameters	**System performance under LM-1**		
No. of DG	**DG=1**	**DG=2**	**DG=3**
Configuration	7,9,14,32,37	7,9,14,28,32,	7,9,14,32,37
P_{FD} (kW)	2929.2	2100.4	1040.8
Q_{FD} (kVAr)	2377.2	2362.9	2355.2
S_{FC} (kVA)	3772.5	3161.5	2574.9
Vi, min	0.9477	0.9617	0.9597
f_{si}	103.64	126.54	168.77
P_L (kW)	100.21	85.65	72.18
CT (sec)	0.0815	0.1188	0.2949
DG Locations (Node)	29	30, 11	23, 16, 27
DG sizes (kW)	885.9	718.1, 982.1	419.2, 408.6, 653.7

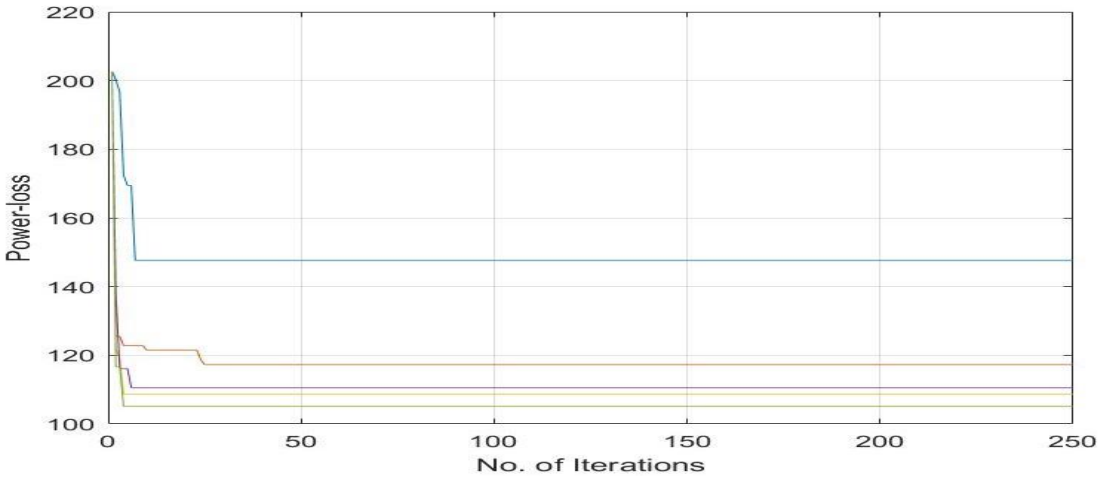

Fig 5.6 Convergence characteristic of optimal configuration under LM-1 with 1-DG

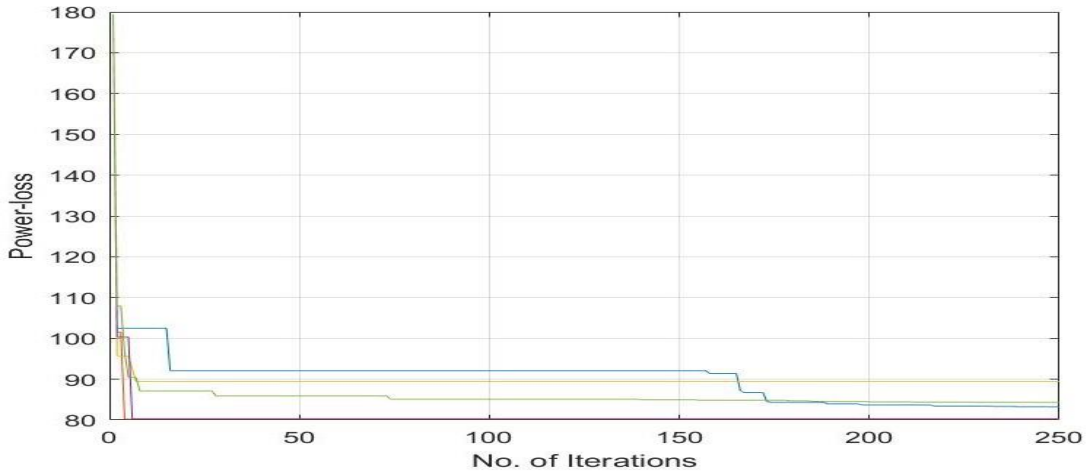

Fig 5.7 Convergence characteristic of optimal configuration under LM-1 with 2-DG

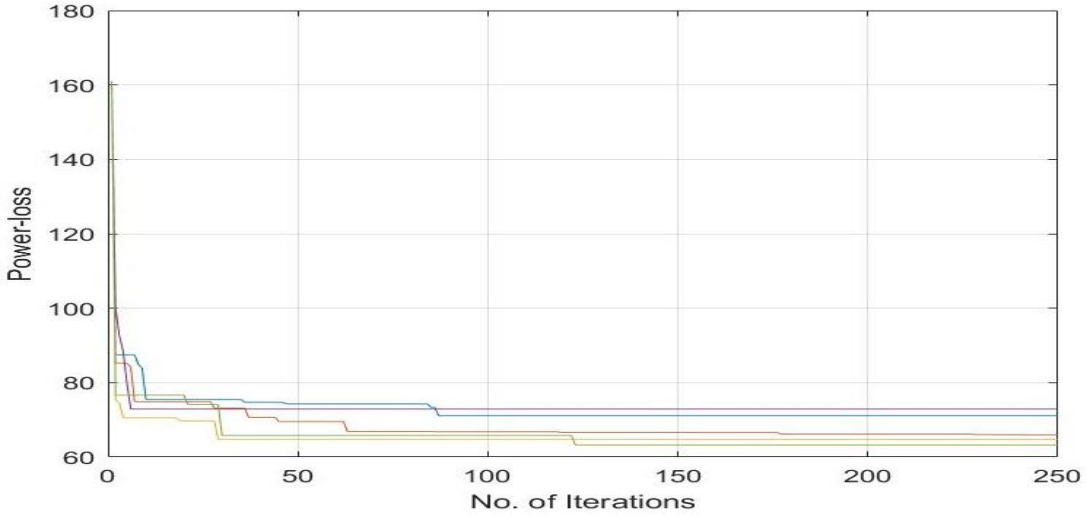

Fig 5.8 Convergence characteristic of optimal configuration under LM-1 with 3-DG

Fig 5.6 to 5.8 show the convergence characteristics of the 33-node system under different load models with single and multiple DG allocation while reconfiguration of network topology. Here, it can be noticed that the convergence has occurred in different number of iterations. The program is run for 250 iterations and the 5 runs. The computational time is evaluated from the average of the time taken to converge in each run. From Fig 5.6-5.8 it can be observed that the convergence rate is slow in Fig 5.8 as compared to the convergence rate in Fig 5.7 and 5.6

5.5.3 Result and discussion for DG allocation in base configuration under LM-2

Table 5.3 shows the test result for DG allocation in the base configuration under load model 2. The DG allocation is performed for single and multi-placement. From the result it can be observed that the variation in various EEDPs is different and optimal DG allocation found to be at different nodes. This is since the optimal DG size and location is highly dependent on the system loading pattern and the node voltage profile.

Table 5.3 EEP after DG allocation in base configuration under LM-2

Parameters	**System performance under LM-2**		
No. of DG	**DG=1**	**DG=2**	**DG=3**
Configuration	33, 34, 35, 36, 37	33, 34, 35, 36, 37	33, 34, 35, 36, 37
P_{FD} (kW)	3043.8	2360.4	1544.0
Q_{FD} (kVAr)	2303.2	2305.3	2307.0
S_{FC} (kVA)	3817.0	3299.7	2776.4
Vi, min	0.9282	0.9407	0.9692
f_{si}	102.11	119.84	148.48
P_L (kW)	136.84	109.83	76.78
CT (sec)	0.4517	0.6319	0.4122
DG Locations (Node)	27	11, 14	32, 7, 18
DG sizes (kW)	677.2	701.0, 671.8	781.4, 991.2, 407.2

The power loss has reduced significantly whereas, the reduction in loss from single DG allocation to the multi DG allocation is not uniform rather with the increment in DG size the overall reduction in loss is 8.08kW, 18.63kW and 51.98kW when DG size is 677.2kW, 1372.8kW and 2179.8kW respectively.

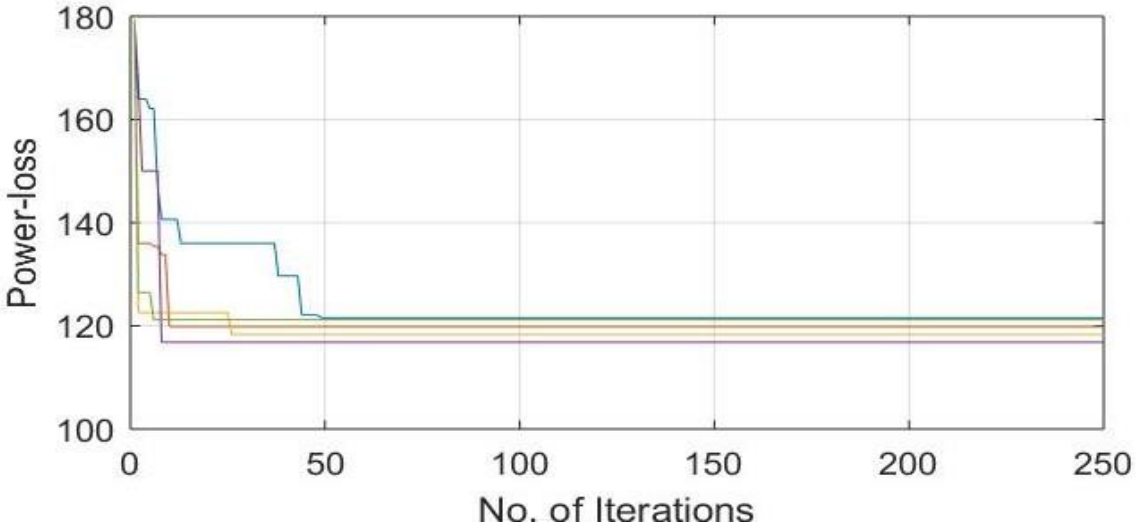

Fig 5.9 Convergence characteristic of base configuration under LM-2 with 1-DG

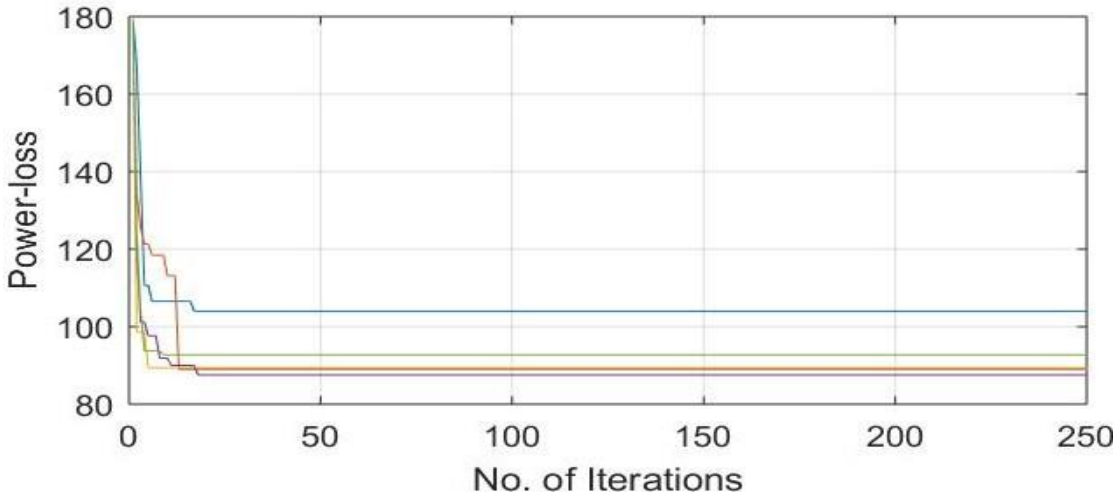

Fig 5.10 Convergence characteristic of base configuration under LM-2 with 2-DG

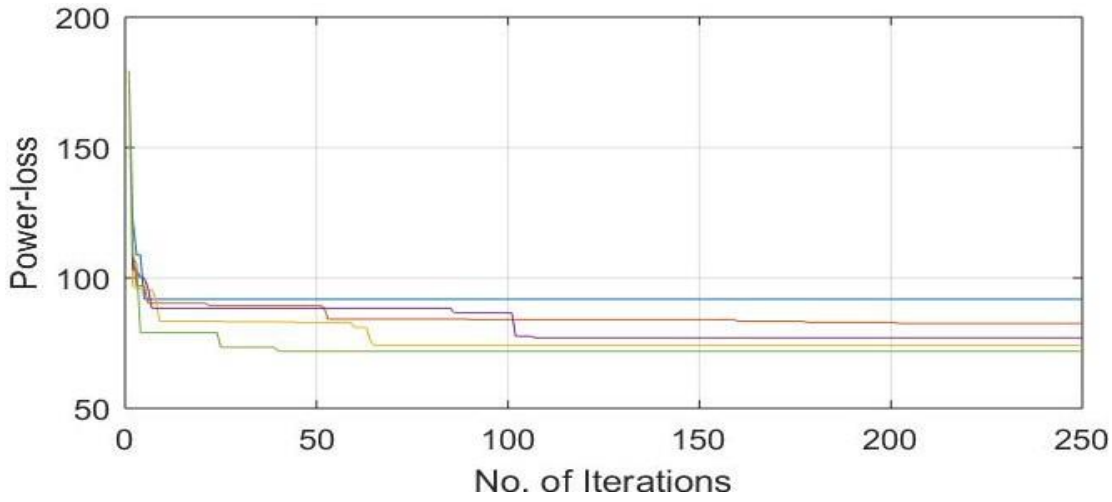

Fig 5.11 Convergence characteristic of base configuration under LM-2 with 3-DG

Fig 5.9 to 5.11 show the convergence characteristics of the 33-node system under different load models while reconfiguration of network topology. Here, it can be noticed that the convergence has occurred in different number of iterations. The program is run for 250 iterations and the 5 runs. The computational time is evaluated from the average of the time taken to converge in each run. From Fig 5.9-5.11 it can be observed that the convergence rate if slow as compared to the convergence rate in Fig 5.10 as compared to the convergence rate in Fig 5.9 and 5.11

5.5.4 Result and discussion for DG allocation in optimal configuration under LM-2

Table 5.4 shows the test result for DG allocation in the base configuration under load model 2. The DG allocation is performed for single and multi-placement. From the result it can be observed that the variation in various EEDPs is different and optimal DG allocation found to be at different nodes. This is due to the fact that the optimal DG size and location is highly dependent on the system loading pattern and the node voltage profile.

The power loss has reduced significantly whereas, the reduction in loss from single DG allocation to the multi DG allocation is not uniform rather with the increment in DG size the overall reduction in loss is 27kW, 38.15kW and 56.71kW when DG size is 545.4kW, 920.6kW and 1481.5kW respectively.

Table 5.4 EEP after fixed size DG allocation in optimal configuration under LM-2

Parameters	**System performance under LM-2**		
No. of DG	**DG=1**	**DG=2**	**DG=3**
Configuration	7,9,14,32,37	7,9,14,28,32,	7,9,14,32,37
P_{FD} (kW)	3175.2	2797.2	2234.1
Q_{FD} (kVAr)	2313.2	2308.4	2304.6
S_{FC} (kVA)	3928.4	3623.5	3209.7
Vi, min	0.9495	0.9558	0.9621
f_{si}	99.07	107.97	123.71
P_L (kW)	101.76	90.61	75.05
CT (sec)	0.1064	0.3441	0.2284
DG Locations (Node)	29	10, 32	6, 18, 28
DG sizes (kW)	545.4	557.8, 362.8	419.2, 408.6, 653.7

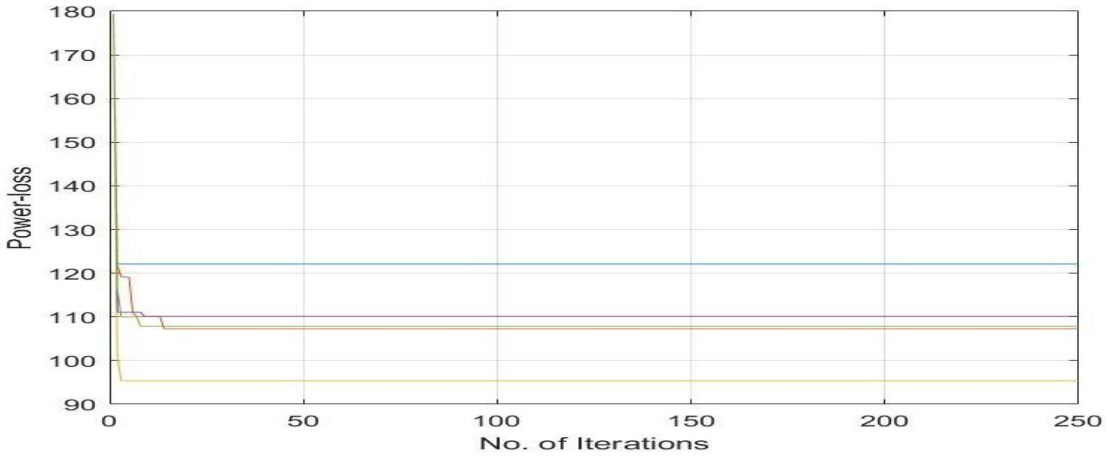

Fig 5.12 Convergence characteristic of optimal configuration under LM-2 with 1-DG

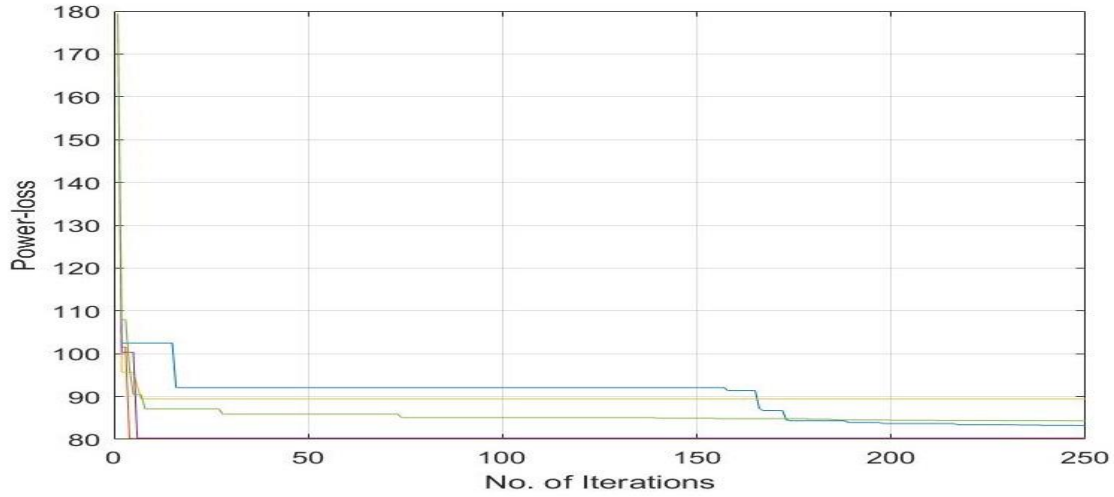

Fig 5.13 Convergence characteristic of optimal configuration under LM-2 with 2-DG

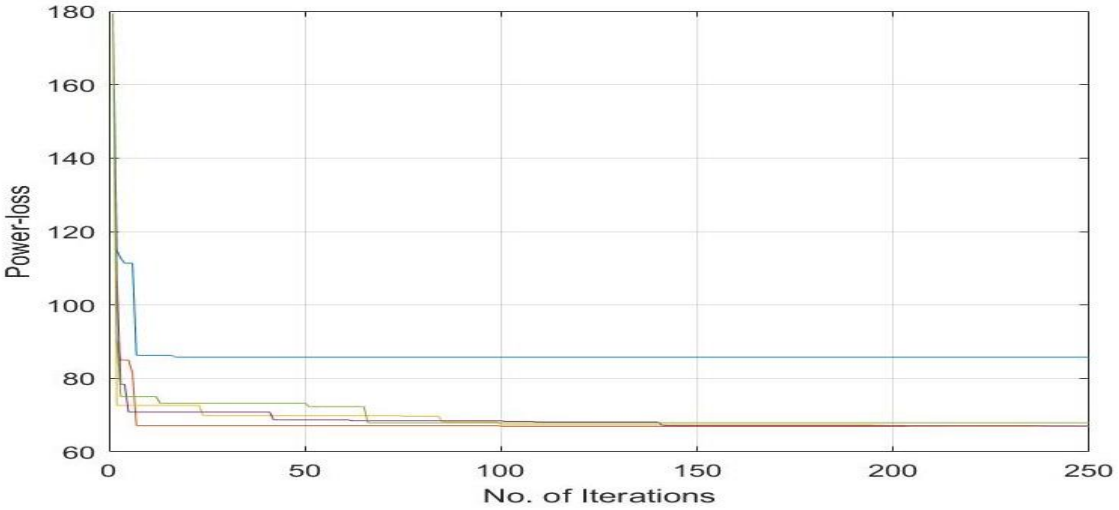

Fig 5.14 Convergence characteristic of optimal configuration under LM-2 with 3-DG

Fig 5.12 to 5.14 show the convergence characteristics of the 33-node system under different load models with single and multiple DG allocation while reconfiguration of network topology. Here, it can be noticed that the convergence has occurred in different number of iterations. The program is run for 250 iterations and the 5 runs. The computational time is evaluated from the average of the time taken to converge in each run. From Fig 5.12-5.14 it can be observed that the convergence rate is slow in Fig 5.12 as compared to the convergence rate in Fig 5.13 and 5.14

5.5.5 Result and discussion for DG allocation in base configuration under LM-3

Table 5.5 shows the test result for DG allocation in the base configuration under load model 3. The DG allocation is performed for single and multi-placement. From the result it can be observed that the variation in various EEDPs is different and optimal DG allocation found to be at different nodes. This is due to the fact that the optimal DG size and location is highly dependent on the system loading pattern and the node voltage profile.

The power loss has reduced significantly whereas, the reduction in loss from single DG allocation to the multi DG allocation is not uniform rather with the increment in DG size the overall reduction in loss is 8.77kW, 39.81kW and 49.22kW when DG size is 863.4kW, 1629.2kW and 2018.3kW respectively.

Table 5.5 EEP with DG Allocation in base configuration under LM-3

Parameters	**System performance under LM-3**		
No. of DG	**DG=1**	**DG=2**	**DG=3**
Configuration	33, 34, 35, 36, 37	33, 34, 35, 36, 37	33, 34, 35, 36, 37
P_{FD} (kW)	2860.1	2087.5	1705.0
Q_{FD} (kVAr)	2078.2	2123.1	2154.4
S_{FC} (kVA)	3535.4	2979.4	2747.5
Vi, min	0.9339	0.9514	0.9664
f_{si}	110.05	133.12	147.25
P_L (kW)	110.17	79.13	69.72
CT (sec)	0.3088	0.4133	0.6235
DG Locations (Node)	33	30, 9	29, 9, 14
DG sizes (kW)	863.4	996.3, 632.9	970.4, 542.3, 505.6

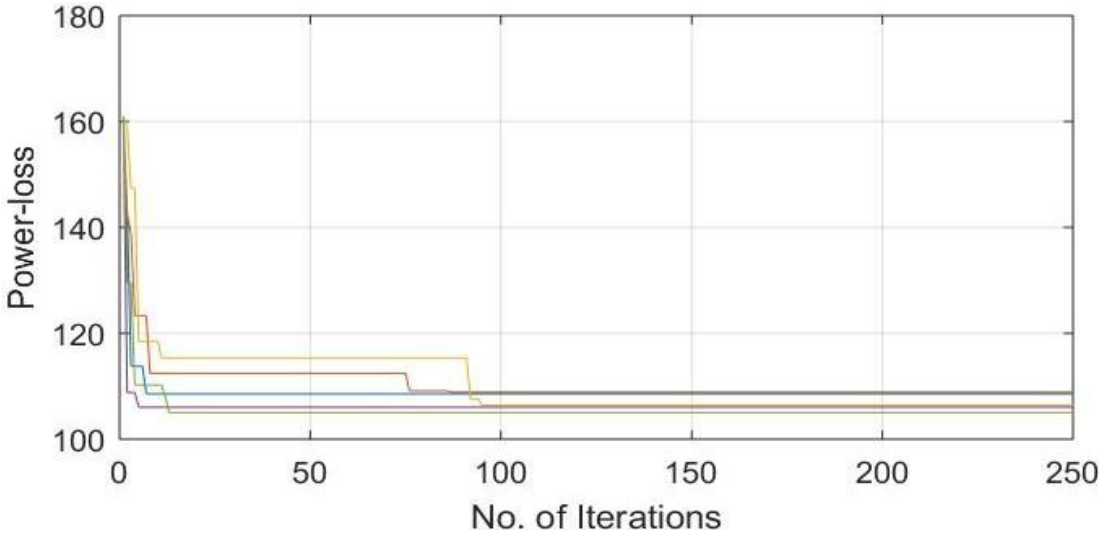

Fig 5.15 Convergence characteristic of base configuration under LM-3 with 1-DG

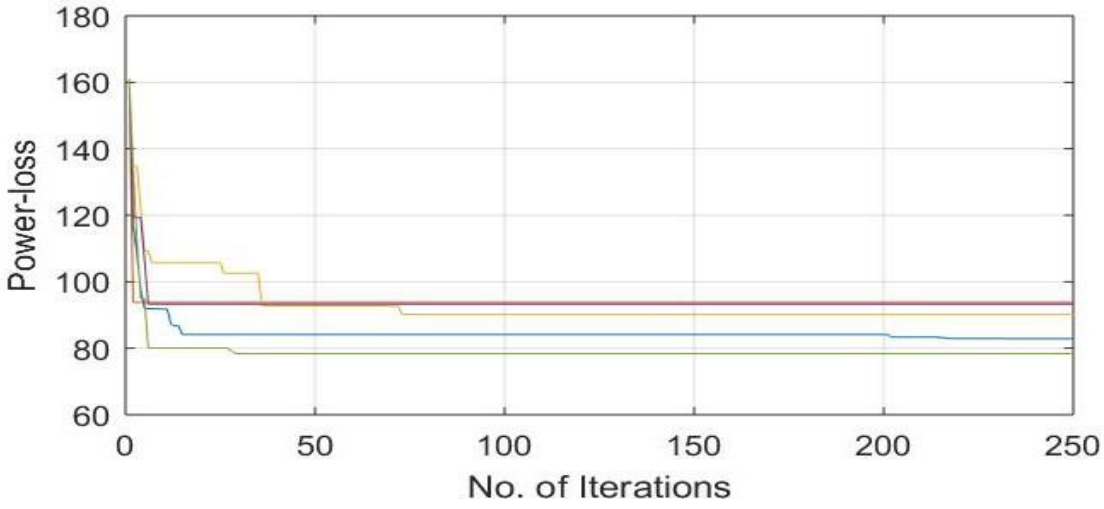

Fig 5.16 Convergence characteristic of base configuration under LM-3 with 2-DG

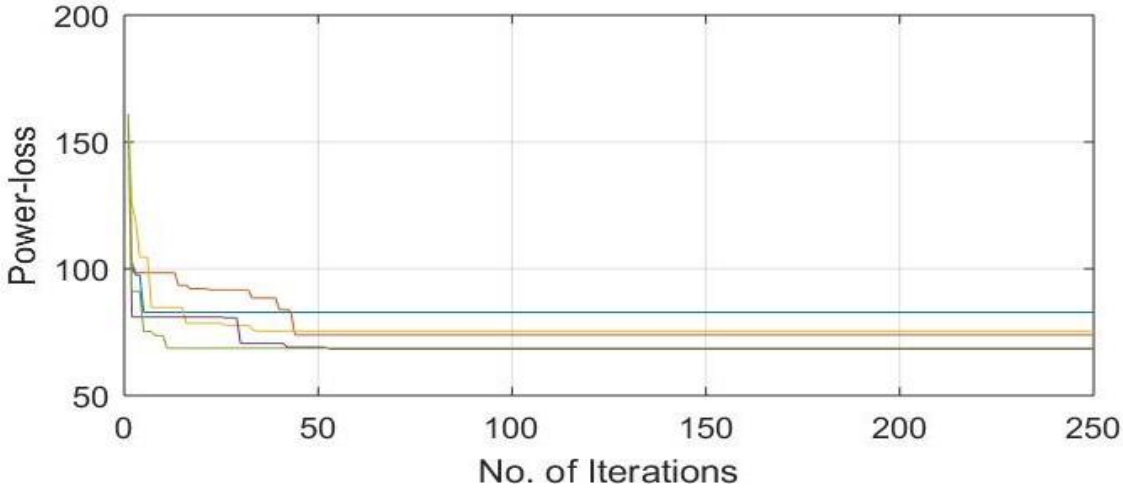

Fig 5.17 Convergence characteristic of base configuration under LM-3 with 3-DG

Fig 5.15 to 5.17 show the convergence characteristics of the 33-node system under different load models while reconfiguration of network topology. Here, it can be noticed that the convergence has occurred in different number of iterations. The program is run for 250 iterations and the 5 runs. The computational time is evaluated from the average of the time taken to converge in each run. From Fig 5.15-5.17 it can be observed that the convergence rate if slow as compared to the convergence rate in Fig 5.15 as compared to the convergence rate in Fig 5.16 and 5.17

5.5.6 Result and discussion for DG allocation in optimal configuration under LM-3

Table 5.6 shows the test result for DG allocation in the base configuration under load model 3. The DG allocation is performed for single and multi-placement. From the result it can be observed that the variation in various EEDPs is different and optimal DG allocation found to be at different nodes. This is due to the fact that the optimal DG size and location is highly dependent on the system loading pattern and the node voltage profile.

The power loss has reduced significantly whereas, the reduction in loss from single DG allocation to the multi DG allocation is not uniform rather with the increment in DG size the overall reduction in loss is 22.21kW, 37.55kW and 53.87kW when DG size is 628.3kW, 1275.1kW and 2130.3kW respectively.

Table 5.6 EEP with DG Allocation in optimal configuration under LM-3

Parameters	**System performance under LM-3**		
No. of DG	**DG=1**	**DG=2**	**DG=3**
Configuration	7,9,14,32,37	7,9,14,28,32,	7,9,14,32,37
P_{FD} (kW)	2099.3	2443.3	1593.1
Q_{FD} (kVAr)	2086.0	2097.1	2182.4
S_{FC} (kVA)	3735.9	3219.9	2702.0
Vi, min	0.9443	0.9473	0.960
f_{si}	103.91	122.17	151.04
P_L (kW)	96.73	81.38	65.07
CT (sec)	0.2457	0.1971	0.4712
DG Locations (Node)	15	15, 24	12, 7, 30
DG sizes (kW)	628.3	386.6, 888.5	680.2, 828.0, 622.1

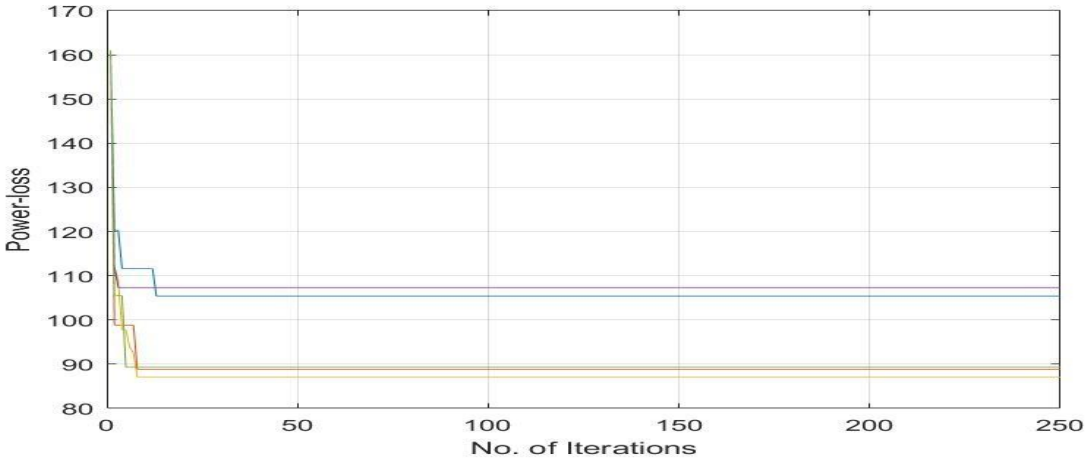

Fig 5.18 Convergence characteristic of optimal configuration under LM-3 with 1-DG

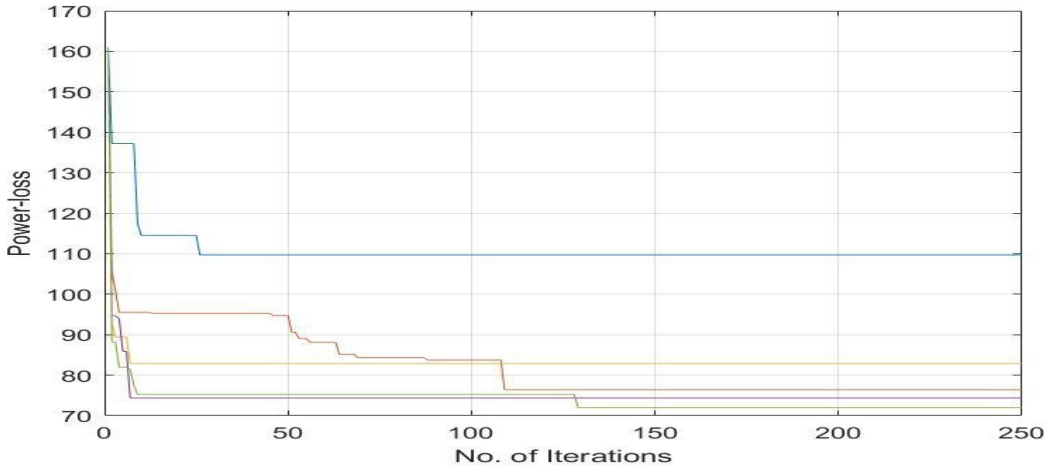

Fig 5.19 Convergence characteristic of optimal configuration under LM-3 with 2-DG

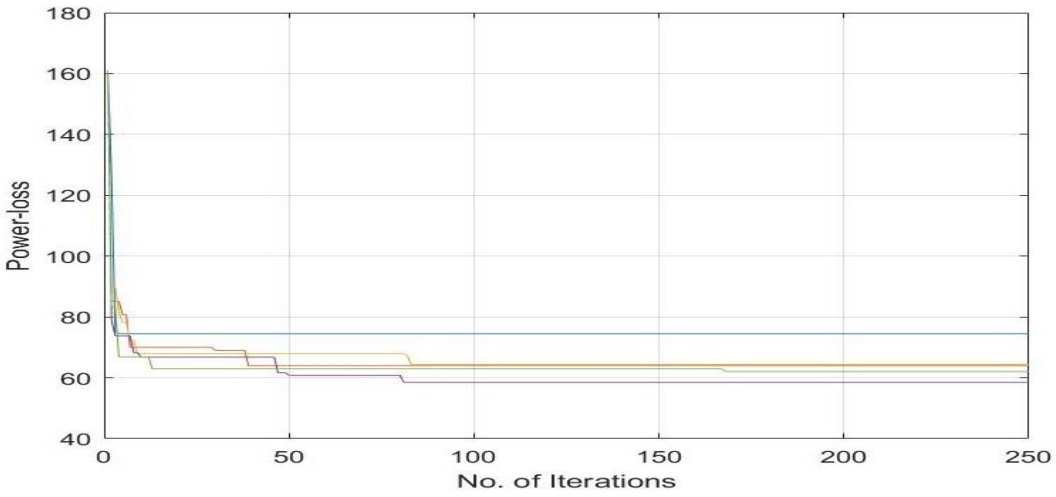

Fig 5.20 Convergence characteristic of optimal configuration under LM-3 with 3-DG

Fig 5.18 to 5.20 show the convergence characteristics of the 33-node system under different load models with single and multiple DG allocation while reconfiguration of network topology. Here, it can be noticed that the convergence has occurred in different number of iterations. The program is run for 250 iterations and the 5 runs. The computational time is evaluated from the average of the time taken to converge in each run. From Fig 5.18-5.20 it can be observed that the convergence rate is slow in Fig 5.18 as compared to the convergence rate in Fig 5.19 and 5.20

5.5.7 Result discussion for fixed DG size in optimal configuration under LM-1

Table 5.7 shows the test result for DG allocation in the base configuration under load model 1. The DG allocation is performed for single and multi-placement. From the result it can be observed that the variation in various EEDPs is different and optimal DG allocation found to be at different nodes. This is since the optimal DG size and location is highly dependent on the system loading pattern and the node voltage profile.

The power loss has reduced significantly whereas, the reduction in loss from single DG allocation to the multi DG allocation is not uniform rather with the increment in DG size the overall reduction in loss is 11.26kW, 28.41kW and 51.66kW when DG size is 500kW, 1000kW and 1500kW respectively.

Table 5.7 EEP after fixed size DG allocation in optimal configuration under LM-1

Parameters	**System performance under LM-1**		
No. of DG	**DG=1**	**DG=2**	**DG=3**
Configuration	7,9,14,32,37	7,9,14,28,32,	7,9,14,32,37
P_{FD} (kW)	3366.0	2767.8	2160.7
Q_{FD} (kVAr)	2399.9	2374.5	2358.9
S_{FC} (kVA)	4133.9	3646.8	3198.9
Vi, min	0.9245	0.9460	0.9528
f_{si}	94.09	107.52	124.73
P_L (kW)	151.23	111.56	88.31
CT (sec)	0.1950	0.0703	0.0499
DG Locations (Node)	13	31, 18	8, 14, 30
DG sizes (kW)	500	500, 500	500, 500, 500

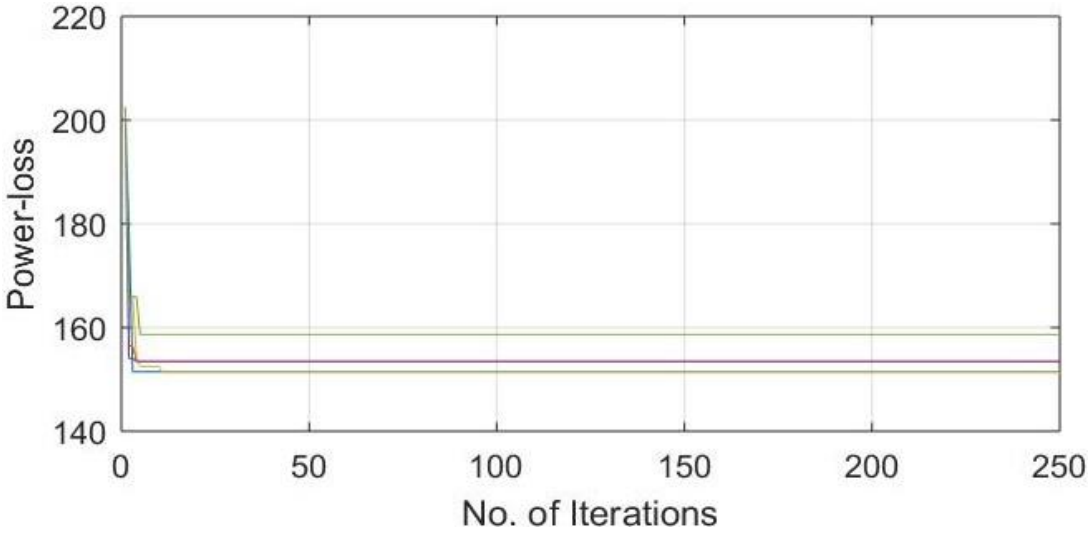

Fig 5.21 Convergence characteristic of optimal configuration under LM-1 with 1-DG

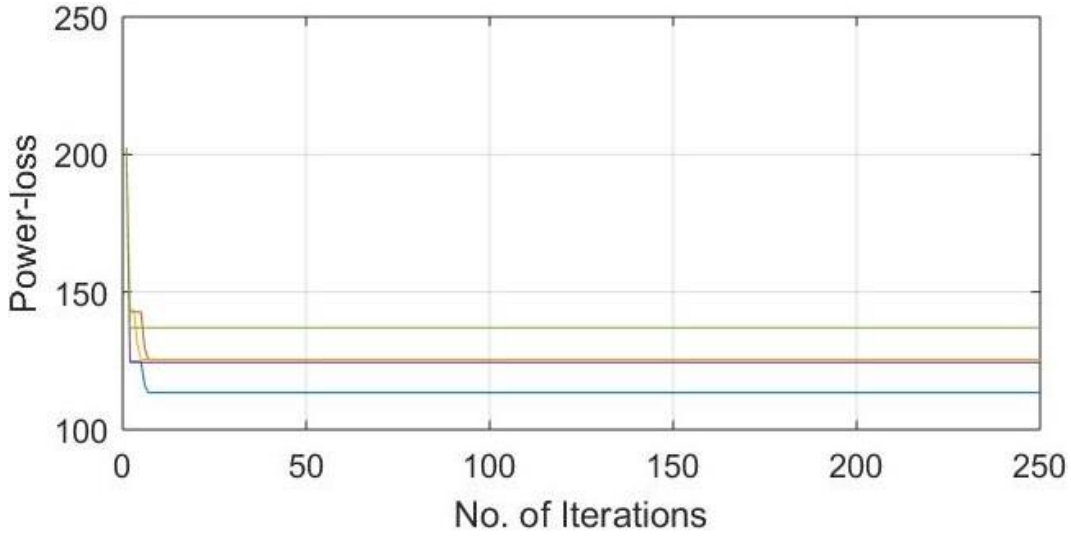

Fig 5.22 Convergence characteristic of optimal configuration under LM-1 with 2-DG

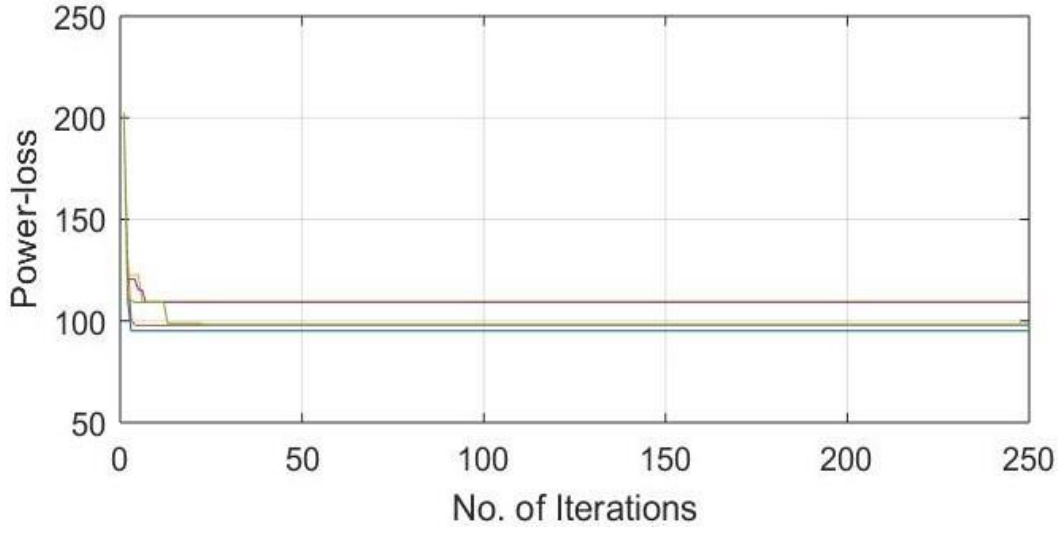

Fig 5.23 Convergence characteristic of optimal configuration under LM-1 with 3-DG

Fig 5.21 to 5.23 show the convergence characteristics of the 33-node system under different load models while reconfiguration of network topology. Here, it can be noticed that the convergence has occurred in different number of iterations. The program is run for 250 iterations and the 5 runs. The computational time is evaluated from the average of the time taken to converge in each run. From Fig 5.21-5.23 it can be observed that the convergence rate if slow as compared to the convergence rate in Fig 5.21 as compared to the convergence rate in Fig 5.22 and 5.23

5.5.8 Result discussion for fixed DG size in optimal configuration under LM-2

Table 5.8 shows the test result for DG allocation in the base configuration under load model 2. The DG allocation is performed for single and multi-placement. From the result it can be observed that the variation in various EEDPs is different and optimal DG allocation found to be at different nodes. This is due to the fact that the optimal DG size and location is highly dependent on the system loading pattern and the node voltage profile.

The power loss has reduced significantly whereas, the reduction in loss from single DG allocation to the multi DG allocation is not uniform rather with the increment in DG size the overall reduction in loss is 9kW, 23.53kW and 40.96kW when DG size is 500kW, 1000kW and 1500kW respectively.

Table 5.8 EEP after fixed size DG allocation in optimal configuration under LM-2

Parameters	**System performance LM-2**		
No. of DG	**DG=1**	**DG=2**	**DG=3**
Configuration	7,9,14,32,37	7,9,14,28,32,	7,9,14,32,37
P_{FD} (kW)	3223.1	2652.9	2068.1
Q_{FD} (kVAr)	2300.3	2297.4	2298.2
S_{FC} (kVA)	3959.8	3509.4	3090.2
Vi, min	0.9291	0.9425	0.9510
f_{si}	98.25	110.29	124.43
P_L (kW)	137.76	105.23	87.80
CT (sec)	0.2481	0.2653	0.2693
DG Locations (Node)	12	33, 10	12, 29, 32
DG sizes (kW)	500	500, 500	500, 500, 500

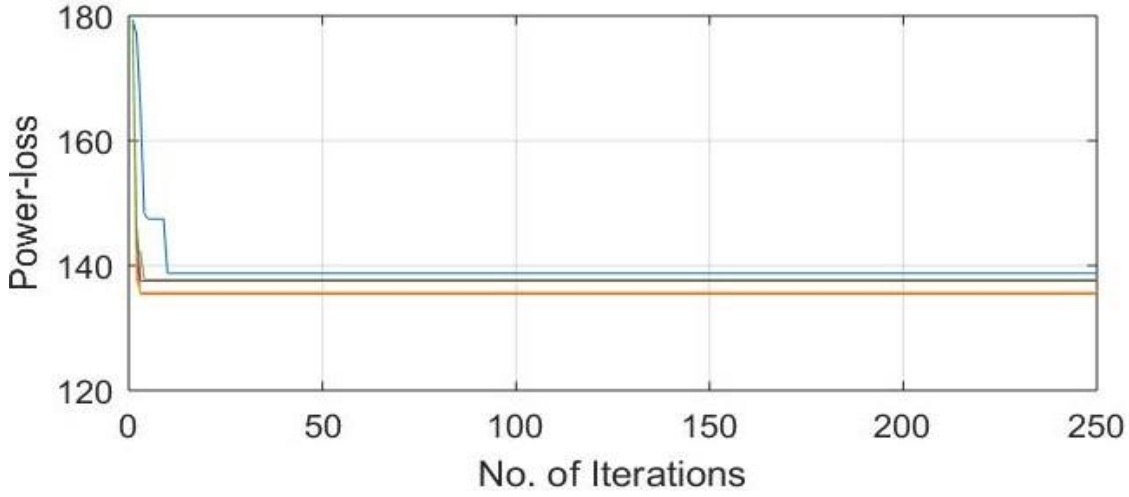

Fig 5.24 Convergence characteristic of optimal configuration under LM-2 with 1-DG

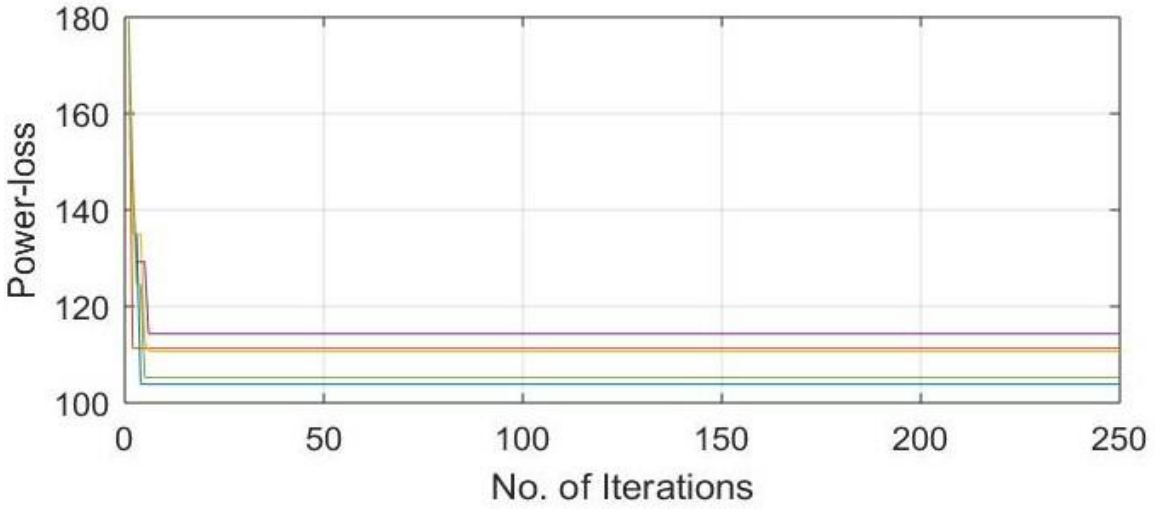

Fig 5.25 Convergence characteristic of optimal configuration under LM-2 with 2-DG

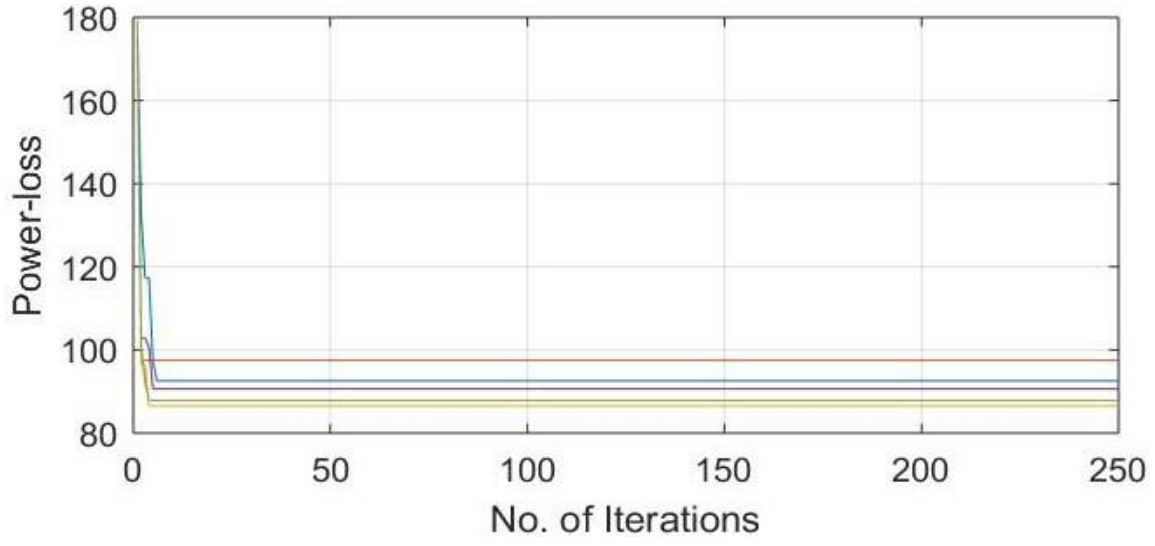

Fig 5.26 Convergence characteristic of optimal configuration under LM-2 with 3-DG

Fig 5.24 to 5.26 show the convergence characteristics of the 33-node system under different load models while reconfiguration of network topology. Here, it can be noticed that the convergence has occurred in different number of iterations. The program is run for 250 iterations and the 5 runs. The computational time is evaluated from the average of the time taken to converge in each run. Fig 5.24-5.26 it can be observed that the convergence rate if slow as compared to the convergence rate in Fig 5.24 as compared to the convergence rate in Fig 5.25 and 5.26

5.5.9 Result discussion for fixed DG size in optimal configuration under LM-3

Table 5.9 shows the test result for DG allocation in the base configuration under load model 3. The DG allocation is performed for single and multi-placement. From the result it can be observed that the variation in various EEDPs is different and optimal DG allocation found to be at different nodes. This is due to the fact that the optimal DG size and location is highly dependent on the system loading pattern and the node voltage profile.

The power loss has reduced significantly whereas, the reduction in loss from single DG allocation to the multi DG allocation is not uniform rather with the increment in DG size the overall reduction in loss is 3.74kW, 24.32kW and 42.33kW when DG size is 500kW, 1000kW and 1500kW respectively.

Table 5.9 EEP after fixed size DG allocation in optimal configuration under LM-3

Parameters	**System performance under LM-3**		
No. of DG	**DG=1**	**DG=2**	**DG=3**
Configuration	7,9,14,32,37	7,9,14,28,32,	7,9,14,32,37
P_{FD} (kW)	3222.0	2653.1	2071.6
Q_{FD} (kVAr)	2037.6	2051.4	2113.0
S_{FC} (kVA)	3812.2	3353.7	2959.1
Vi, min	0.9294	0.9415	0.9497
f_{si}	101.69	116.29	143.04
P_L (kW)	122.68	94.62	76.61
CT (sec)	0.0988	0.3788	0.5019
DG Locations (Node)	33	15, 26	30, 26, 17
DG sizes (kW)	500	500, 500	500, 500, 500

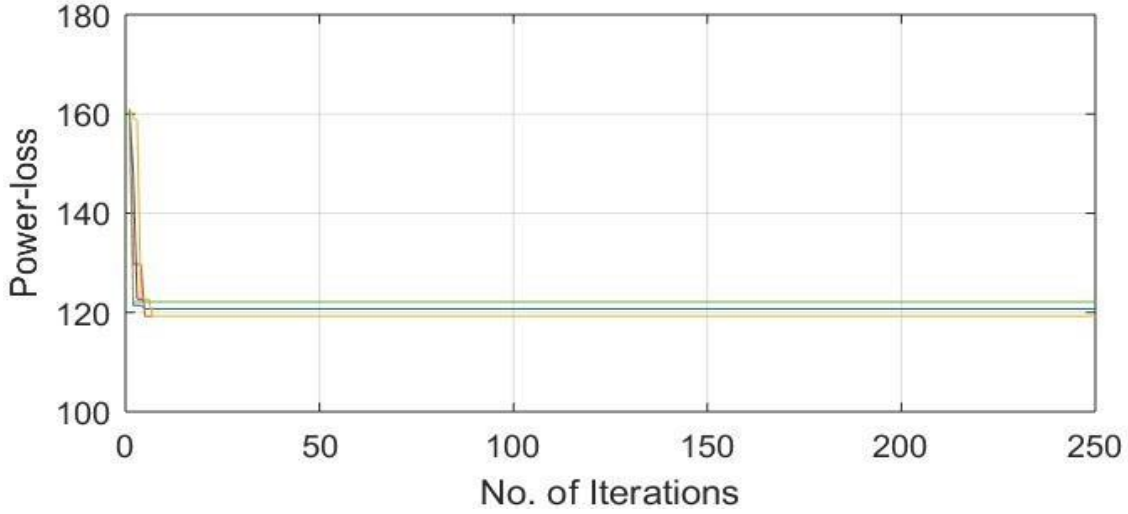

Fig 5.27 Convergence characteristic of optimal configuration under LM-3 with 1-DG

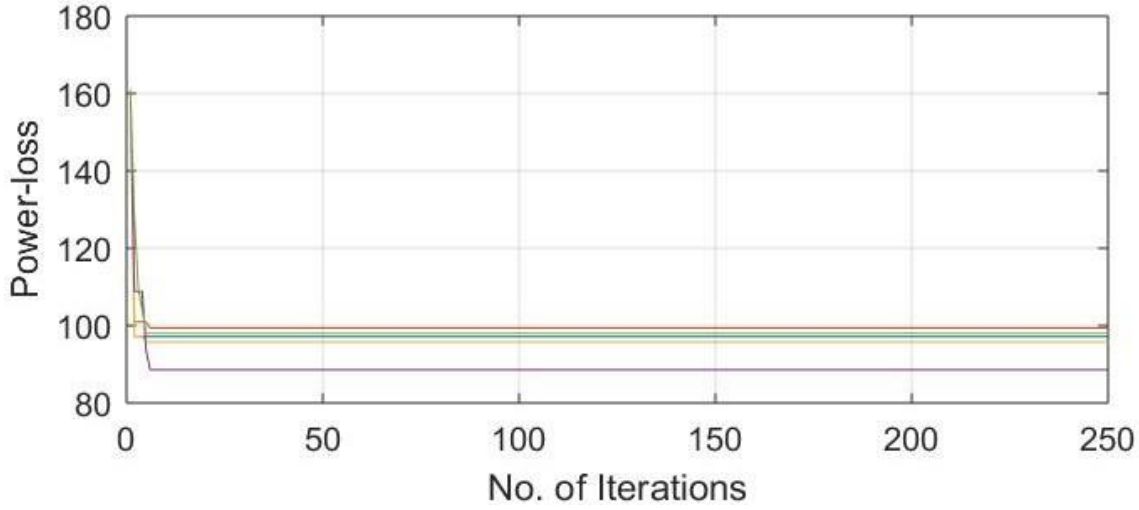

Fig 5.28 Convergence characteristic of optimal configuration under LM-3 with 2-DG

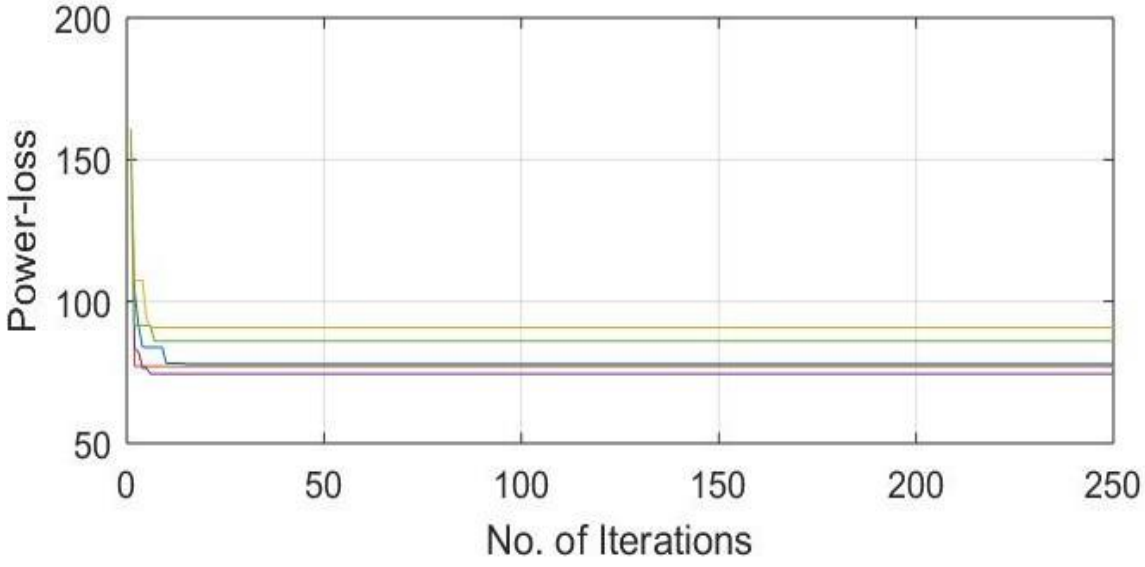

Fig 5.29 Convergence characteristic of optimal configuration under LM-3 with 3-DG

Fig 5.27 to 5.29 show the convergence characteristics of the 33-node system under different load models while reconfiguration of network topology. Here, it can be noticed that the convergence has occurred in different number of iterations. The program is run for 250 iterations and the 5 runs. The computational time is evaluated from the average of the time taken to converge in each run. Fig 5.27-5.29 it can be observed that the convergence rate if slow as compared to the convergence rate in Fig 5.27 as compared to the convergence rate in Fig 5.28 and 5.29

5.5.10 Result discussion for fixed DG location in optimal configuration under LM-1

Table 5.10 shows the test result for DG allocation in the base configuration under load model 1. The DG allocation is performed for single and multi-placement. From the result it can be observed that the variation in various EEDPs is different and optimal DG allocation found to be at different nodes. This is due to the fact that the optimal DG size and location is highly dependent on the system loading pattern and the node voltage profile.

The power loss has reduced significantly whereas, the reduction in loss from single DG allocation to the multi DG allocation is not uniform rather with the increment in DG size the overall reduction in loss is 18.87kW, 16.28kW and 16.39kW when DG size is 999.3kW, 1363kW and 1361.3kW respectively.

Table 5.10 EEP after fixed location DG allocation in optimal configuration under LM-1

Parameters	**System performance under LM-1**		
No. of DG	**DG=1**	**DG=2**	**DG=3**
Configuration	7,9,14,32,37	7,9,14,28,32,	7,9,14,32,37
P_{FD} (kW)	2728.2	2515.5	2477.2
Q_{FD} (kVAr)	2314.7	2386.6	2386.7
S_{FC} (kVA)	3577.8	3467.5	3449.0
Vi, min	0.9324	0.9331	0.9336
f_{si}	109.52	113.80	114.58
P_L (kW)	121.10	123.69	123.58
CT (sec)	0.4996	0.5774	0.9336
DG Locations (Node)	33	33, 31	33, 31, 32
DG sizes (kW)	999.3	389.8, 973.2	021.7, 848.9, 490.7

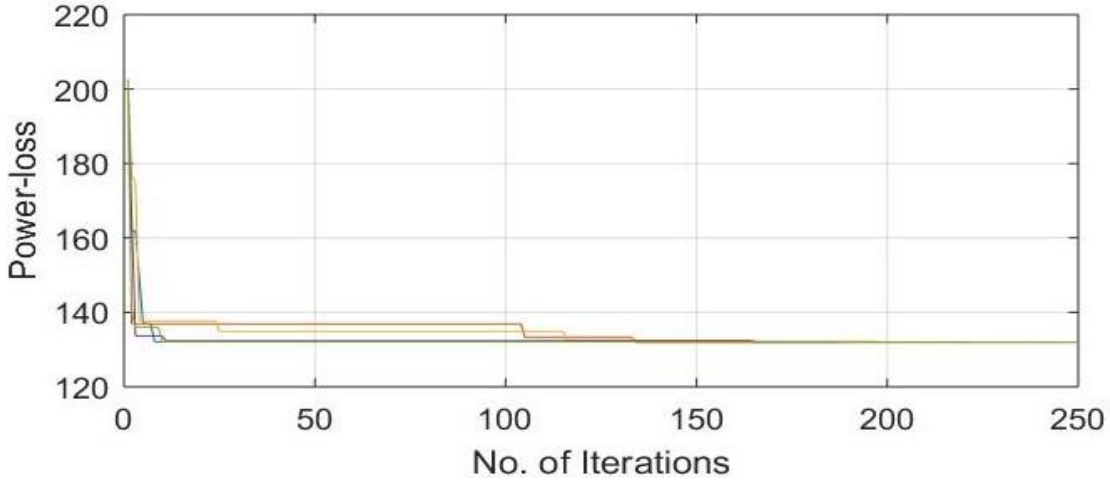

Fig 5.30 Convergence characteristic of optimal configuration under LM-1 with 1-DG

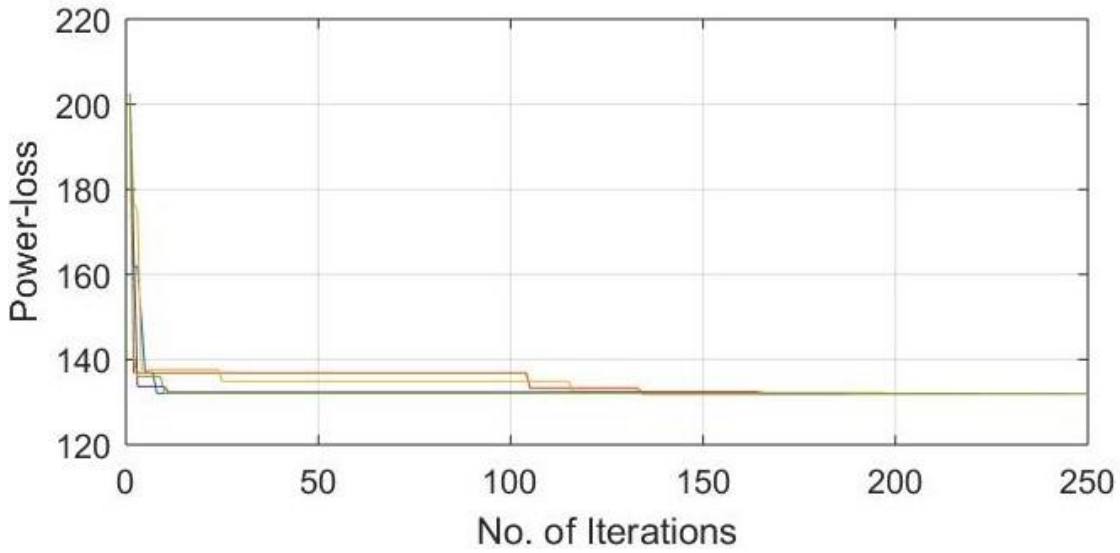

Fig 5.31 Convergence characteristic of optimal configuration under LM-1 with 2-DG

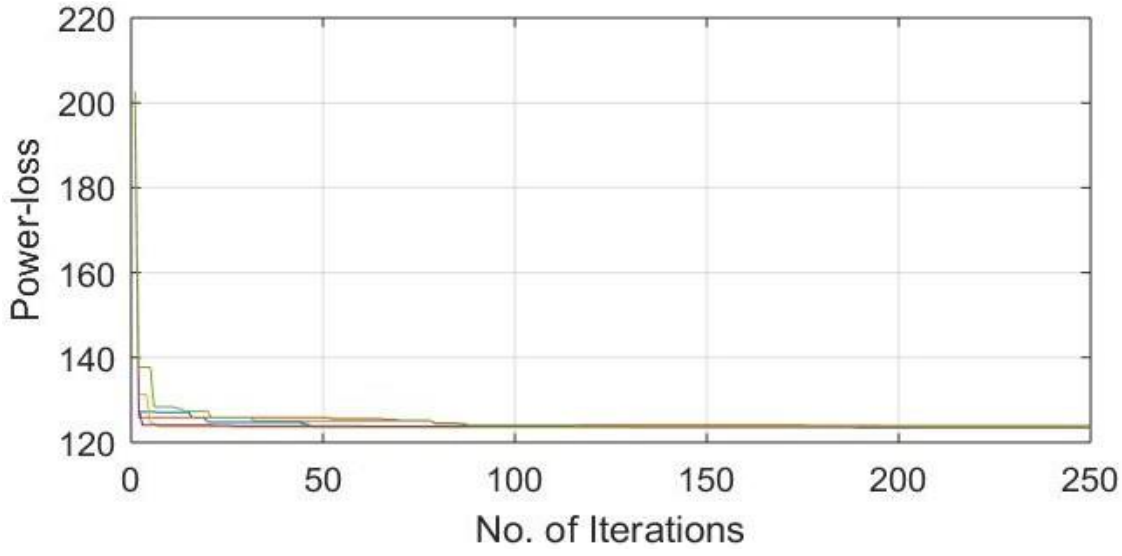

Fig 5.32 Convergence characteristic of optimal configuration under LM-1 with 3-DG

Fig 5.30 to 5.32 show the convergence characteristics of the 33-node system under different load models while reconfiguration of network topology. Here, it can be noticed that the convergence has occurred in different number of iterations. The program is run for 250 iterations and the 5 runs. The computational time is evaluated from the average of the time taken to converge in each run. Fig 5.30-5.32 it can be observed that the convergence rate if slow as compared to the convergence rate in Fig 5.30 as compared to the convergence rate in Fig 5.31 and 5.32

5.5.11 Result discussion for fixed DG location in optimal configuration under LM-2

Table 5.11 shows the test result for DG allocation in the base configuration under load model 2. The DG allocation is performed for single and multi-placement. From the result it can be observed that the variation in various EEDPs is different and optimal DG allocation found to be at different nodes. This is due to the fact that the optimal DG size and location is highly dependent on the system loading pattern and the node voltage profile.

The power loss has reduced significantly whereas, the reduction in loss from single DG allocation to the multi DG allocation is not uniform rather with the increment in DG size the overall reduction in loss is 7.66kW, 13.67kW and 13.77kW when DG size is 999.3kW, 3369.2kW and 1252.8kW respectively.

Tab 5.11 EEP after fixed location DG allocation in optimal configuration under LM-2

Parameters	**System performance under LM-2**		
No. of DG	**DG=1**	**DG=2**	**DG=3**
Configuration	7,9,14,32,37	7,9,14,28,32,	7,9,14,32,37
P_{FD} (kW)	2728.2	2495.9	2478.7
Q_{FD} (kVAr)	2314.7	2317.7	2318.3
S_{FC} (kVA)	3577.8	3406.0	3393.9
Vi, min	0.9324	0.9355	0.9357
f_{si}	109.52	115.68	116.15
P_L (kW)	121.10	115.09	114.99
CT (sec)	0.4996	0.6029	1.0077
DG Locations (Node)	33	33, 31	33, 31, 32
DG sizes (kW)	999.3	2371.1, 998.1	203.0, 841.4, 208.4

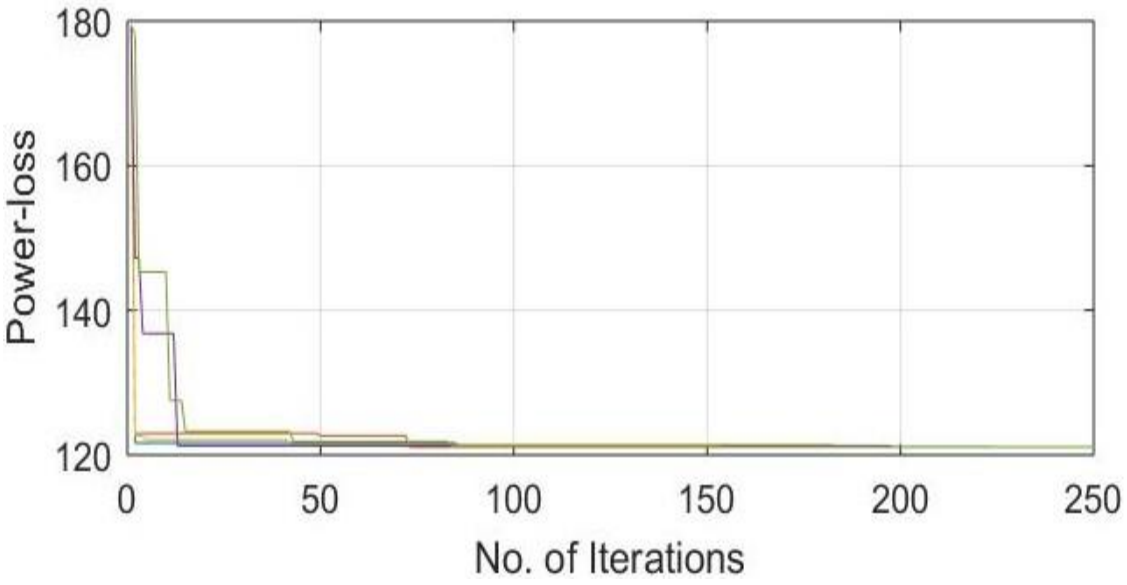

Fig 5.33 Convergence characteristic of optimal configuration under LM-2 with 1-DG

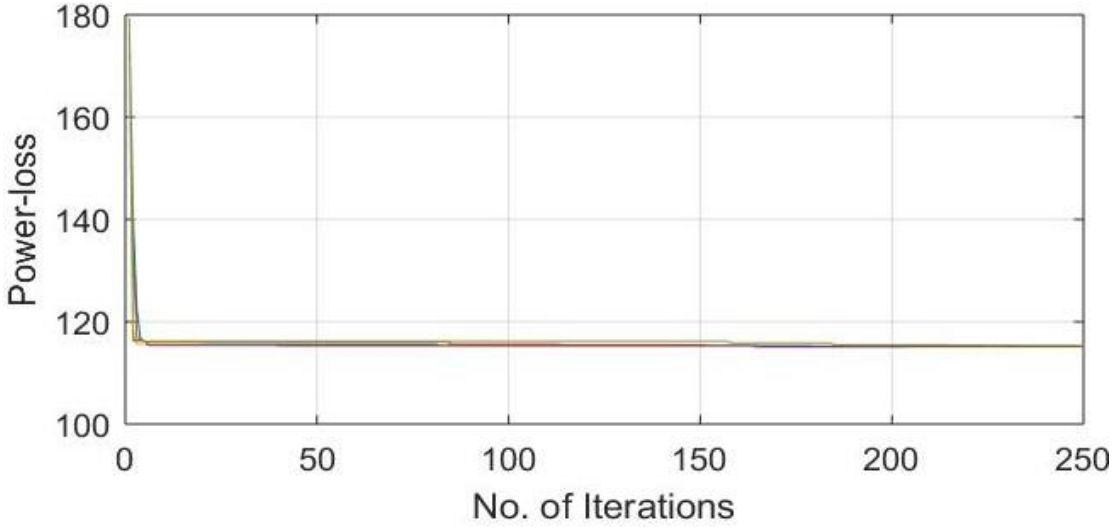

Fig 5.34 Convergence characteristic of optimal configuration under LM-2 with 2-DG

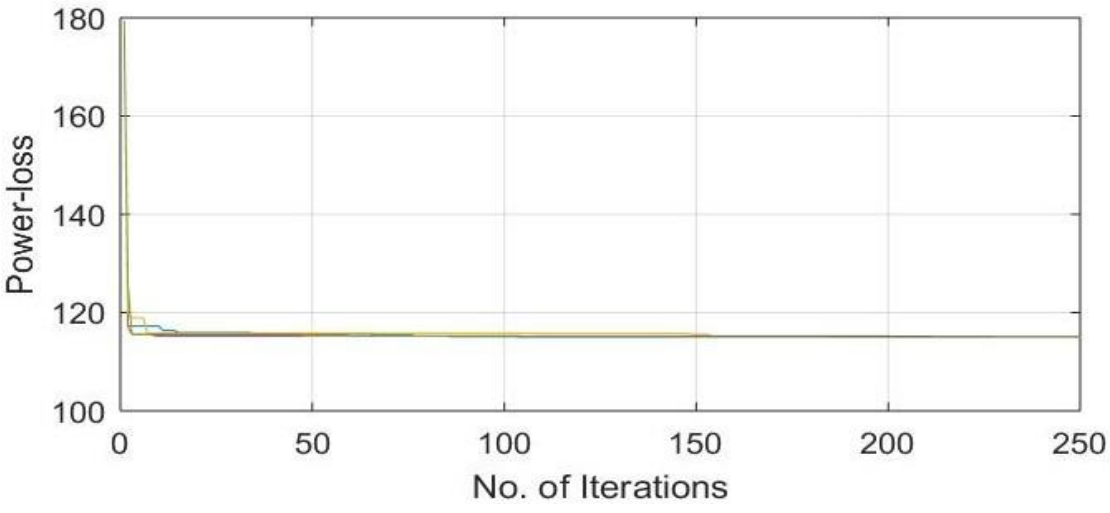

Fig 5.35 Convergence characteristic of optimal configuration under LM-2 with 3-DG

Fig 5.33 to 5.35 show the convergence characteristics of the 33-node system under different load models while reconfiguration of network topology. Here, it can be noticed that the convergence has occurred in different number of iterations. The program is run for 250 iterations and the 5 runs. The computational time is evaluated from the average of the time taken to converge in each run. Fig 5.33-5.35 it can be observed that the convergence rate if slow as compared to the convergence rate in Fig 5.33 as compared to the convergence rate in Fig 5.34 and 5.35

5.5.12 Result discussion for fixed DG location in optimal configuration under LM-3

Table 5.12 shows the test result for DG allocation in the base configuration under load model 3. The DG allocation is performed for single and multi-placement. From the result it can be observed that the variation in various EEDPs is different and optimal DG allocation found to be at different nodes. This is due to the fact that the optimal DG size and location is highly dependent on the system loading pattern and the node voltage profile.

The power loss has reduced significantly whereas, the reduction in loss from single DG allocation to the multi DG allocation is not uniform rather with the increment in DG size the overall reduction in loss is 10.38kW, 15.12kW and 15.16kW when DG size is 999.6kW, 1178.6kW and 1173kW respectively.

Table 5.12 EEP after fixed location DG allocation in optimal configuration under LM-3

Parameters	**System performance under LM-3**		
No. of DG	**DG=1**	**DG=2**	**DG=3**
Configuration	7,9,14,32,37	7,9,14,28,32,	7,9,14,32,37
P_{FD} (kW)	2727.6	2550.0	2554.7
Q_{FD} (kVAr)	2095.6	2113.9	2113.3
S_{FC} (kVA)	3439.7	3312.3	3315.4
Vi, min	0.9355	0.9377	0.9376
f_{si}	113.35	118.14	118.01
P_L (kW)	108.56	103.84	103.78
CT (sec)	0.5839	0.6205	0.6528
DG Locations (Node)	33	33, 31	33, 31, 32
DG sizes (kW)	999.3	193.0, 985.6	063.8, 896.4, 213.6

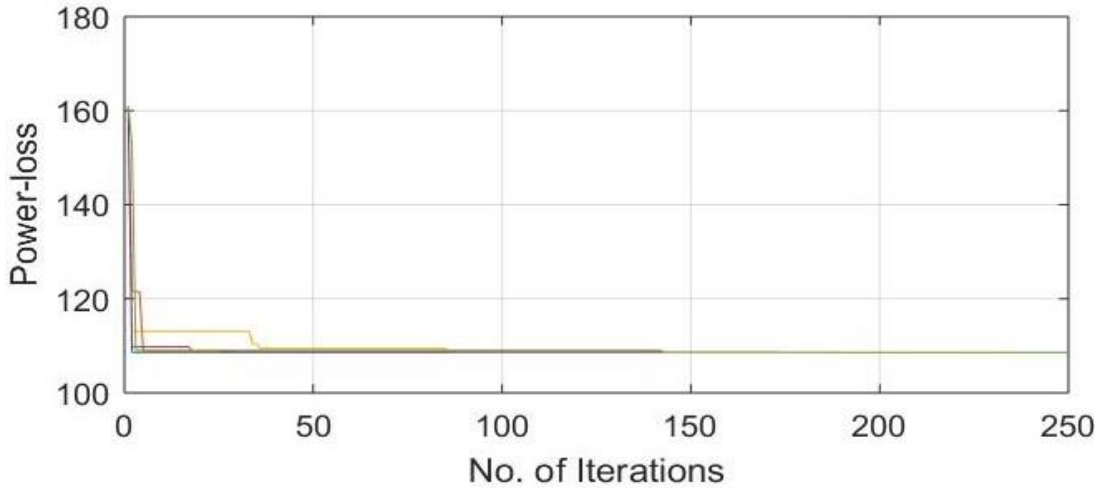

Fig 5.36 Convergence characteristic of optimal configuration under LM-3 with 1-DG

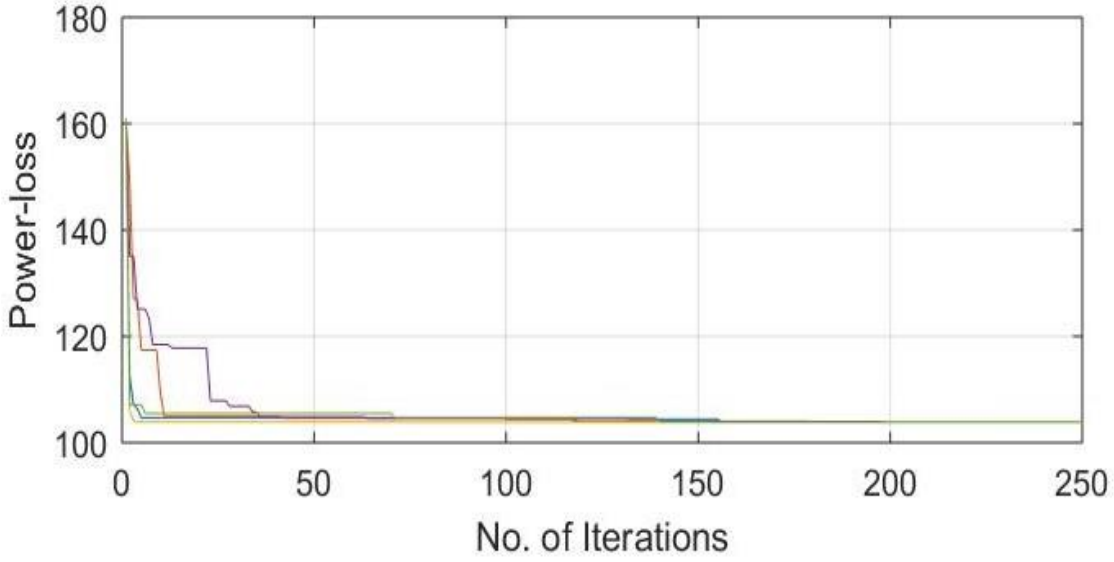

Fig 5.37 Convergence characteristic of optimal configuration under LM-3 with 2-DG

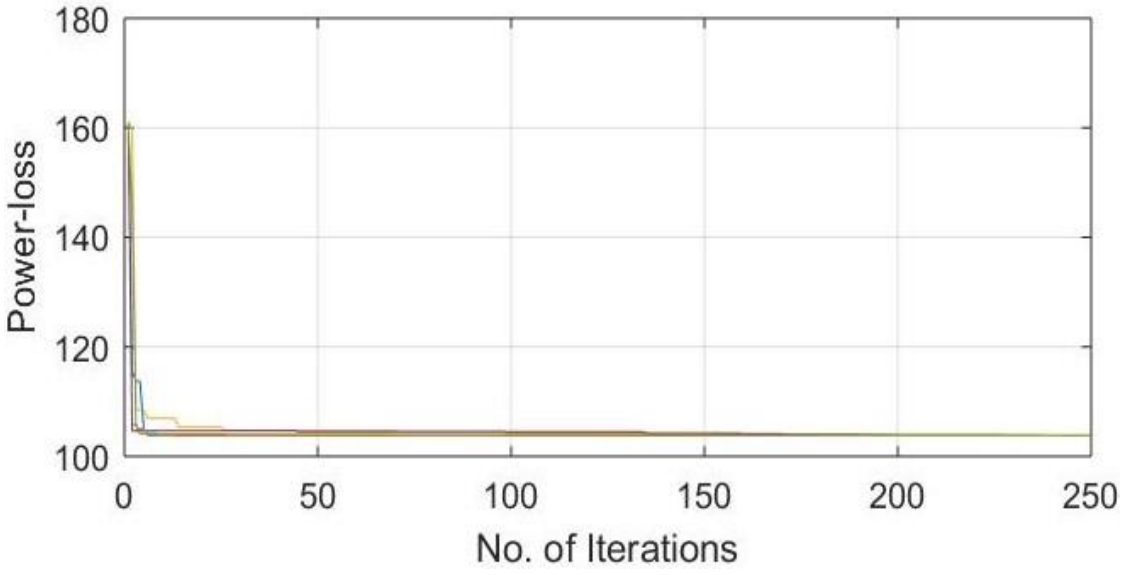

Fig 5.38 Convergence characteristic of optimal configuration under LM-3 with 3-DG

Fig 5.36 to 5.38 show the convergence characteristics of the 33-node system under different load models while reconfiguration of network topology. Here, it can be noticed that the convergence has occurred in different number of iterations. The program is run for 250 iterations and the 5 runs. The computational time is evaluated from the average of the time taken to converge in each run. Fig 5.36-5.38 it can be observed that the convergence rate if slow as compared to the convergence rate in Fig 5.36 as compared to the convergence rate in Fig 5.36 and 5.38

5.6 Conclusion

In this section, a method to optimally allocate DG in radial distribution schemes is based on the peak load capacity of the system. This method represents to allocate (locations and calculation of DG size) DG in system. And it is also examined that the proposed method is adequate for loss minimization and boost maximum loadability in comparison to existing method. It is also tested on distinct load designs and high load capacity and steady impedance load after DG positioning, but at the same time constant load is small in many instances.

Chapter 6

Synchronized DG Allocation and Reconfiguration

6.1 Introduction

The electric powered strength move is conveying through the distribution gadget to customer. In general, distribution feeders are in radial network which allows to lessen over cutting-edge safety, even though transmission lines are framing with the meshed community. When fault occurs inside the line due to any motives, it makes interruption to patron, to deliver again power at once to load facet, most feeders have tie-switches to adjacent feeders.

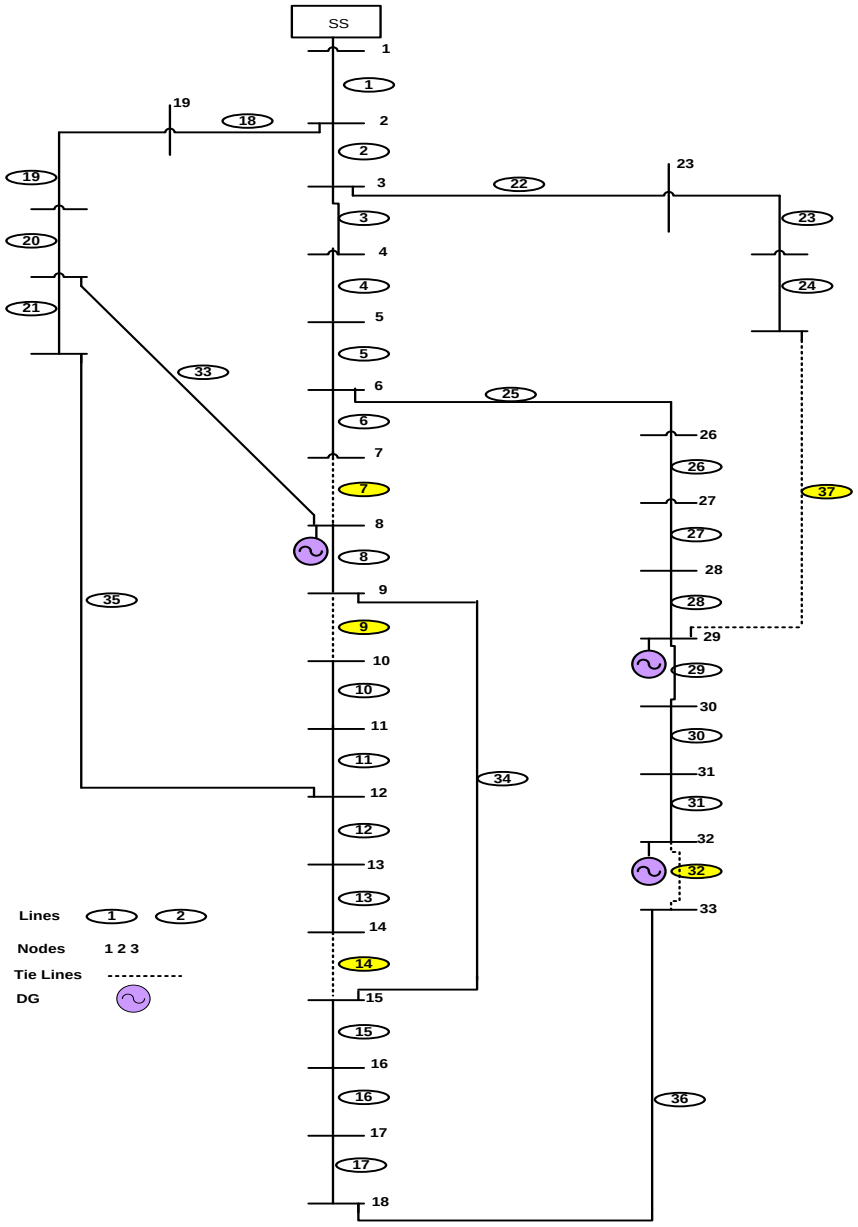

Fig 6.1 IEEE 33-node radial distribution system with reconfiguration and DG Allocation

The plans of electrical tool plans within the presence of distribution generation (DG) requires the definition of several factors, such as: the excellent technology to be used, the wide range and potential of the devices, the wide area, the form of community connection and many others. DG placement inside the distribution machine, leave the large change in operating traits to makes the device extra powerful and efficient compared to the preceding or without DG with respect to the voltage losses, voltage profile, stability, and reliability as properly.

There is some principal difficulty with DG placement with appreciate to the size and place. It ought to be in suitable manner otherwise placement of DG at non-foremost website will increase the losses and that is why cost may even increase, consequently awareness of the website and length of DG is important.

The RDS reconfiguration of distribution automation allowance and such an arrangement could be beneficially implemented for growth of execution. One of the main estimates of execution that could be advanced among others is the MVA element or margin to the final loadability factor. In order to achieve this goal, two problems need to be targeted, in particular the estimation of correct closeness to the maximum factor of severe loadability and the most appropriate reconfiguration scheme to reconfigure the network for maximum loadability.

6.2 Algorithm

Step1: Read the line and load data.

Step2: Set the HSA parameters.

Step3: Generate solution vectors for

i. Tie line
ii. DG location
iii. DG size

Step4: Initialize the HM with discrete and continuous solution vector

iii. Discrete vectors: tie line and DG location
iv. Continuous vector: DG size

Step5: Improvise the HM based on HSA rules.

Step6: Compare the new harmony with existing harmony.

Step7: If new harmony is better than old harmony, update the solution vector, else discard.

Step8: Repeat the step 5-7 till maximum improvisation.

Step9: Print the best harmony and load flow result.

Step10: Stop.

6.3 Flowchart

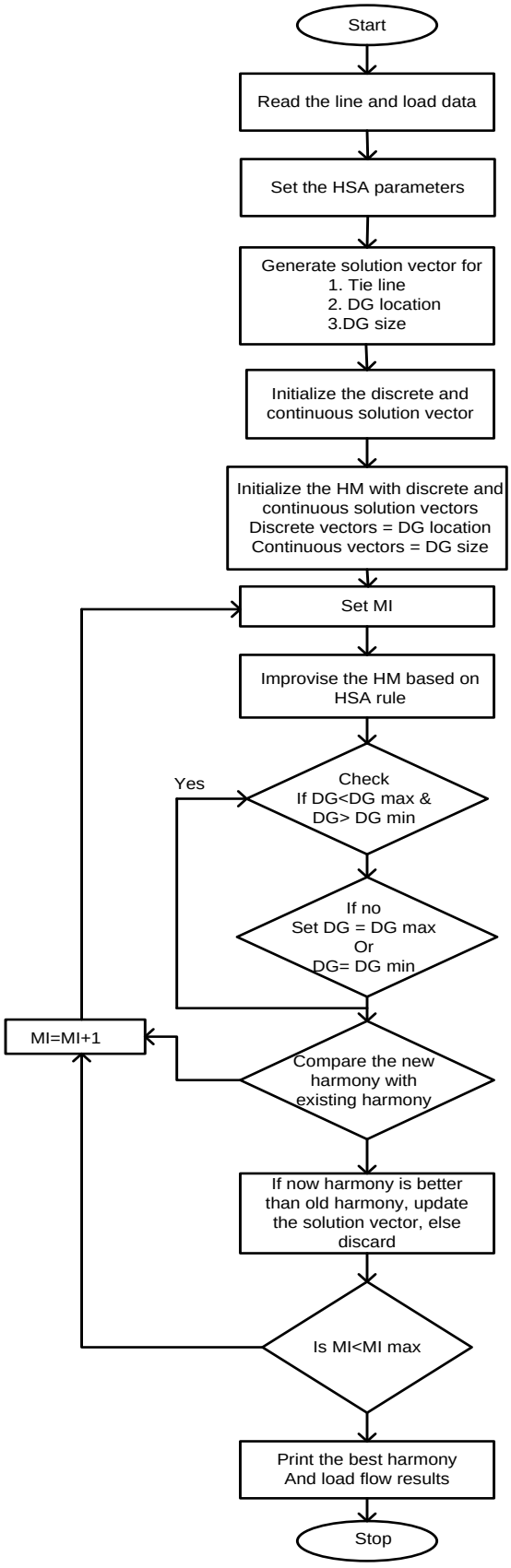

Fig 6.2 Flow chart for DG allocation and reconfiguration

6.4 Result and discussions

In the reconfiguration and DG allocation result and discussion, different load models along with variation of DG's and fixed size, location are discussed below:

6.4.1 Result discussion for DG allocation and reconfiguration under LM-1

Table 6.1 shows the test result for DG allocation in the base configuration under load model 1. The DG allocation is performed for single and multi-placement. From the result it can be observed that the variation in various EEDPs is different and optimal DG allocation found to be at different nodes. This is due to the fact that the optimal DG size and location is highly dependent on the system loading pattern and the node voltage profile.

The power loss has reduced significantly whereas, the reduction in loss from single DG allocation to the multi DG allocation is not uniform rather with the increment in DG size the overall reduction in loss is 29.45kW, 58.59kW and 81.87kW when DG size is 920.1kW, 1481.2kW and 2539kW respectively.

Table 6.1 EEP after reconfigurations and DG allocation under LM-1

Parameters	**System performance underLM-1**		
No. of DG	**DG=1**	**DG=2**	**DG=3**
Configuration	33,14,10,32,28	7,34,8,36,28	7,13,11,36,27
P_{FD} (kW)	2905.4	2315.1	1234.1
Q_{FD} (kVAr)	2378.2	2361.1	2343.0
S_{FC} (kVA)	3754.6	3306.8	2648.2
Vi, min	0.9423	0.9544	0.9750
f_{si}	104.18	119.98	160.40
P_L (kW)	110.52	81.38	58.10
CT (sec)	1.3073	1.1651	2.1818
DG Locations (Node)	8	31, 22	25, 9, 31
DG sizes (kW)	920.1	915.6, 565.6	890.0, 856.5, 792.5

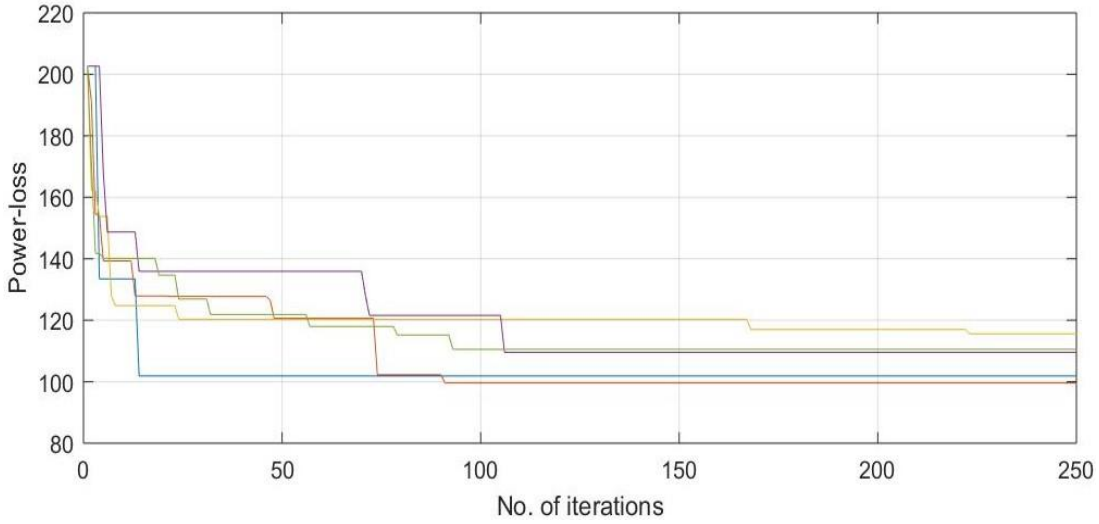

Fig 6.3 Convergence characteristic of optimal configuration under LM-1 with 1-DG

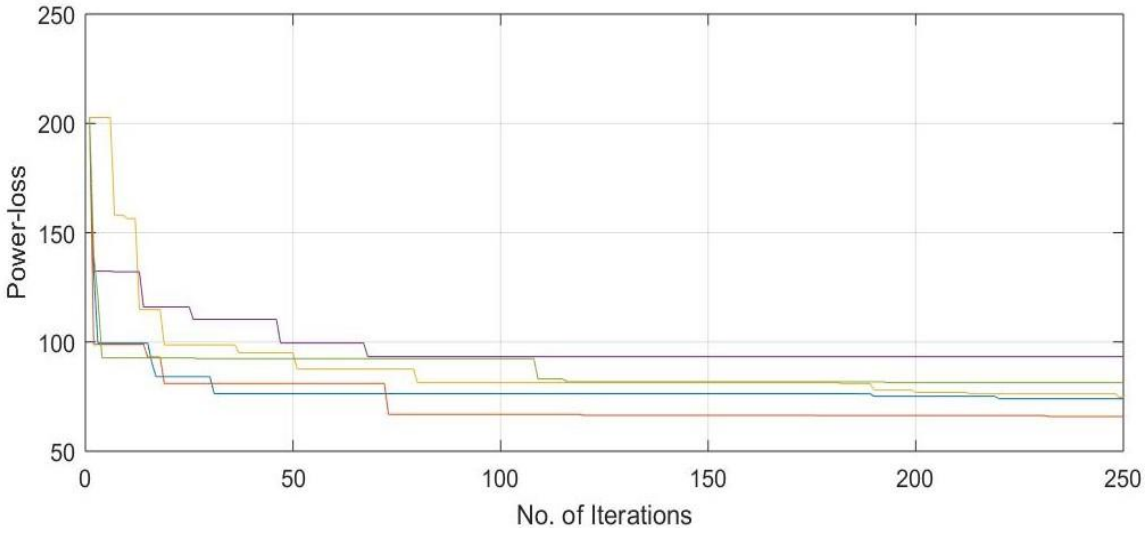

Fig 6.4 Convergence characteristic of optimal configuration under LM-1 with 2-DG

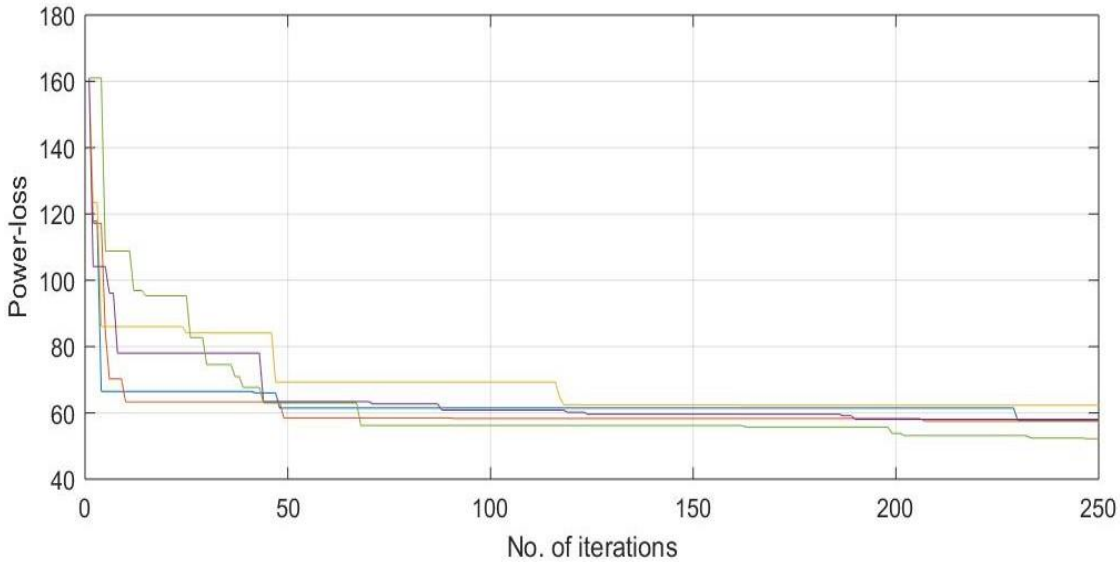

Fig 6.5 Convergence characteristic of optimal configuration under LM-1 with 3-DG

Fig 6.3 to 6.5 show the convergence characteristics of the 33-node system under different load models while reconfiguration of network topology. Here, it can be noticed that the convergence has occurred in different number of iterations. The program is run for 250 iterations and the 5 runs. The computational time is evaluated from the average of the time taken to converge in each run. Fig 6.3-6.5 it can be observed that the convergence rate if slow as compared to the convergence rate in Fig 6.5 as compared to the convergence rate in Fig 6.4 and 6.3

6.4.2 Result discussion for reconfiguration and DG allocation under LM-2

Table 6.2 shows the test result for DG allocation in the base configuration under load model 2. The DG allocation is performed for single and multi-placement. From the result it can be observed that the variation in various EEDPs is different and optimal DG allocation found to be at different nodes. This is due to the fact that the optimal DG size and location is highly dependent on the system loading pattern and the node voltage profile.

The power loss has reduced significantly whereas, the reduction in loss from single DG allocation to the multi DG allocation is not uniform rather with the increment in DG size the overall reduction in loss is 27.94kW, 60.25kW and 72.37kW when DG size is 724.1kW, 1843.5kW and 2550.6kW respectively.

Table 6.2 EEP after reconfigurations and DG allocation under LM-2

Parameters	**System performance under LM-2**		
No. of DG	**DG=1**	**DG=2**	**DG=3**
Configuration	6,34,9,32,37	7,14,9,32,28	7,12,10,32,25
P_{FD} (kW)	2996.8	1865.9	1169.8
Q_{FD} (kVAr)	2303.8	2302.3	2309.2
$S_{FC,}$ (kVA)	3780.0	2963.5	2588.7
Vi, min	0.9446	0.9615	0.9768
f_{si}	103.17	136.20	164.92
P_L (kW)	100.82	68.51	56.39
CT (sec)	0.9891	1.1590	1.4377
DG Locations (Node)	13	29, 21	25, 15, 31
DG sizes (kW)	724.1	999.1, 844.4	984.7, 811.6, 754.3

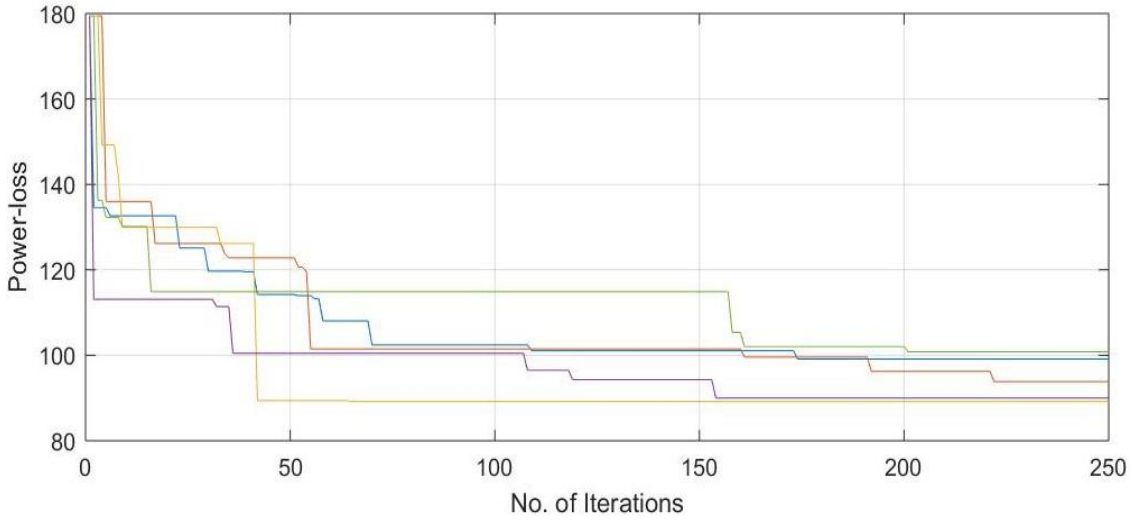

Fig 6.6 Convergence characteristic of optimal configuration under LM-2 with 1-DG

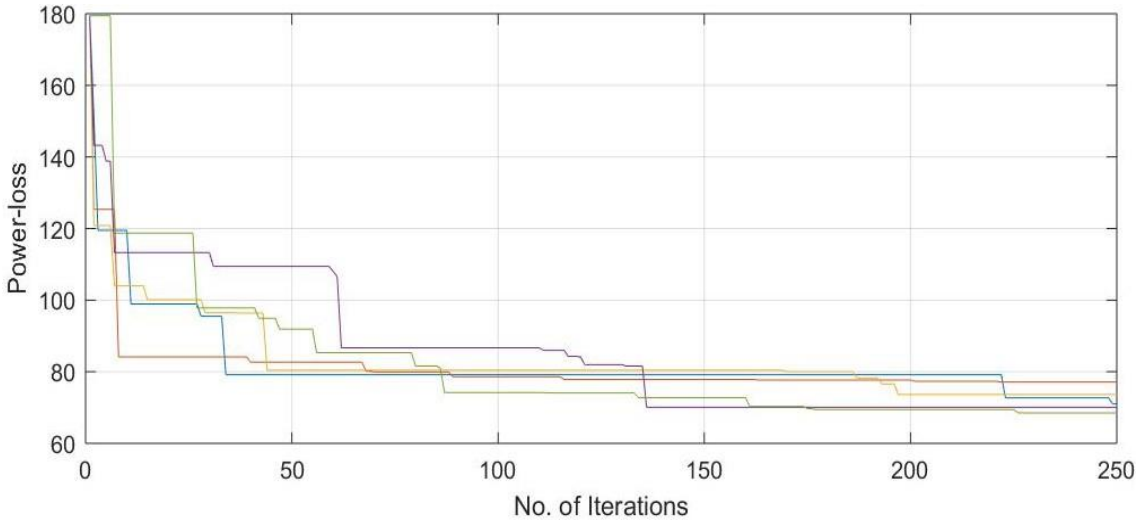

Fig 6.7 Convergence characteristic of optimal configuration under LM-2 with 2-DG

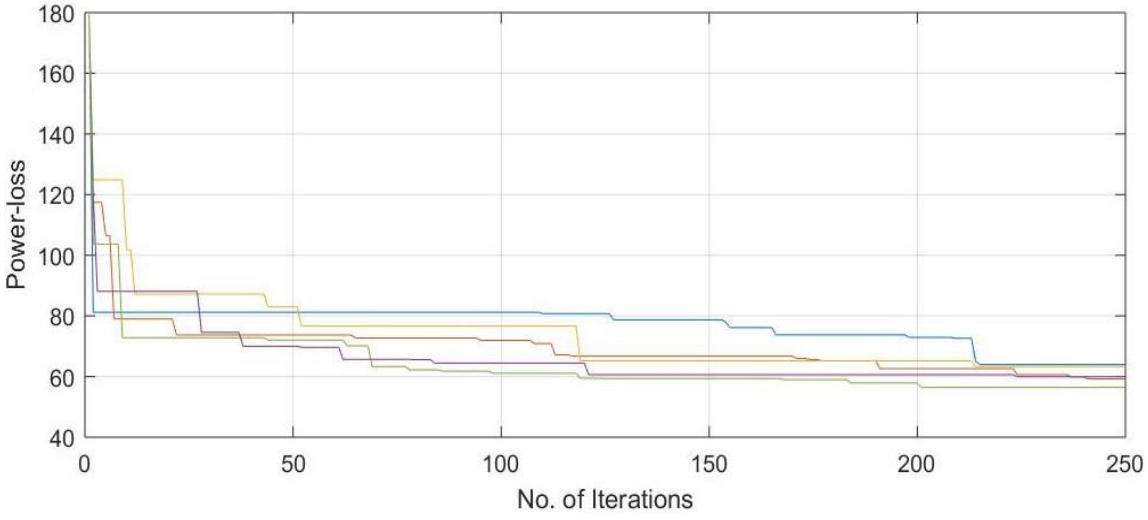

Fig 6.8 Convergence characteristic of optimal configuration under LM-2 with 3-DG

Fig 6.6 to 6.8 show the convergence characteristics of the 33-node system under different load models while reconfiguration of network topology. Here, it can be noticed that the convergence has occurred in different number of iterations. The program is run for 250 iterations and the 5 runs. The computational time is evaluated from the average of the time taken to converge in each run. Fig 6.6-6.8 it can be observed that the convergence rate if slow as compared to the convergence rate in Fig 5.8 as compared to the convergence rate in Fig 5.7 and 5.6

6.4.3 Result discussion for reconfiguration and DG allocation under LM-3

Table 6.3 shows the test result for DG allocation in the base configuration under load model 3. The DG allocation is performed for single and multi-placement. From the result it can be observed that the variation in various EEDPs is different and optimal DG allocation found to be at different nodes. This is due to the fact that the optimal DG size and location is highly dependent on the system loading pattern and the node voltage profile.

The power loss has reduced significantly whereas, the reduction in loss from single DG allocation to the multi DG allocation is not uniform rather with the increment in DG size the overall reduction in loss is 32.95kW, 55.72kW and 66.76kW when DG size is 930kW, 1713.7kW and 2640.8kW respectively.

Table 6.3 EEP after reconfigurations and DG allocation under LM-3

Parameters	**System performance under LM-3**		
No. of DG	**DG=1**	**DG=2**	**DG=3**
Configuration	33,14,8,30,26	6,14,11,32,26	7,12,10,31,27
P_{FD} (kW)	2790.9	1991.5	1067.4
Q_{FD} (kVAr)	2108.2	2118.0	2166.6
S_{FC} (kVA)	3497.6	2907.2	2415.3
Vi, min	0.9582	0.9603	0.9612
f_{si}	111.40	136.91	177.38
P_L (kW)	85.99	63.22	52.18
CT (sec)	1.5257	1.7387	1.1202
DG Locations (Node)	18	25, 9	29, 9, 16
DG sizes (kW)	930.0	865.8, 847.9	892.4, 967.9, 780.5

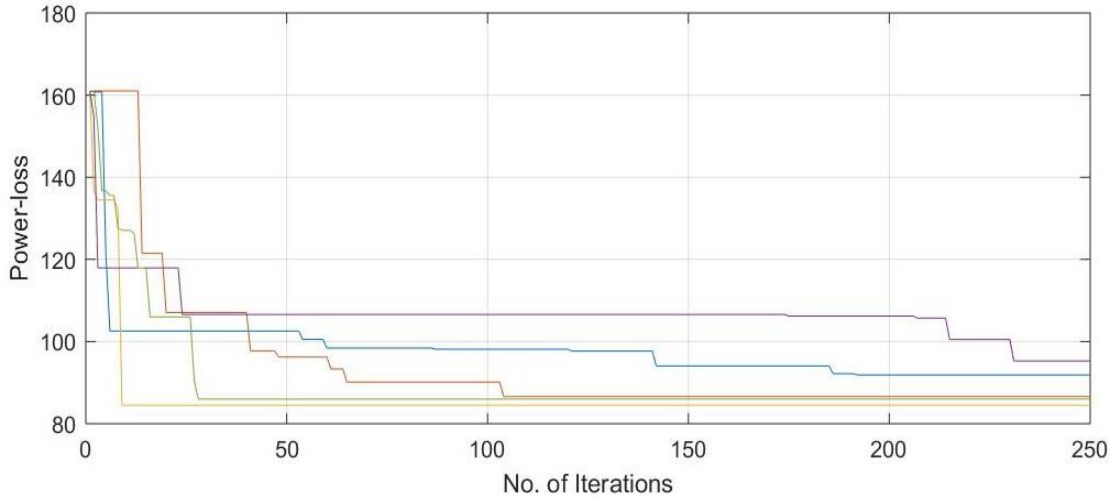

Fig 6.9 Convergence characteristic of optimal configuration under LM-3 with 1- DG

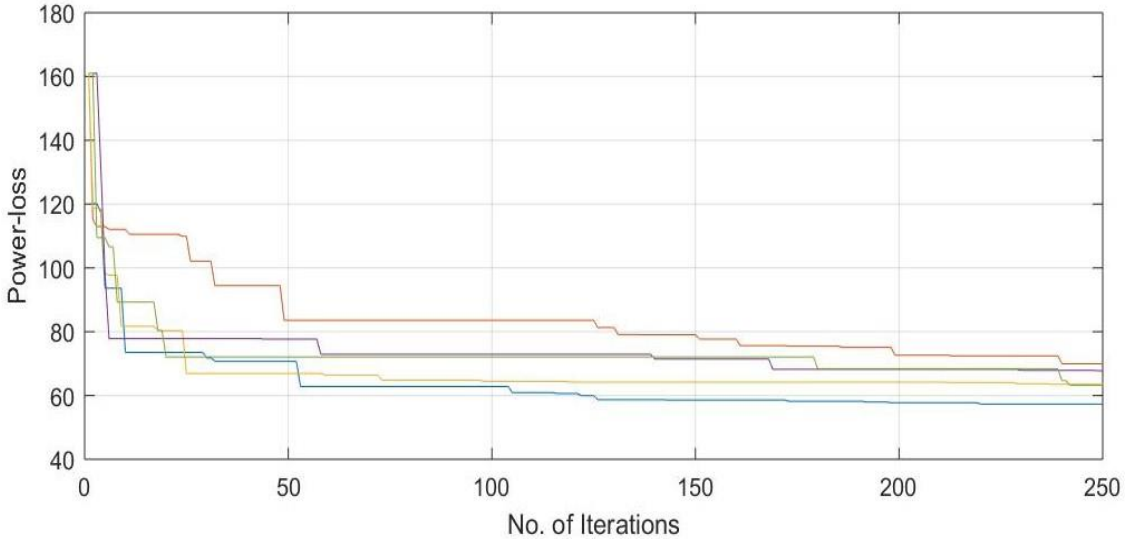

Fig 6.10 Convergence characteristic of optimal configuration under LM-3 with 2-DG

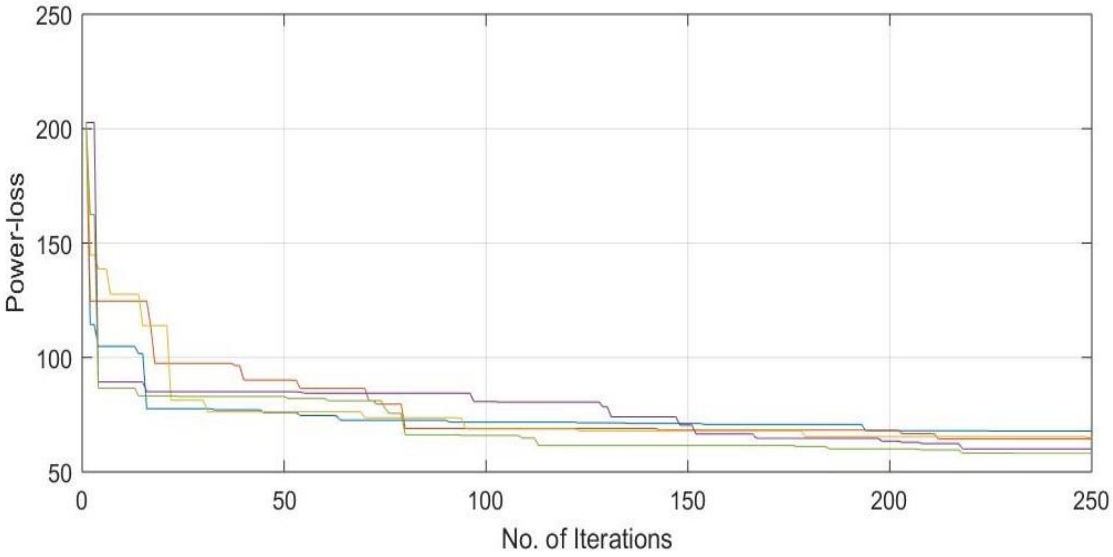

Fig 6.11 Convergence characteristic of optimal configuration under LM-3 with 3-DG

Fig 6.9 to 6.11 show the convergence characteristics of the 33-node system under different load models while reconfiguration of network topology. Here, it can be noticed that the convergence has occurred in different number of iterations. The program is run for 250 iterations and the 5 runs. The computational time is evaluated from the average of the time taken to converge in each run. Fig 6.9-6.11 it can be observed that the convergence rate if slow as compared to the convergence rate in Fig 6.11 as compared to the convergence rate in Fig 6.10 and 6.9

6.4.4 Result discussion for reconfiguration and DG allocation (size fixed) under LM-1

Table 6.4 shows the test result for DG allocation in the base configuration under load model 1. The DG allocation is performed for single and multi-placement. From the result it can be observed that the variation in various EEDPs is different and optimal DG allocation found to be at different nodes. This is due to the fact that the optimal DG size and location is highly dependent on the system loading pattern and the node voltage profile.

The power loss has reduced significantly whereas, the reduction in loss from single DG allocation to the multi DG allocation is not uniform rather with the increment in DG size the overall reduction in loss is 32.08kW, 45.93kW and 67.69kW when DG size is 500kW, 1000kW and 1500kW respectively.

Table 6.4 EEP after reconfigurations and fixed DG size allocation under LM-1

Parameters	**System performance under LM-1**		
No. of DG	**DG=1**	**DG=2**	**DG=3**
Configuration	33,34,9,30,28	7,14,11,36,28	7,14,9,31,37
P_{FD} (kW)	3297.0	2724.6	2118.8
Q_{FD} (kVAr)	2381.2	2368.9	2352.0
S_{FC} (kVA)	4067.0	3610.4	3165.7
Vi, min	0.8337	0.9519	0.9599
f_{si}	95.68	108.69	126.22
P_L (kW)	107.89	94.04	72.28
CT (sec)	0.8337	0.5525	0.9536
DG Locations (Node)	18	30, 21	27, 12, 26
DG sizes (kW)	500	500, 500	500, 500, 500

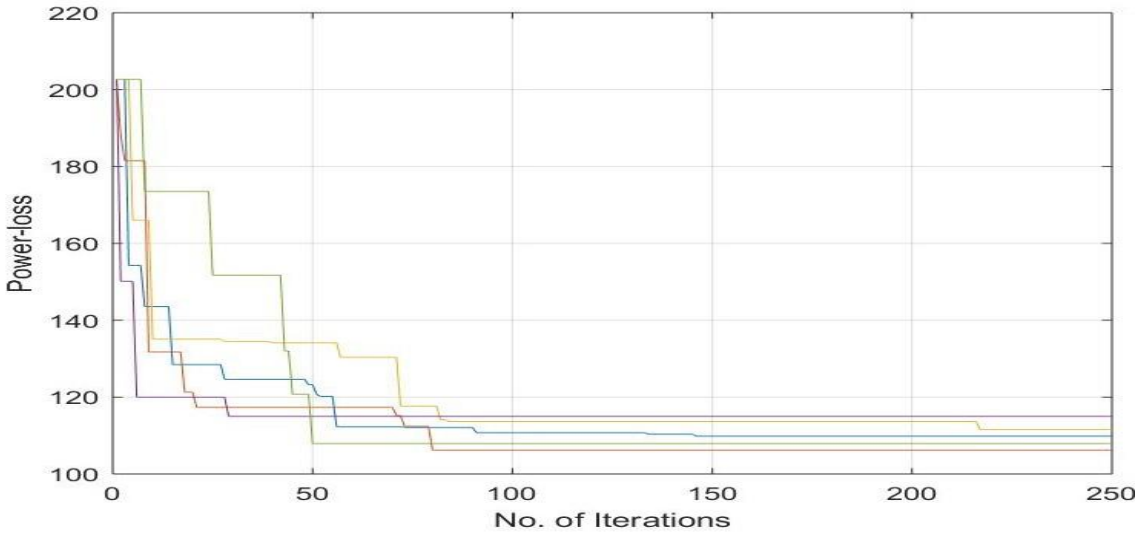

Fig 6.12 Convergence characteristic of optimal configuration under LM-1 with 1-DG

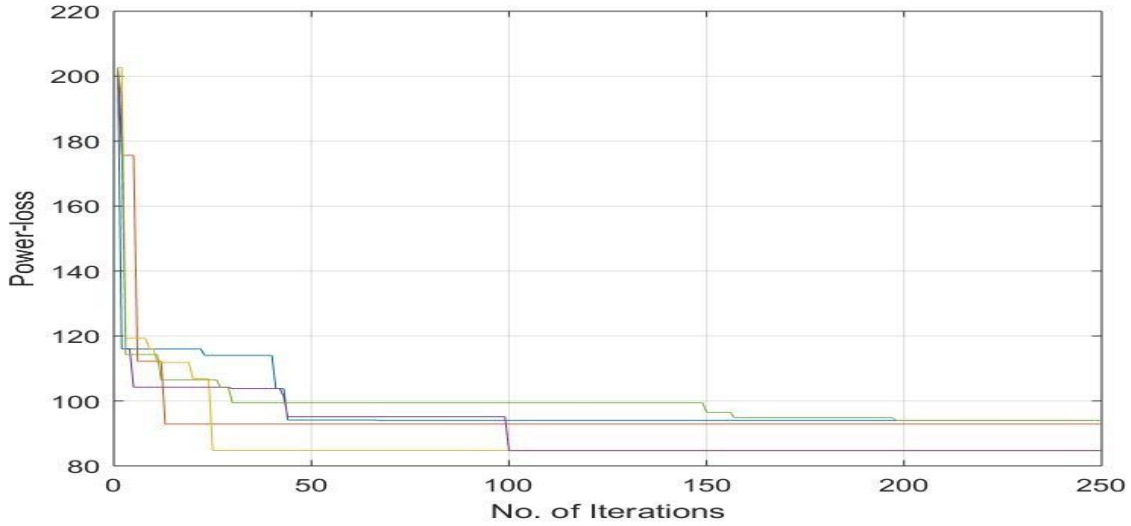

Fig 6.13 Convergence characteristic of optimal configuration under LM-1 with 2-DG

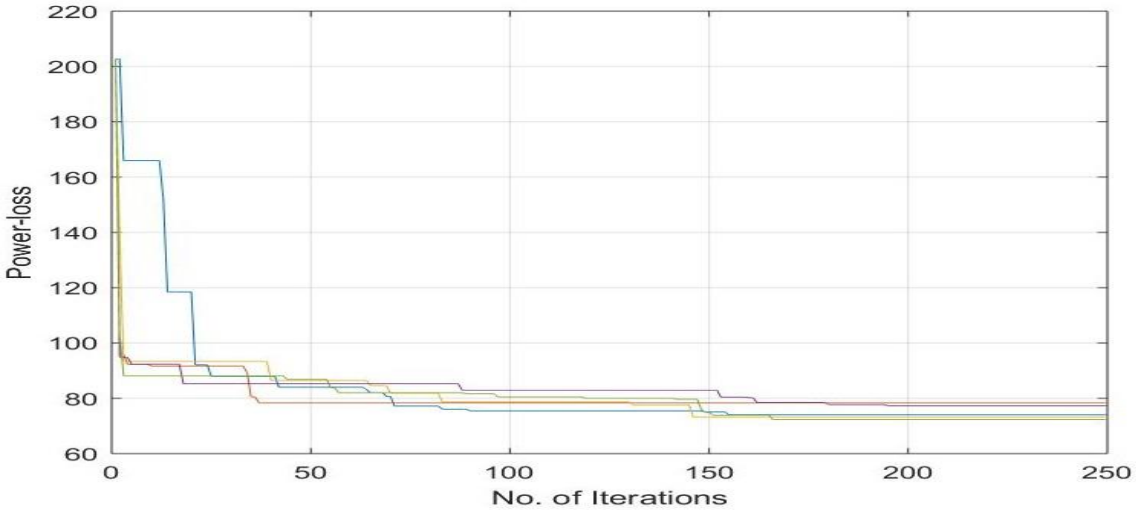

Fig 6.14 Convergence characteristic of optimal configuration under LM-1 with 3-DG

Fig 6.12 to 6.14 show the convergence characteristics of the 33-node system under different load models while reconfiguration of network topology. Here, it can be noticed that the convergence has occurred in different number of iterations. The program is run for 250 iterations and the 5 runs. The computational time is evaluated from the average of the time taken to converge in each run. Fig 6.12-6.14 it can be observed that the convergence rate if slow as compared to the convergence rate in Fig 6.14 as compared to the convergence rate in Fig 6.13 and 6.14

6.5.5 Result discussion for reconfiguration and DG allocation (size fixed) under LM-2

Table 6.5 shows the test result for DG allocation in the base configuration under load model 2. The DG allocation is performed for single and multi-placement. From the result it can be observed that the variation in various EEDPs is different and optimal DG allocation found to be at different nodes. This is due to the fact that the optimal DG size and location is highly dependent on the system loading pattern and the node voltage profile.

The power loss has reduced significantly whereas, the reduction in loss from single DG allocation to the multi DG allocation is not uniform rather with the increment in DG size the overall reduction in loss is 19.73kW, 51.27kW and 49.54kW when DG size is 500kW, 1000kW and 1500kW respectively.

Table 6.5 EEP after reconfigurations and fixed DG size allocation under LM-2

Parameters	**System performance under LM-2**		
No. of DG	**DG=1**	**DG=2**	**DG=3**
Configuration	6,34,8,31,28	7,14,8,31,28	7,14,10,32,25
P_{FD} (kW)	3182.7	2619.3	2039.1
Q_{FD} (kVAr)	2310.3	2300.6	2300.0
S_{FC} (kVA)	3932.8	3486.2	3073.7
Vi, min	0.9349	0.9578	0.9555
f_{si}	98.95	112.62	130.18
P_L (kW)	109.03	77.49	79.22
CT (sec)	1.1246	1.1148	0.7018
DG Locations (Node)	13	25, 32	23, 26, 8
DG sizes (kW)	500	500, 500	500, 500, 500

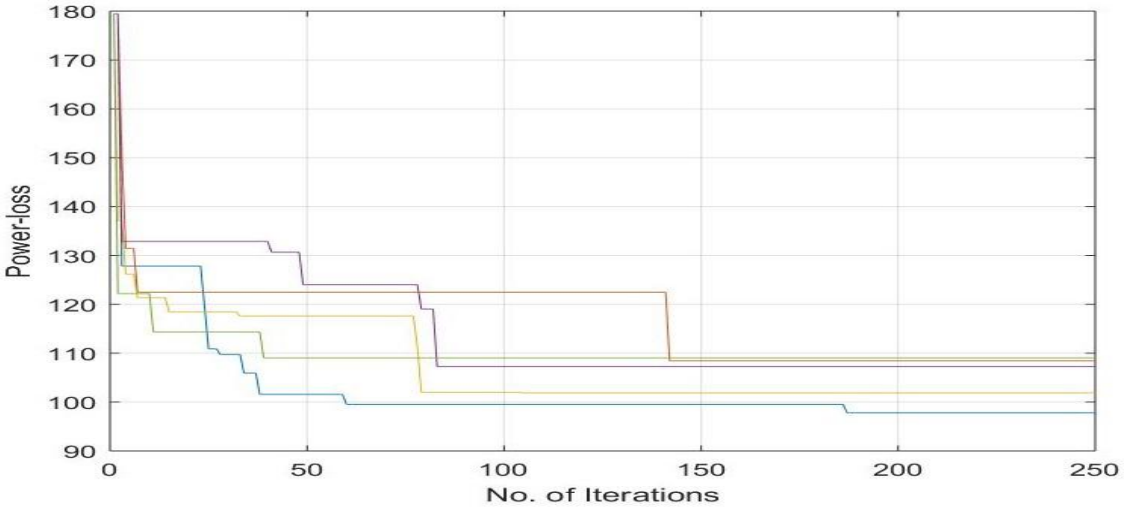

Fig 6.15 Convergence characteristic of optimal configuration under LM-2 with 1-DG

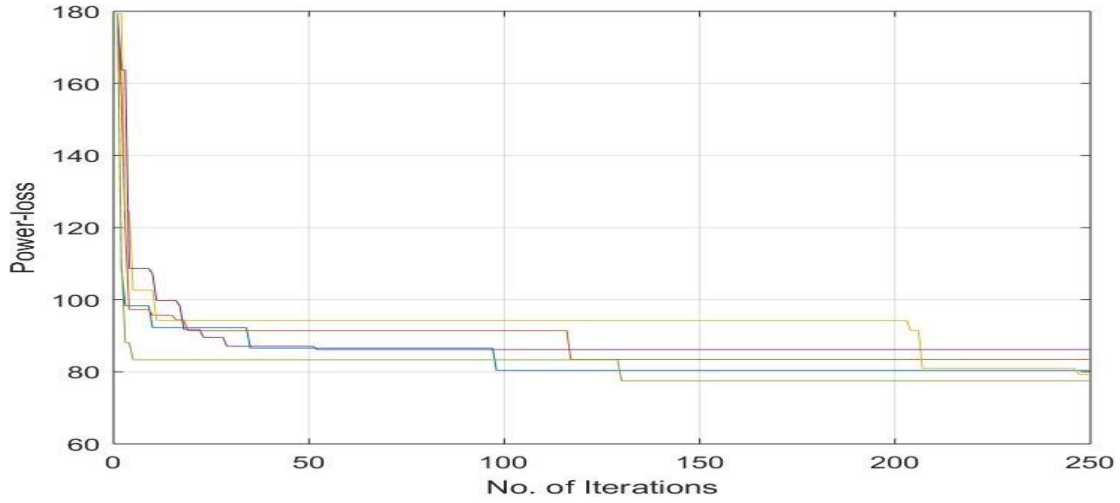

Fig 6.16 Convergence characteristic of optimal configuration under LM-2 with 2-DG

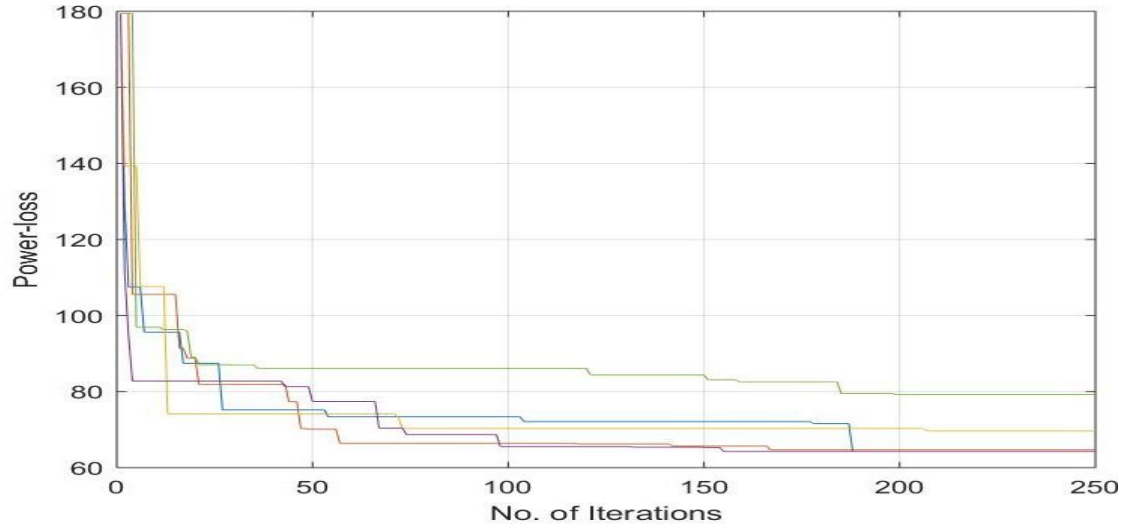

Fig 6.17 Convergence characteristic of optimal configuration under LM-2 with 3-DG

Fig 6.15 to 6.17 show the convergence characteristics of the 33-node system under different load models while reconfiguration of network topology. Here, it can be noticed that the convergence has occurred in different number of iterations. The program is run for 250 iterations and the 5 runs. The computational time is evaluated from the average of the time taken to converge in each run. Fig 6.15-6.17 it can be observed that the convergence rate if slow as compared to the convergence rate in Fig 6.17 as compared to the convergence rate in Fig 6.16 and 5.15

6.4.6 Result discussion for reconfiguration and DG allocation (size fixed) in LM-3

Table 6.6 shows the test result for DG allocation in the base configuration under load model 3. The DG allocation is performed for single and multi-placement. From the result it can be observed that the variation in various EEDPs is different and optimal DG allocation found to be at different nodes. This is due to the fact that the optimal DG size and location is highly dependent on the system loading pattern and the node voltage profile.

The power loss has reduced significantly whereas, the reduction in loss from single DG allocation to the multi DG allocation is not uniform rather with the increment in DG size the overall reduction in loss is 14.49kW, 44.51kW and 59.95kW when DG size is 863.4kW, 1629.2kW and 2018.3kW respectively.

Table 6.6 EEP after reconfigurations and fixed DG size allocation under LM-3

Parameters	**System performance under LM-3**		
No. of DG	**DG=1**	**DG=2**	**DG=3**
Configuration	7,14,35,36,27	6,12,9,36,37	7,14,11,30,28
P_{FD} (kW)	3193.1	2627.2	2046.9
Q_{FD} (kVAr)	2080.1	2116.3	2161.6
S_{FC} (kVA)	3810.8	3373.6	2976.9
Vi, min	0.9479	0.9597	0.9737
f_{si}	101.79	115.82	133.63
P_L (kW)	104.45	74.43	58.99
CT (sec)	0.5386	1.3043	0.5451
DG Locations (Node)	25	33, 9	30, 32, 15
DG sizes (kW)	500	500, 500	500, 500, 500

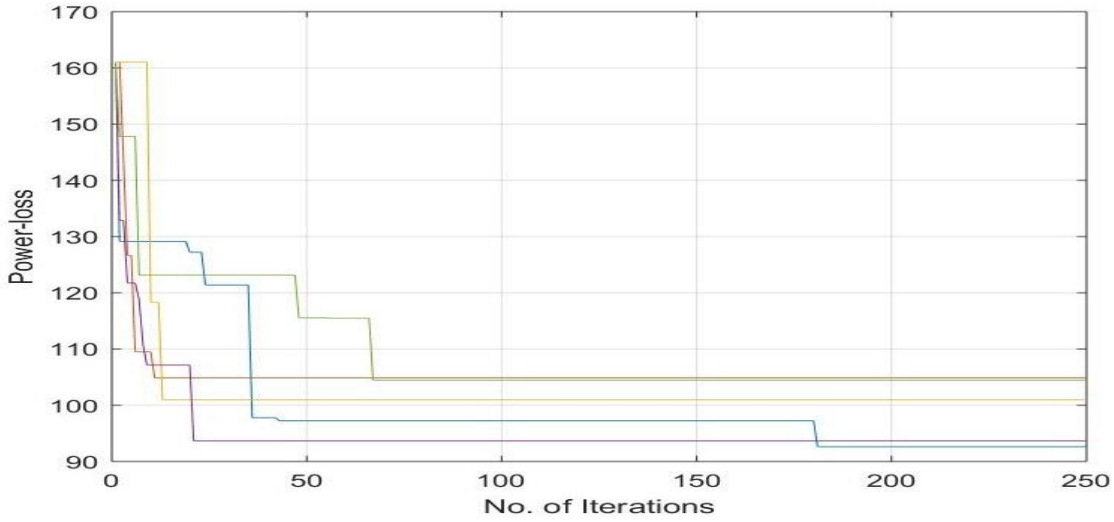

Fig 6.18 Convergence characteristic of optimal configuration under LM-3 with 1-DG

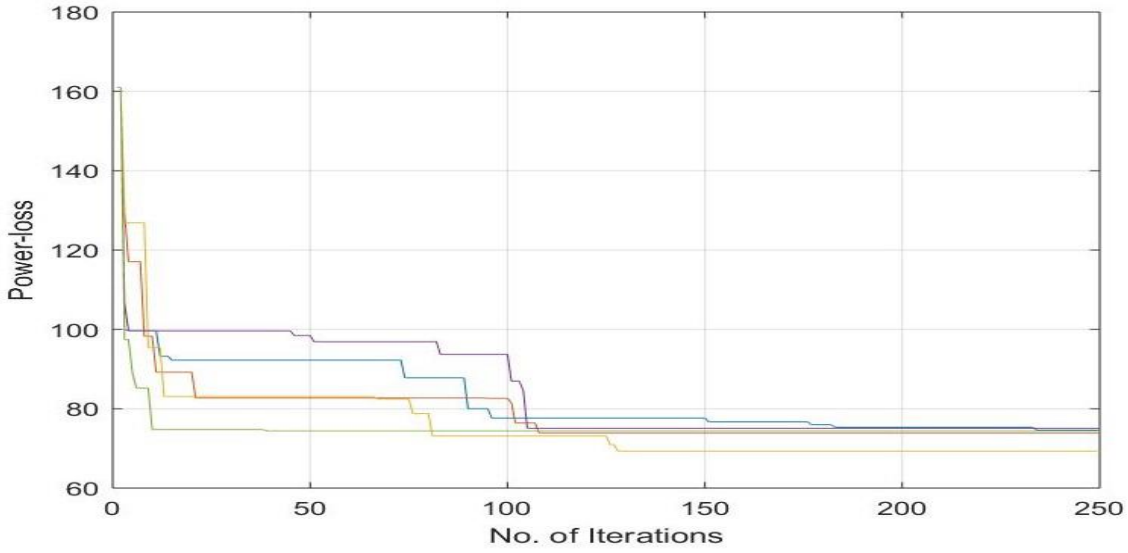

Fig 6.19 Convergence characteristic of optimal configuration under LM-3 with 2-DG

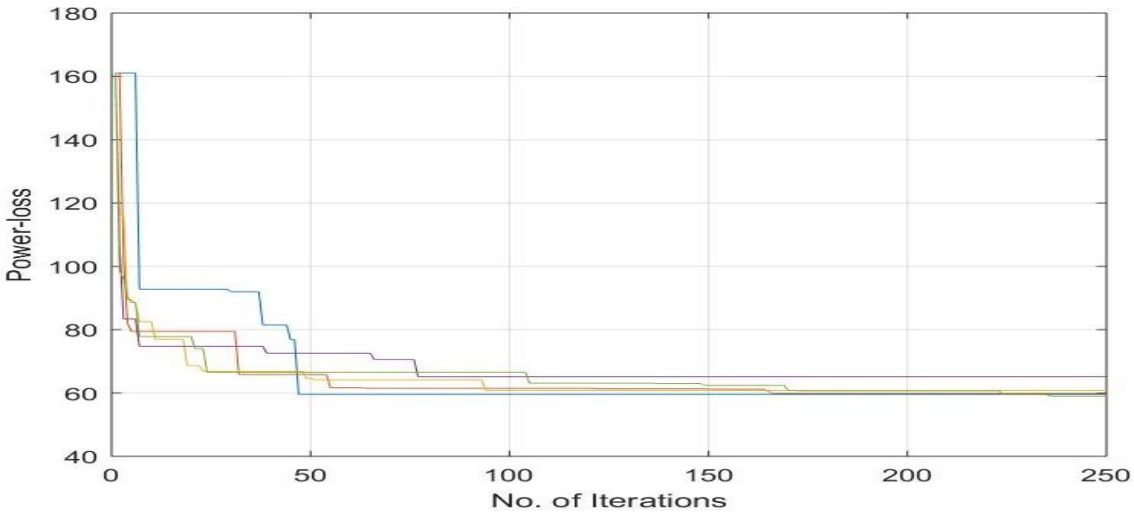

Fig 6.20 Convergence characteristic of optimal configuration under LM-3 with 3-DG

Fig 6.18 to 6.20 show the convergence characteristics of the 33-node system under different load models while reconfiguration of network topology. Here, it can be noticed that the convergence has occurred in different number of iterations. The program is run for 250 iterations and the 5 runs. The computational time is evaluated from the average of the time taken to converge in each run. Fig 6.18-6.20 it can be observed that the convergence rate if slow as compared to the convergence rate in Fig 6.20 as compared to the convergence rate in Fig 6.19 and 6.18

6.4.7 Result discussion for reconfiguration and fixed DG location under LM-1

Table 6.7 shows the test result for DG allocation in the base configuration under load model 1. The DG allocation is performed for single and multi-placement. From the result it can be observed that the variation in various EEDPs is different and optimal DG allocation found to be at different nodes. This is due to the fact that the optimal DG size and location is highly dependent on the system loading pattern and the node voltage profile.

The power loss has reduced significantly whereas, the reduction in loss from single DG allocation to the multi DG allocation is not uniform rather with the increment in DG size the overall reduction in loss is 48.9kW, 66.91kW and 67.29kW when DG size is 996.7kW, 1594kW and 1750.2kW respectively. Here, the increment in DG size is twofold from 2DG to 3DG allocation whereas the reduction in loss is mere 0kW.

Table 6.7 EEP after reconfigurations and fixed DG location allocation under LM-1

Parameters	**System performance under LM-1**		
No. of DG	**DG=1**	**DG=2**	**DG=3**
Configuration	7,14,9,15,28	7,13,9,32,28	7,12,10,320,28
P_{FD} (kW)	2809.9	2194.1	2038.0
Q_{FD} (kVAr)	2369.0	2354.8	2335.1
S_{FC} (kVA)	3675.3	3218.6	3114.5
Vi, min	0.9617	0.9710	0.9701
f_{si}	106.59	123.78	128.77
P_L (kW)	91.07	73.06	72.68
CT (sec)	0.9037	0.9432	0.8530
DG Locations (Node)	33	33, 31	33, 31, 32
DG sizes (kW)	996.7	596.2, 997.8	608.1, 699.9, 442.2

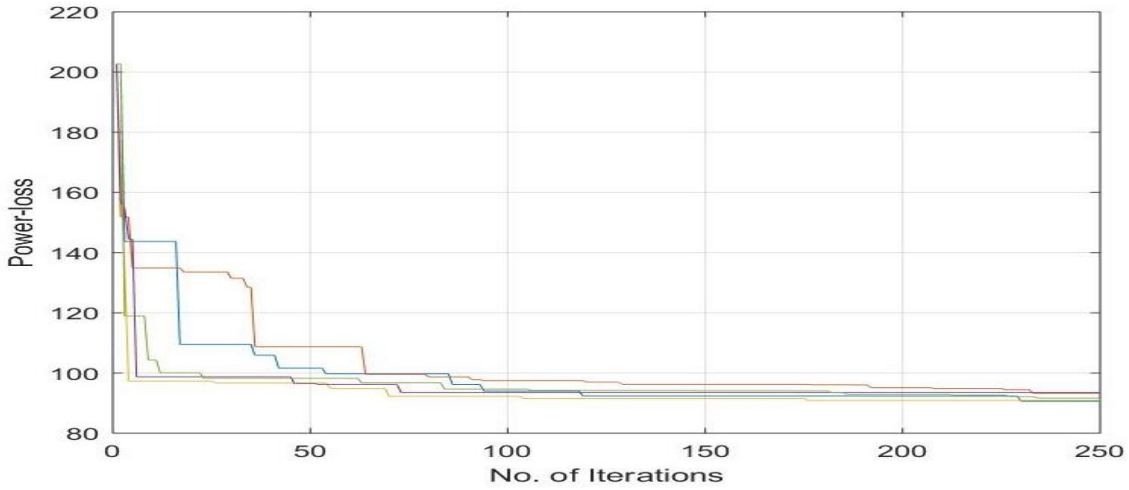

Fig 6.21 Convergence characteristic of optimal configuration under LM-1 with 1-DG

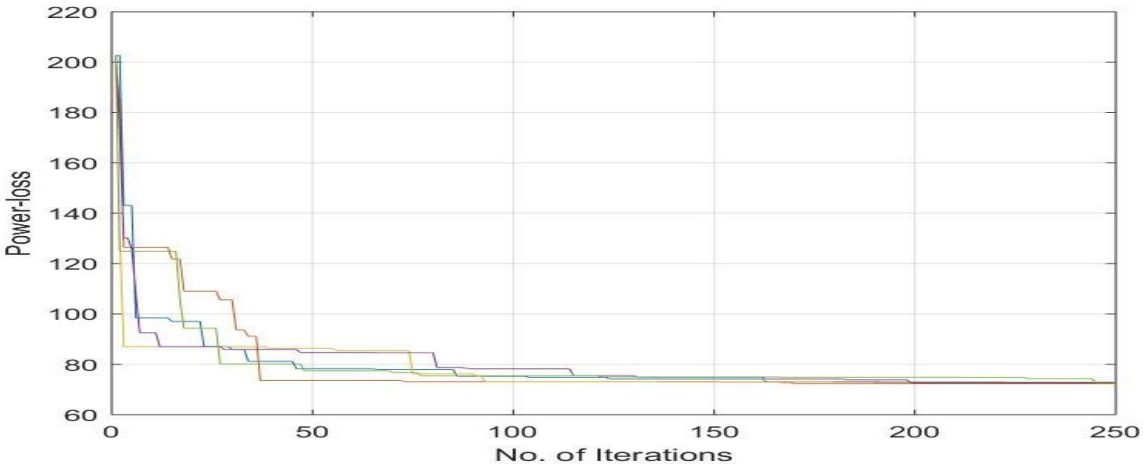

Fig 6.22 Convergence characteristic of optimal configuration under LM-1 with 2-DG

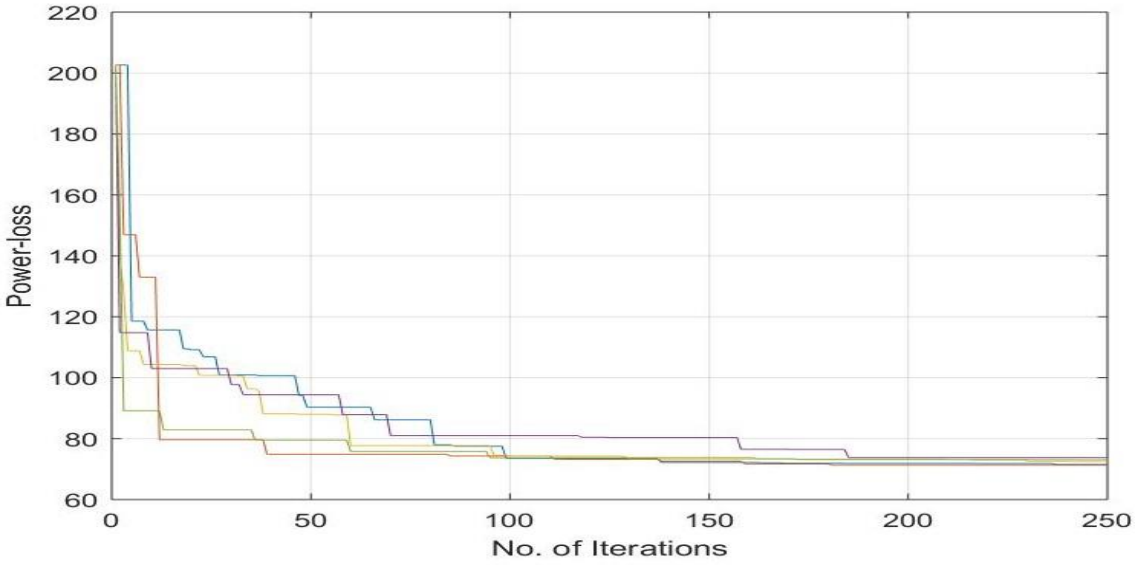

Fig 6.23 Convergence characteristic of optimal configuration under LM-1 with 3-DG

Fig 6.21 to 6.23 show the convergence characteristics of the 33-node system under different load models while reconfiguration of network topology. Here, it can be noticed that the convergence has occurred in different number of iterations. The program is run for 250 iterations and the 5 runs. The computational time is evaluated from the average of the time taken to converge in each run. Fig 6.21-6.23 it can be observed that the convergence rate if slow as compared to the convergence rate in Fig 6.23 as compared to the convergence rate in Fig 6.22 and 6.21

6.4.8 Result discussion for reconfiguration and fixed DG location under LM-2

Table 6.8 shows the test result for DG allocation in the base configuration under load model 2. The DG allocation is performed for single and multi-placement. From the result it can be observed that the variation in various EEDPs is different and optimal DG allocation found to be at different nodes. This is due to the fact that the optimal DG size and location is highly dependent on the system loading pattern and the node voltage profile.

The power loss has reduced significantly whereas, the reduction in loss from single DG allocation to the multi DG allocation is not uniform rather with the increment in DG size the overall reduction in loss is 42.94kW, 56.71kW and 57.8kW when DG size is 885.3kW, 1345.8kW and 1718.2kW respectively.

Table 6.8 EEP after reconfigurations and fixed DG location allocation under LM-2

Parameters	**System performance under LM-2**		
No. of DG	**DG=1**	**DG=2**	**DG=3**
Configuration	7,14,10,30,37	7,34,10,32,28	7,14,10,32,28
P_{FD} (kW)	2834.0	2366.9	2001.8
Q_{FD} (kVAr)	2306.1	2303.2	2314.7
S_{FC} (kVA)	3653.8	3303.2	3060.2
Vi, min	0.9677	0.9861	0.8385
f_{si}	107.01	119.67	131.06
P_L (kW)	85.82	72.05	70.96
CT (sec)	0.9677	0.9861	0.8385
DG Locations (Node)	33	33, 31	33, 31, 32
DG sizes (kW)	885.3	466.8, 879.0	493.7, 608.0, 616.50

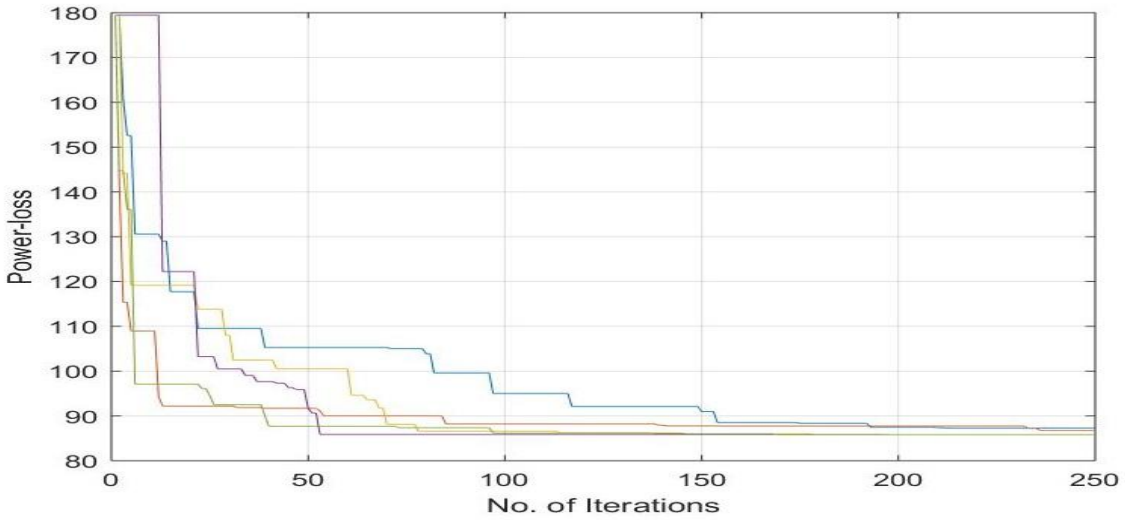

Fig 6.24 Convergence characteristic of optimal configuration under LM-2 with 1-DG

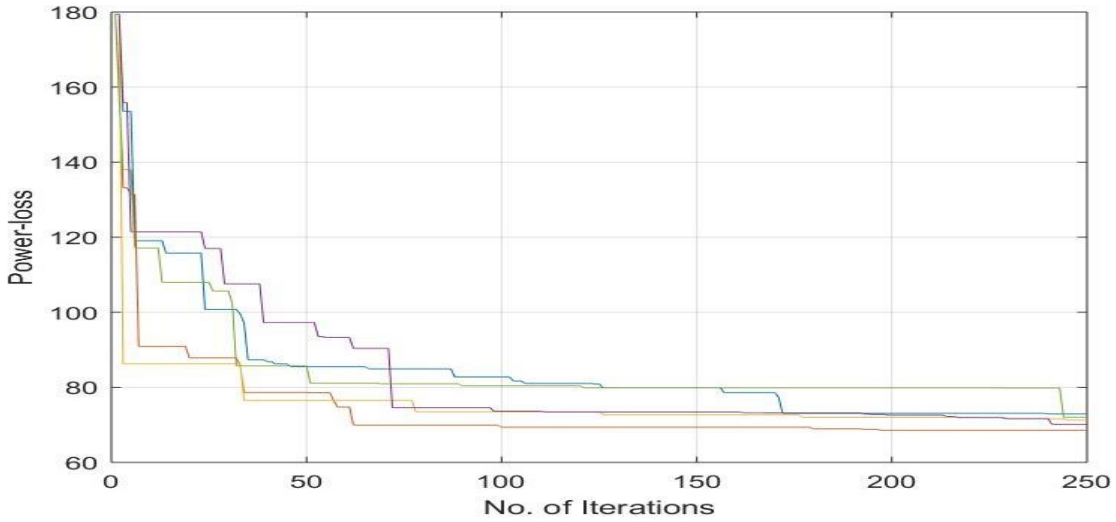

Fig 6.25 Convergence characteristic of optimal configuration under LM-2 with 2-DG

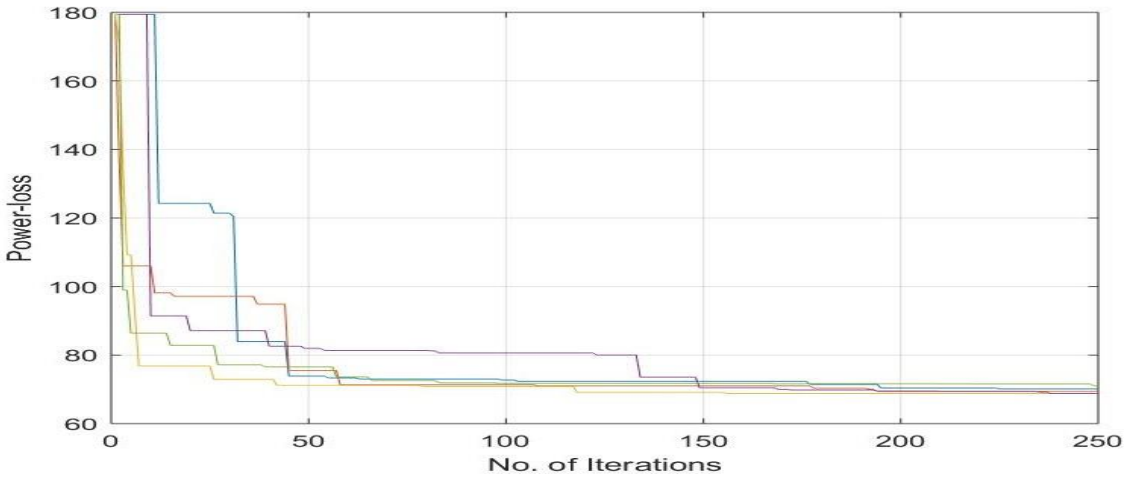

Fig 6.26 Convergence characteristic of optimal configuration under LM-2 with 3-DG

Fig 6.24 to 6.26 show the convergence characteristics of the 33-node system under different load models while reconfiguration of network topology. Here, it can be noticed that the convergence has occurred in different number of iterations. The program is run for 250 iterations and the 5 runs. The computational time is evaluated from the average of the time taken to converge in each run. Fig 6.24-6.26 it can be observed that the convergence rate if slow as compared to the convergence rate in Fig 6.24 as compared to the convergence rate in Fig 6.25 and 6.26

6.4.9 Result discussion for reconfiguration and fixed DG location under LM-3

Table 6.9 shows the test result for DG allocation in the base configuration under load model 3. The DG allocation is performed for single and multi-placement. From the result it can be observed that the variation in various EEDPs is different and optimal DG allocation found to be at different nodes. This is due to the fact that the optimal DG size and location is highly dependent on the system loading pattern and the node voltage profile.

The power loss has reduced significantly whereas, the reduction in loss from single DG allocation to the multi DG allocation is not uniform rather with the increment in DG size the overall reduction in loss is 40.59kW, 54.41kW and 55.09kW when DG size is 901.2kW, 1591kW and 1604.7kW respectively.

Table 6.9 EEP after reconfigurations and fixed DG location allocation under LM-3

Parameters	**System performance under LM-3**		
No. of DG	**DG=1**	**DG=2**	**DG=3**
Configuration	7,3,10,30,37	33,34,8,31,28	7,13,9,32,28
P_{FD} (kW)	2816.7	2125.5	2115.3
Q_{FD} (kVAr)	2119.0	2163.0	2167.3
S_{FC} (kVA)	3524.8	3032.5	3028.5
Vi, min	0.9619	0.9699	0.9742
f_{si}	110.53	130.78	131.03
P_L (kW)	78.35	64.53	63.85
CT (sec)	0.9606	0.8809	0.6647
DG Locations (Node)	33	33, 31	33, 31, 32
DG sizes (kW)	901.2	710.3, 880.7	565.5, 911.5, 127.7

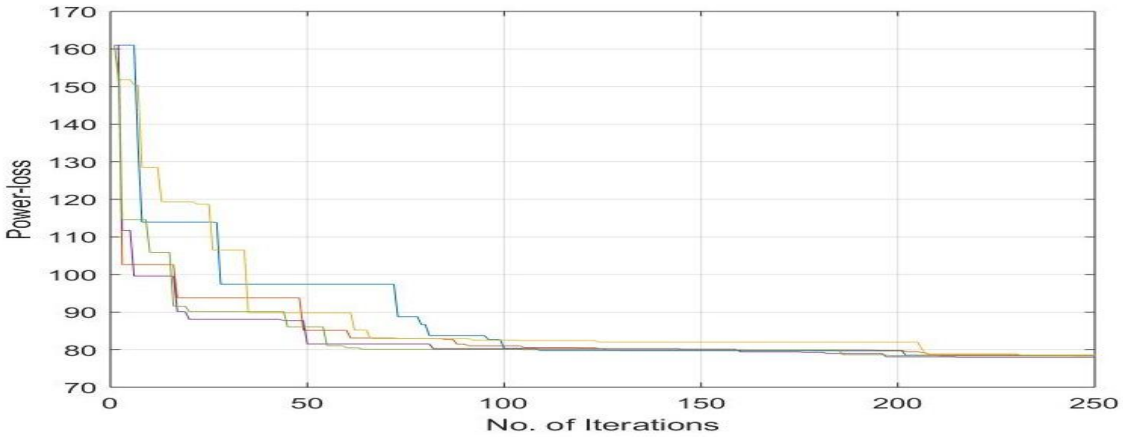

Fig 6.27 Convergence characteristic of optimal configuration under LM-3 with 1-DG

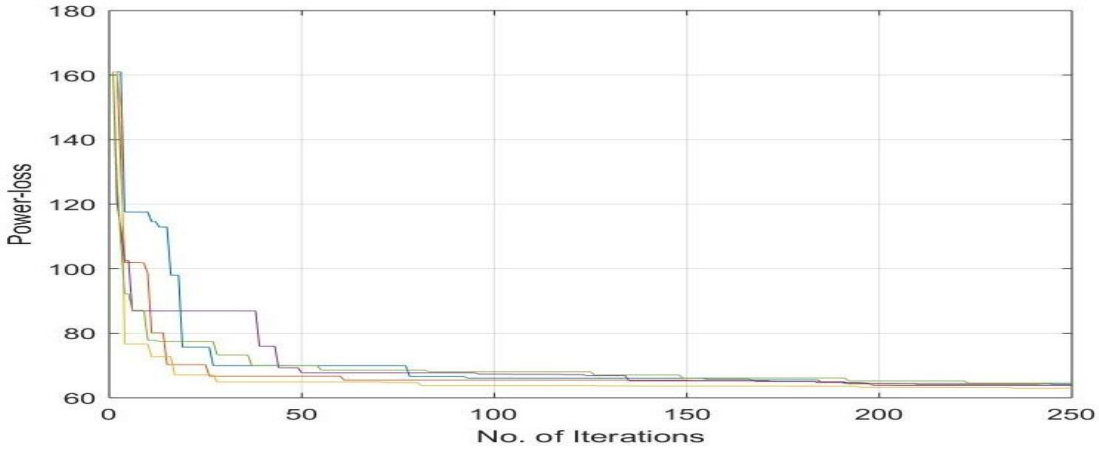

Fig 6.28 Convergence characteristic of optimal configuration under LM-3 with 2-DG

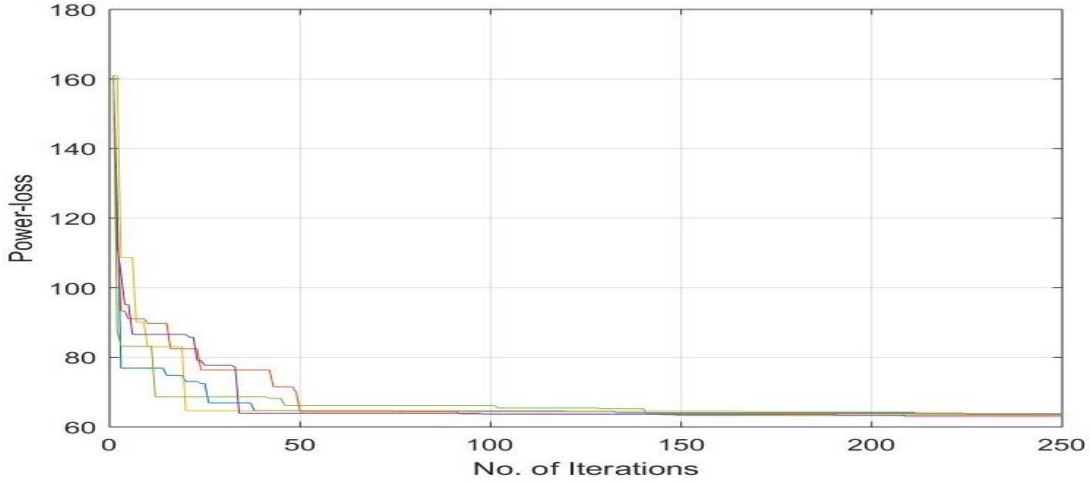

Fig 6.29 Convergence characteristic of optimal configuration under LM-3 with 3-DG

Fig 6.27 to 6.29 show the convergence characteristics of the 33-node system under different load models while reconfiguration of network topology. Here, it can be noticed that the convergence has occurred in different number of iterations. The program is run for 250 iterations and the 5 runs. The computational time is evaluated from the average of the time

taken to converge in each run. Fig 6.27-6.29 it can be observed that the convergence rate if slow as compared to the convergence rate in Fig 6.27 as compared to the convergence rate in Fig 6.28 and 6.29

Table 6.10 Result analysis for IEEE 33-Bus system

Case/Methods	Configuration	Power loss (kW)	DG size	DG location
Base Configuration	33,34,35,36,37	202.67	--	--
Optimal configuration	7, 9, 14, 32, 37	139.55	--	--
DG allocation in base Configuration under,				
LM-1	33,34,35,36,37	78.25	652.3, 999.8, 656.7	14, 26, 32
LM-2		76.78	781.4, 991.2, 407.2	32, 7, 18
LM-3		69.72	970.4, 542.3, 505.6	29, 9, 14
DG allocation in optimal configuration under,				
LM-1	7,9,14,32,37	72.19	968.5, 780.3, 997.6	23, 16,27
LM-2		75.05	419.4, 408.6, 653.7	6, 18, 28
LM-3		65.07	680.2, 828, 622.1	12, 7, 30
DG allocation and Reconfiguration under,				
LM-1	7, 13, 11, 36, 27	58.10	890, 856.5, 792.5	25, 9, 31
LM-2	7, 12, 10, 32, 25	56.39	984.7, 811.6, 754.3	25, 15, 31
LM-3	7, 12, 10, 31, 27	52.18	892.4, 967.9, 780.5	29, 9, 16
Ref. [41]				
IPSO	33, 34, 9, 32, 28	59.63	557, 922, 931	18, 7, 30
TLBO	6,14, 10, 32, 37	58.08	1329, 1172, 726	8, 24, 31
PSO	7, 13, 11, 32, 27	59.37	1732, 809, 550	29, 16, 7
Jaya	33, 13, 9, 28, 30	58.49	801, 1215, 745	18, 25, 9
Ref. [43]	7, 14, 10, 31, 28	73.05	526, 559, 584	28, 31, 33
Ref. [44]	7, 9, 14, 17, 37	92.98	55, 151, 103	18, 31, 32

6.5 Conclusion

In this chapter, the following important outcome are examined: when reconfigure network and DG placement done in radial distribution at same time, it gives effective result in power loss reduction including improvement of voltage profile too. The recommended technique tested on different load models and it has been observed that after reconfiguration and DG placement, maximum loadability of constant impedance load was high and low in the constant power load model in maximum test cases.

Chapter 7

Conclusions

7.1. Summary

This thesis was conducted on a redial distribution system with 33 nodes. The aim of the thesis was to minimize the losses and made the system more reliable as compared to previous. It was carried out by the reconfiguration and DG allocation on the RDS. DG of optimal size is allocated by HSA.

In chapter 1, distribution system discussed in terms of definition, classification, load classes in different types such as residential, commercial and industrial, types of construction ring and radial form, load type like constant voltage load, constant current load and constant impedance load, load model and load combinations as well. Hence in this chapter a brief information delivered.

In chapter 2, literature review has been discussed. From the literature review it has been observed that the single problem can be solved in different way based upon the operating constraints and the methodologies. The objective of reconfiguration and DG placement have been solved by the research using several heuristic and meta-heuristic approaches. In the literature, the loading is considered constant power type whereas in practical system the loads vary with time and state of economy. Therefore, it is a big challenge to solve the objective of reconfiguration and DG allocation in coordination under different loading pattern. In this work, this objective is thoroughly studied.

In chapter 3, the mathematical formulation of various energy efficiency different parameters like node voltages, loadability index is presented for radial network / system nodes beyond particular node have been identified. An efficient load flow method, based on backward /forward sweep, is presented and fundamental of HSA are discuss for formulation.

Chapter 4 presented the network reconfiguration of distribution system. Due to reconfiguration of network, power losses of distribution system can be minimized and with the minimization of power loss, voltage profile has improved. The proposed approach is also examined for distinct load models and the variation in different parameters have been observed. This variation is highly dependent on the level of voltage and proximity to the source node. Further, the convergence of algorithm found different under load model.

Chapter 5 presented, a method to optimally allocate DG in radial distribution schemes is based on the peak load capacity of the system. This method represents to allocate (locations and calculation of DG size) DG in system. And it is also examined that the proposed method is adequate for loss minimization and boost maximum loadability in comparison to existing method. It is also tested on distinct load designs and high load capacity and steady impedance load after DG positioning, but at the same time constant load is small in many instances.

In chapter 6, the following important outcome are examined: when reconfigure network and DG placement done in radial distribution at same time, it gives effective result in power loss reduction including improvement of voltage profile too. The recommended technique tested on different load models and it has been observed that after reconfiguration and DG placement, maximum loadability of constant impedance load was high and low in the constant power load model in maximum test cases.

7.2. Future scope

This work presented the three aspects of the energy efficiency performance of the distribution system which includes; reconfiguration only, DG allocation only and the synchronized DG allocation and reconfiguration. The performance of the sample IEEE 33-node distribution system is evaluated, and it has been observed that the energy efficiency performance in above three objectives found varying differently under different loading patterns. Therefore, it further needs to be investigated the effect of loading pattern through demand side management for the objective of reconfiguration, DG allocation and their synchronized operation as well.

REFERENCES

[1] I. Ali, M. S. Thomas, and P. Kumar, "Energy efficient reconfiguration for practical load combinations in distribution systems," *IET Generation, Transmission & Distribution*, vol. 9, no. 11, pp. 1051–1060, 2015.

[2] P. Kumar, I. Ali, and M. S. Thomas**,** "Energy efficiency of reconfigured distribution system for practical loads," *Elsevier Perspectives in science*, vol. 8, pp. 498-501, 2016.

[3] P. Kumar, I. Ali, M. S. Thomas and S. Singh**,** "Imposing voltage security and network radiality for reconfiguration of distribution systems using efficient heuristic and metaheuristic approach," *IET Generation, Transmission & Distribution*, vol. 11, pp. 2457-2467, 2016.

[4] B. Venkatesh, R. Ranjan, and H. Gooi, "Optimal reconfiguration of radial distribution systems to maximize loadability," *IEEE Transactions on power systems*, vol. 19, no. 1, pp. 260–266, 2004.

[5] S. Sivanagaraju, N. Visali, V. Sankar, and T. Ramana, "Enhancing voltage stability of radial distribution systems by network reconfiguration," *Electric power components and systems*, vol. 33, no. 5, pp. 539–550, 2005.

[6] A. Saffar, R. Hooshmand, and A. Khodabakhshian, "A new fuzzy optimal reconfiguration distribution systems for loss reduction and load balancing using ant colony search-based algorithm," *Applied Soft Computing*, vol. 11, no. 5, pp. 4021–4028, 2011.

[7] M. E. Baran and F. F. Wu, "Network reconfiguration in distribution systems for loss reduction and load balancing," *IEEE Transactions on power delivery*, vol. 4, no. 2, pp. 1401–1407, 1989.

[8] J. Subrahmanyam and C. Radhakrishna, "A simple method for feeder reconfiguration of balanced and unbalanced distribution systems for loss minimization," *Electric Power Components and Systems*, vol. 38, no. 1, pp. 72–84, 2009.

[9] S. Rao, S. V. L. Narasimham, M. R. Raju, andA. S. Rao, "Optimal network reconfiguration of large-scale distribution system using harmony search algorithm," *IEEE Transactions on power systems*, vol. 26, no. 3, pp. 1080–1088, 2011.

[10] C. Ababei and R. Kavasseri, “Efficient network reconfiguration using minimum cost maximum flow-based branch exchanges and random walks-based loss estimations,” *IEEE Transactions on Power Systems*, vol. 26, no. 1, pp. 30–37, 2011.

[11] K. Nara, “Implementation of genetic algorithm for distribution system loss minimum re-configuration,” *IEEE Trans. on Power Systems*, vol. 5, pp. 1902–1909, 1992.

[12] D. Zhang, Z. Fu, and L. Zhang, “An improved ts algorithm for loss-minimum reconfiguration in large-scale distribution systems,” *Electric Power Systems Research*, vol. 77, no. 5-6, pp. 685–694, 2007.

[13] G. V. Raju and P. Bijwe, “Efficient reconfiguration of balanced and unbalanced distribution systems for loss minimisation,” *IET Generation, Transmission & Distribution*, vol. 2, no. 1, pp. 7–12, 2008.

[14] C.-T. Su, C.-F. Chang, and J.-P. Chiou, “Distribution network reconfiguration for loss reduction by ant colony search algorithm,” *Electric Power Systems Research*, vol. 75, no. 2-3, pp. 190–199, 2011.

[15] R. Hooshmand and E. Mashhoor, “Application of fuzzy algorithm in optimal reconfiguration of distribution networks for loss reduction and load balancing,” *Engineering intelligent systems for electrical engineering and communications*, vol. 14, no. 1, pp. 15– 2006

[16] V. Farahani, B. Vahidi, and H. A. Abyaneh, “Reconfiguration and capacitor placement simultaneously for energy loss reduction based on an improved reconfiguration method,” *IEEE Transactions on power systems*, vol. 27, no. 2, p. 587, 2012.

[17] R. A. Jabr, R. Singh, and B. C. Pal, “Minimum loss network reconfiguration using mixed-integer convex programming,” *IEEE Transactions on Power systems*, vol. 27, no. 2, pp. 1106–1115, 2012.

[18] E. J. de Oliveira, G. J. Rosseti, L. W. de Oliveira, F. V. Gomes, and W. Peres, “New algorithm for reconfiguration and operating procedures in electric distribution systems,” *International Journal of Electrical Power & Energy Systems*, vol. 57, pp. 129–134, 2014.

[19] M. M. Aman, G. B. Jasmon, A. H. Abu Bakar, H. Mokhlis, and K. Naidu, “Graph theory-based radial load flow analysis to solve the dynamic network reconfiguration problem”, *International Transactions on Electrical Energy Systems*, vol. 26, no. 4, pp. 783–808, 2016.

[20] M.-R. Andervazh, J. Olamaei, and M.-R. Haghifam, “Adaptive multi-objective distribution network reconfiguration using multi-objective discrete particles swarm optimisation algorithm and graph theory,” *IET Generation, Transmission & Distribution*, vol. 7, no. 12, pp. 1367–1382, 2013.

[21] J. Mendoza, M. Lopez, C. C. Coello, and E. Lopez, “Microgenetic multiobjective reconfiguration algorithm considering power losses and reliability indices for medium voltage distribution network,” *IET Generation,Transmission & Distribution*, vol. 3, no. 9, pp. 825–840, 2009.

[22] M. R. Narimani, A. A. Vahed, R. Azizipanah-Abarghooee, and M. Javidsharifi, “Enhanced gravitational search algorithm for multi-objective distribution feeder reconfigu- ration considering reliability, loss and operational cost,” *IET Generation, Transmission & Distribution*, vol. 8, no. 1, pp. 55–69, 2014.

[23] N. Gupta, A. Swarnkar, and K. Niazi, “Distribution network reconfiguration for power quality and reliability improvement using genetic algorithms,” *International Journal of Electrical Power & Energy Systems*, vol. 54, pp. 664–671, 2014.

[24] J. C. Lopez, M. Lavorato, J. F. Franco, and M. J. Rider, “Robust optimisation applied to the reconfiguration of distribution systems with reliability constraints,” *IET Generation, Transmission & Distribution*, vol. 10, no. 4, pp. 917–927, 2016.

[25] B. Khorshid-Ghazani, H. Seyedi, B. Mohammadiivatloo, K. Zare, and S. Shargh, “Reconfiguration of distribution networks considering coordination of the protective devices,” *IET Generation, Transmission & Distribution*, vol. 11, no. 1, pp. 82–92, 2011

[26] I. Ali, M. S. Thomas, and P. Kumar, “Effect of loading pattern on the performance of reconfigured medium size distribution system,” *in Power India Conference, 2012 IEEE Fifth*, pp. 1–6, IEEE, 2012.

[27] P. Kumar and S. Singh, “Reconfiguration of radial distribution system with static load models for loss minimization,” *in Power Electronics, Drives and Energy Systems (PEDES), 2014 IEEE International Conference on*, pp. 1–5, IEEE, 2014.

[28] G. Celli, S. Mocci, F. Pilo, and G. Soma, “A multi-objective approach for the optimal distributed generation allocation with environmental constraints,” *in Probabilistic Methods*

Applied to Power Systems, 2008. PMAPS'08. Proceedings of the 10th International Conference on, pp. 1–8, IEEE, 2008.

[29] P. Chiradeja and R. Ramakumar, "An approach to quantify the technical benefits of distributed generation," *IEEE Transactions on energy conversion*, vol. 19, no. 4, pp. 764–773, 2004.

[30] D. Q. Hung, N. Mithulananthan, and R. Bansal, "Analytical expressions for dg allocation in primary distribution networks," *IEEE Transactions on energy conversion*, vol. 25, no. 3, pp. 814–820, 2010.

[31] N. Khalesi, N. Rezaei, and M.-R. Haghifam, "Dg allocation with application of dynamic programming for loss reduction and reliability improvement," *International Journal of Electrical Power & Energy Systems*, vol. 33, no. 2, pp. 288–295, 2011.

[32] S. Ganguly and D. Samajpati, "Distributed generation allocation on radial distribution networks under uncertainties of load and generation using genetic algorithm," *IEEE Transactions on Sustainable Energy*, vol. 6, no. 3, pp. 688–697, 2015.

[33] A. Soroudi, M. Ehsan, R. Caire, and N. Hadjsaid, "Hybrid immune-genetic algorithm method for benefit maximisation of distribution network operators and distributed generation owners in a deregulated environment," *IET generation, transmission & distribution*, vol. 5, no. 9, pp. 961–972, 2011.

[34] C. J. Dent, L. F. Ochoa, and G. P. Harrison, "Network distributed generation capacity analysis using opf with voltage step constraints," *IEEE Transactions on Power systems*, vol. 25, no. 1, pp. 296–304, 2010.

[35] A. Mahari and E. Babaei, "Optimal dg placement and sizing in distribution systems using imperialistic competition algorithm," *IEEE 5th India International Conference* on, pp. 1–6, IEEE, 2012.

[36] V. A. Evangelopoulos and P. S. Georgilakis, "Optimal distributed generation placement under uncertainties based on point estimate method embedded genetic algorithm," *IET Generation, Transmission & Distribution*, vol. 8, no. 3, pp. 389–400, 2014.

[37] A. Keane, Q. Zhou, J. W. Bialek, and M. O'Malley, "Planning and operating non-firm distributed generation," *IET Renewable Power Generation*, vol. 3, no. 4, pp. 455–464,2009.

[38] M. Haghifam, H. Falaghi, and O. Malik, “Risk-based distributed generation placement,” *IET Generation, Transmission & Distribution*, vol. 2, no. 2, pp. 252, 2008.

[39] A. Keane, L. F. Ochoa, C. L. Borges, G. W. Ault, A. D. Alarcon-Rodriguez, R. A. Currie, F. Pilo, C. Dent, and G. P. Harrison, “State-of-the-art techniques and challenges ahead for distributed generation planning and optimization,” *IEEE Transactions on Power Systems*, vol. 28, no. 6, 2013.

[40] S. Kamel, A. Awed, H.B. Mawgoud and F. Jarado, “Optimal DG allocation for enhancing voltage stability and minimizing power loss using hybrid gray wolf optimizer,” *Turkish Journal of electrical engineering and computer sciences*, doi: 10.3906/elk-1805-66, 2018

[41] M.S. Rawat and S. Vadhera, “Heuristic optimization techniques for DG stability enhance for radial distribution network with simultaneous consideration for DG sizing and allocations,” *Turkish Journal of electrical engineering and computer sciences*, vol. 27, no. 1, pp. 330-345, 2019

[42] S. Rao, Narasimham, Raju and Rao, “Optimal reconfiguration of large-scale distribution system using harmony search algorithm,” *IEEE transaction on power system*, vol. 26, no. 3, pp. 1080-1088, 2011.

[43] S. Rao, K. Ravindra, K. Satish, and S.V.L Narasimham, “Power loss minimization in distribution system using network reconfiguration in the presence of distribution generation,” *IEEE Transaction on power system*, vol. 28, no. 1, pp. 1317-328, 2013.

[44] H. Esmaeilian, and R. Fadaeinagjad, “Energy loss minimization in distribution system utilizing and enhanced reconfiguration method integrating distribution generation,” *IEEE system journal*, vol. 9, no. 9, pp. 1430-1439, 2015.

Thesis22

ORIGINALITY REPORT

8%	1%	4%	6%
SIMILARITY INDEX	INTERNET SOURCES	PUBLICATIONS	STUDENT PAPERS

PRIMARY SOURCES

1	Submitted to Jawaharlal Nehru Technological University Student Paper	1%
2	Submitted to Malaviya National Institute of Technology Student Paper	1%
3	Submitted to Jawaharlal Nehru Technological University Kakinada Student Paper	1%
4	Submitted to Thapar University, Patiala Student Paper	1%
5	Xiaolei Wang, Xiao-Zhi Gao, Kai Zenger. "An Introduction to Harmony Search Optimization Method", Springer Nature, 2015 Publication	1%
6	Srinivasa Rao, Rayapudi, Sadhu Venkata Lakshmi Narasimham, Manyala Ramalinga Raju, and A. Srinivasa Rao. "Optimal Network Reconfiguration of Large-Scale Distribution System Using Harmony Search Algorithm",	1%

IEEE Transactions on Power Systems, 2011.
Publication

7	Wei Sun, Xingyan Chang. "An Improved Harmony Search Algorithm for Power Distribution Network Planning", Journal of Electrical and Computer Engineering, 2015 Publication	<1%
8	Submitted to The University of Manchester Student Paper	<1%
9	Submitted to Jawaharlal Nehru Technological University Anantapur Student Paper	<1%
10	"ENHANCING THE MAXIMUM LOADABILITY OF RADIAL DISTRIBUTION SYSTEM BY NETWORK RECONFIGURATION", International Journal of Power and Energy Systems, 2009 Publication	<1%
11	Submitted to VIT University Student Paper	<1%
12	Ali, Ikbal, Mini S. Thomas, and Pawan Kumar. "Energy efficient reconfiguration for practical load combinations in distribution systems", IET Generation Transmission & Distribution, 2015. Publication	<1%
13	Submitted to SASTRA University Student Paper	